Review article

Recycling of crustal materials through study of ultrahigh-pressure minerals in collisional orogens, ophiolites, and mantle xenoliths: A review

Juhn G. Liou [a,*], Tatsuki Tsujimori [b], Jingsui Yang [c], R.Y. Zhang [a], W.G. Ernst [a]

[a] Department of Geological and Environmental Sciences, Stanford University, Stanford, CA 94305-2115, USA
[b] Pheasant Memorial Laboratory, Institute for Study of the Earth's Interior, Okayama University, 827 Yamada, Misasa-cho, Tottori-ken 682-0193, Japan
[c] CARMA and SKLCTD, Institute of Geology, Chinese Academy of Geological Sciences, 26 Baiwanzhuang Road, Beijing 100037, China

ARTICLE INFO

ABSTRACT

Newly recognized occurrences of ultrahigh-pressure (UHP) minerals including diamonds in ultrahigh-temperature (UHT) felsic granulites of orogenic belts, in chromitites associated with ophiolitic complexes, and in mantle xenoliths suggest the recycling of crustal materials through deep subduction, mantle upwelling, and return to the Earth's surface. This circulation process is supported by crust-derived mineral inclusions in deep-seated zircons, chromites, and diamonds from collision-type orogens, from eclogitic xenoliths in kimberlites, and from chromitites of several Alpine–Himalayan and Polar Ural ophiolites; some of these minerals contain low-atomic number elements typified by crustal isotopic signatures. Ophiolite-type diamonds in placer deposits and as inclusions in chromitites together with numerous highly reduced minerals and alloys appear to have formed near the mantle transition zone. In addition to ringwoodite and inferred stishovite, a number of nanometric minerals have been identified as inclusions employing state-of-the-art analytical tools. Reconstitution of now-exsolved precursor UHP phases and recognition of subtle decompression microstructures produced during exhumation reflect earlier UHP conditions. For example, Tibetan chromites containing exsolution lamellae of coesite + diopside suggest that the original chromitites formed at $P > 9$–10 GPa at depths of >250–300 km. The precursor phase most likely had a Ca-ferrite or a Ca-titanite structure; both are polymorphs of chromite and (at 2000 °C) would have formed at minimum pressures of $P > 12.5$ or 20 GPa respectively. Some podiform chromitites and host peridotites contain rare minerals of undoubted crustal origin, including zircon, feldspars, garnet, kyanite, andalusite, quartz, and rutile; the zircons possess much older U–Pb ages than the time of ophiolite formation. These UHP mineral-bearing chromitite hosts evidently had a deep-seated evolution prior to extensional mantle upwelling and partial melting at shallow depths to form the overlying ophiolite complexes. These new findings together with stable isotopic and inclusion characteristics of diamonds provide compelling evidence for profound underflow of both oceanic and continental lithosphere, recycling of surface 'organic' carbon into the lower mantle, and ascent to the Earth's surface through mantle upwelling. Intensified study of UHP granulite-facies lower crustal basement and ophiolitic chromitites should allow a better understanding of the geodynamics of subduction and crustal cycling.

© 2014 Elsevier Ltd. All rights reserved.

Contents

* Corresponding author.

1. UHP crustal terranes

1.1. Introduction for UHP crustal terranes

An explosion in current research on continental UHP terranes reflects their significance regarding mantle dynamics and the tectonics of continental subduction, collision, exhumation, crustal growth, mantle-lithospheric slab interactions, and geochemical recycling (e.g., Zheng, 2012a,b; Janák et al., 2013a; Spandler and Pirard, 2013; Hermann and Rubatto, 2014). Since our previous review in 2009, several special issues related to UHP metamorphism

and tectonics have been published (e.g., Dobrzhinetskaya et al., 2011; Yang et al., 2011; Dobrzhinetskaya and Faryad, 2011; Dobrzhinetskaya, 2012; Zheng et al., 2012; Dobrzhinetskaya et al., 2013a; Faryad et al., 2013; Gilotti, 2013; Yui et al., 2013). Among many new petrochemical descriptions and their tectonic origins, the most startling discoveries include (1) finding of UHP relict minerals and a possible remnant of ringwoodite in a Paleoproterozoic (~1.8 Ga) collisional suture in West Greenland (Glassley et al., 2014), (2) microdiamond (±coesite) inclusions in minerals of Variscan HT granulites and garnet peridotites of the North Bohemian basement (Kotková et al., 2011; Naemura et al., 2011, 2013) and in

UH*T* felsic granulites of the Betic-Rif Cordillera in NW Africa and SE Spain (Ruiz Cruz and Sanz de Galdeano, 2012, 2013, 2014), and (3) *in-situ* microdiamond, possible stishovite and other UH*P* minerals in chromitites associated with low-*P* mineral inclusions in crustal zircons associated with Tibetan and Ural ophiolites (e.g., Robinson et al., 2004; Yang et al., 2007, 2014a,b; Yamamoto et al., 2013).

These new results reflect numerous petrochemical studies of mineral inclusions in tough, rigid minerals such as chromite, diamond, zircon, garnet, omphacite and kyanite using sophisticated analytical tools. Similar approaches have also been applied for investigation of mineral inclusions in diamonds and other mantle minerals from kimberlitic mantle xenoliths (e.g., Walter et al., 2011; Schulze et al., 2013; Pearson et al., 2014). The first finding of terrestrial ringwoodite with 1.5–1.4 wt% H_2O as an inclusion in a Brazilian diamond by Pearson et al. (2014) supports the suggestion of a hydrous mantle transition zone and the possibility of vast amounts of fluids being recycled to the deep mantle through subduction (e.g., Schulze et al., 2014; Pearson et al., 2014 and references). Furthermore, the nano- to micron-size ion microprobe (secondary ion mass-spectrometry: SIMS) has been used to characterize U–Pb ages and C-isotopes of zircon and diamond respectively, and to interpret the primary origin and evolution of their host minerals and rocks. In the present review, we integrate some mineralogical–petrochemical and C-isotope evidence of UH*P* minerals in orogenic belts, in chromitites associated with ophiolites, and in kimberlitic xenoliths. Based on this summary, we postulate their evolution through subduction of oceanic + continental lithosphere, recycling of surface 'organic' carbon into the lower mantle, and exhumation to the Earth's surface through deep mantle circulation (for other recent reviews, see Spandler and Pirard, 2013; Shirey et al., 2013; Helmstaedt, 2013; Arai, 2013).

Fig. 1 is a schematic cross section of the Earth's outer shells showing recycling of crustal materials in different tectonic regimes. Bold black arrows represent global pathways of continental materials to the Earth's surface and to the mantle–core boundary. Label A is a general trajectory of subduction/exhumation of UH*P* metamorphic rocks in a collision-type orogen. Label B represents UH*P*-mineral-bearing ophiolites; unusual chromitites with UH*P*-minerals and/or crustal-derived minerals might have formed from recycled materials. Subduction of terrigenous materials in Pacific-type orogens transports significant volumes of continental crust into the transition zone. Label C is a kimberlite pipe where diamondiferous materials of the subcontinental lithospheric mantle (SCLM) as well as superdeep mantle materials can be transported surfaceward (Maruyama et al., 2007; Liou and Tsujimori, 2013). Mineral abbreviations throughout this work are mostly after Whitney and Evans (2010).

1.2. Definition of UHP and UHT metamorphism

1.2.1. Ultrahigh-pressure metamorphism

Ultrahigh-pressure metamorphism involves the mineralogic and structural transformation of continental ± oceanic crustal rocks at subduction-zone depths greater than 90–100 km. Fig. 2 illustrates the stabilities fields of UH*P* index minerals including high-P polymorphs of SiO_2, C, TiO_2 and higher proportions of majoritic component in garnet solid solution. The discovery of at least 31 tracts of upper continental crust metamorphosed under mantle pressure–temperature (*P–T*) conditions has stimulated intensive study in the Earth sciences over the last three decades (Fig. 3; Table 1). High-pressure (H*P*)–UH*P* metamorphism is a hallmark of subduction zones; exhumed assemblages of rocks mark compressional plate sutures (e.g., Ernst, 1970, 1972, 1973, 2005; Maruyama et al., 1996; Liou et al., 2004; Tsujimori and Ernst, 2014). Two distinct convergent plate-tectonic regimes, Pacific-type active and Alpine-type passive margins, have been identified, although a continuum of intermediate types exists. Pacific-type convergence reflects subduction of an oceanic plate and landward development of an accretionary complex, a forearc basin, and a
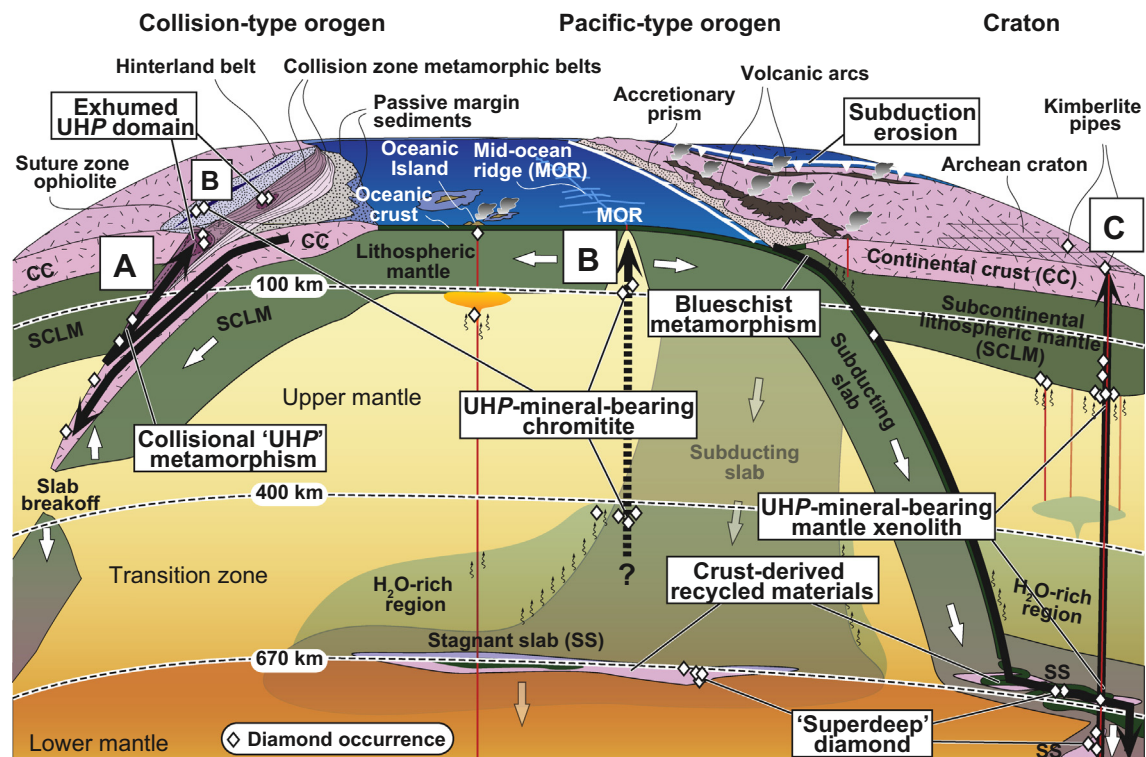
Fig. 1. A schematic cross section of the Earth's outer shells showing recycling of crustal materials in different tectonic regimes (modified after Liou and Tsujimori, 2013; see text for details).
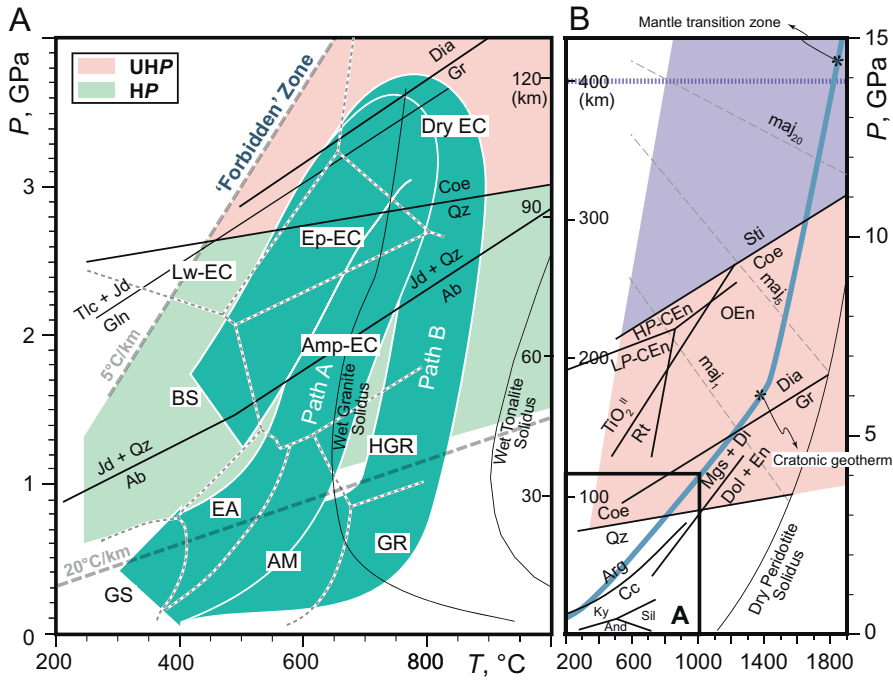
Fig. 2. (A) P–T regimes at different scales assigned to various metamorphic types: (1) ultrahigh-P, (2) high-P, (3) low-P and (4) "forbidden zone" and stabilities of coesite and diamond (modified after Liou et al., 2004; 2009a). Path A and B represent P-T paths of small/thin UHP terranes and large/thick terranes, respectively (modified after Kylander-Clark et al., 2012). (B) P–T stabilities of additional UHP index minerals including pseudomorphic stishovite, majoritic garnet, high-P clinoenstatite and TiO$_2^{II}$ (α-PbO$_2$ structured TiO$_2$) are shown (modified from Fig. 1 of Liou et al., 2009a and Fig. 1 of Schertl and O'Brien, 2013).
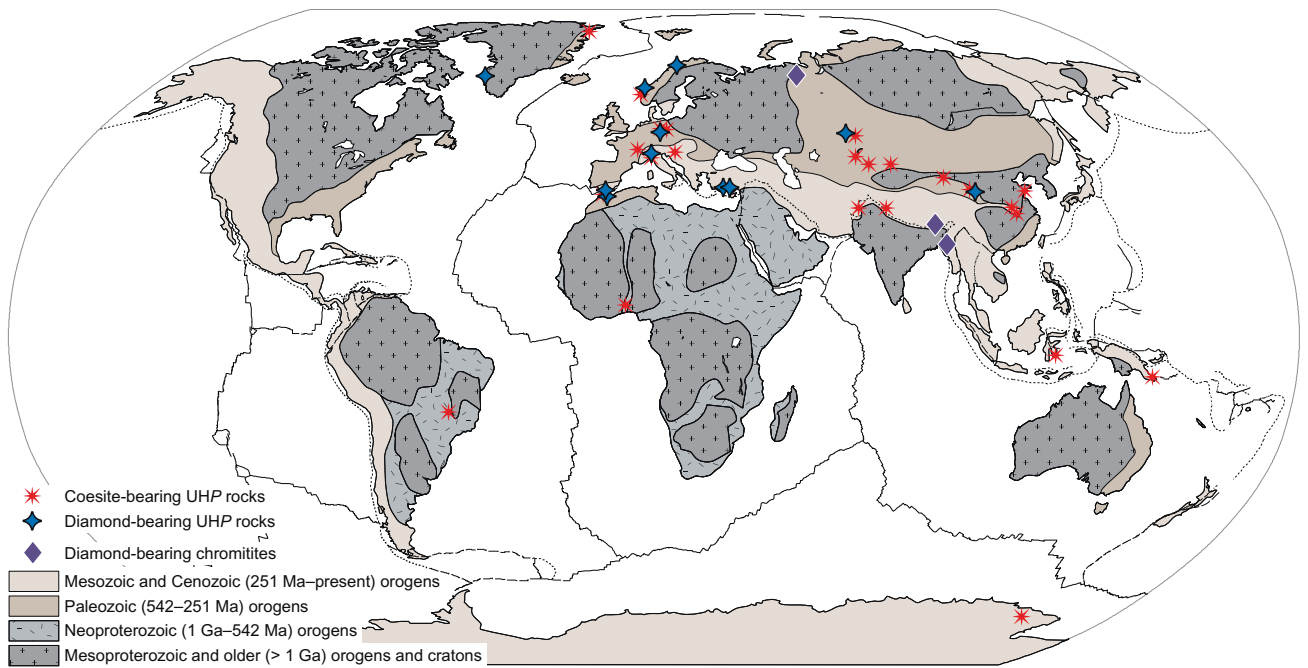
Fig. 3. Global distribution and peak metamorphic age of recognized coesite-, and diamond-bearing UHP terranes (modified after Liou et al., 2004; Tsujimori et al., 2006; Stern et al., 2013).

huge calc-alkaline magmatic arc. In Pacific-type margins, protoliths for HP–UHP metamorphism consist of oceanic materials (bedded cherts, pillow basalts) and associated trench sediments derived from the inboard igneous arc. In contrast, Alpine-type HP–UHP rocks include old continental granitic basement complexes and their overlying sediments, including pelites, carbonates, quartzites, and volcaniclastic rocks, as well as minor ultramafic–mafic fragments.

1.2.2. Ultrahigh-temperature metamorphism

Ultrahigh-temperature metamorphism represents crustal recrystallization at temperatures exceeding 900 °C (Fig. 2). Granulite-facies rocks metamorphosed under such extreme conditions were identified in the early 1980s; it took another decade for the geoscience community to recognize UHT metamorphism as a common regional phenomenon. Petrological evidence based on characteristic mineral assemblages backed by experimental and

Table 1
Global UHP terranes recognized in the previous review papers of Liou et al. (2009a,b) and Gilotti (2013).

UHP terranes	Age (Ma)	Index
West Greenland	~1800	PT, Dia*
Mali, W Africa	620	Coe
Pompangeo schist, Brazil	630	Coe+
Kokchetav massif, Kazakhstan	537–527	Coe, Dia
Makbal, Krygyzstan	510–500	Coe
At-bashy, Krygyzstan	324–327	Coe+
Qinling, China	507	Coe, Dia
Altyn Tagh, Western China	509–493	Coe*
Lanterman Range, Antarctica	500	Coe
NE Greenland	365–350	Coe
Tromsø, Norway	452	Dia
Northern Qaidam, NE Tibetan Plateau, China	446–423	Coe
Massif Central, France	420–400	Coe
Western Gneiss Region, Norway	405–400, 407	Coe, Dia
Maksyutov complex, Russia	388	Dia*
Bohemian massif, Central Sudetes, Poland	389–381	Coe*
Bohemian massif, Germany/Czech Republic	337	Coe, Dia
Betic-Riff, NW Africa/SE Spain	330?, 18–14?	Coe, Dia
Qinling, China	240–220	Coe
Dabie, E China	240–220	Coe
Sulu, E China	240–220	Coe
Tianshan, W China	320	Coe
Ngoc Linh complex, Kontum, Vietnam	250	Dia+
Kimi complex, E Rhodope, NE Greece	202	Coe, Dia
Austroalpine basement, Pohorje, Austria	≈92	Coe*
As Sifah, Oman	79	PT
Tso Morari, India	53–48	Coe
Kaghan Valley, Pakistan	46	Coe
Zermatt–Saas-Fee, West Alps, Italy/Switzerland	44–41	Coe, Dia
Dora Maira, West Alps, Italy	35	Coe
SE Sundaland margin, Sulawesi, Indonesia	27–20	Dia+
Papua New Guinea	8–7	Coe

Coe—coesite; Dia—diamond; PT—PT estimation; *—pseudomorph; +—incomplete documentation.

thermodynamic relations demonstrated that the Earth's crust can attain very high temperatures (900–1000 °C) with partial melting to various extents. UHT assemblages of pelitic restites include Opx + Sil + Qz ± Osm ± Crd, Spr + Qz or Spl + Qz, whereas mafic ones are typical Opx + Cpx + Pl ± Grt (or Spl) ± Qz; these rocks are commonly associated with migmatites in the mid- to upper crust (e.g., Harley, 1998; Brown, 2007; Kelsey, 2008). UHT rocks occur in all major continents and span different geological ages ranging from c. 3178 to 35 Ma; more than 46 localities/terranes with diagnostic UHT indicators have been reported in both extensional and collisional orogens.

1.2.3. Types of UHP terranes

Kylander-Clark et al. (2012) classified UHP terranes as of two types based on the estimated exposed areas of eclogite-facies rocks. Small, thin terranes including Dora Maira, New Guinea, Kaghan, Tso Morari, Kokchetav and Erzgebirge evidently were subducted and exhumed rapidly, whereas large, thick terranes such as Dabie-Sulu, the Western Gneiss Region of Norway, and Northern Qaidam (see Fig. 2 for their P–T paths and Fig. 3 for locations) were subducted and exhumed more slowly. The former may be created during the early stages of continental subduction when the volume of negatively buoyant, subducted oceanic lithosphere—and thus forces that pull the subducting lithosphere down—prevail; rapid, steep-angle subduction results. The latter may form during the later stages of continent collision when subduction of massive, buoyant continental lithosphere leads to slow, low-angle subduction.

1.3. P–T regimes and types of eclogites

Classical metamorphic facies of high-P–T conditions includes blueschist-, eclogite-, amphibolite- and granulite-facies named

after the typical metamorphic rocks of basaltic composition (Fig. 2). Eclogites formed under lower crust/mantle conditions with $P > 1.2$ GPa (45 km depth) over a T range of >400–1000 °C. Coleman et al. (1965) and Carswell (1990) grouped these eclogites into 3 types based on their tectonic origin: Group A high-T eclogites occur as mantle xenoliths; Group B eclogites are associated with HP granulites within the crustal basement of orogenic belts; and Group C eclogites are important subduction products in active continental margins. Following the same scheme, we divide UHP eclogite-facies rocks into three types: Group-A kimberlitic UHP eclogites (e.g., Roberts Victor Mine, Udachnaya, e.g., Schulze et al., 2013), Group-B UHP eclogites (e.g., Kokchetav, Bohemia, e.g., Liou et al., 2009a) in Alpine orogens, and Group-C lawsonite UHP eclogites (e.g. South Motagua Mélange, Guatemala, e.g., Tsujimori and Ernst, 2014) in Pacific-type orogens.

Fig. 2 shows relevant P–T conditions defining both UHP–HP and UHT–HT eclogites, and UHT–HT granulites based mainly on experimental phase equilibria. In addition, subduction geotherms of about 5 °C/km (extremely cold), 20 °C/km (old, downgoing plates) and 25 °C/km (labeled as cratonic geotherm in Fig. 2b) are illustrated. UHP and HP metamorphic conditions are separated by the Qz–Coe phase boundary; the graphite-diamond boundary further subdivides the UHP regime into diamond (±Coe) and graphite (±Coe) P–T fields (e.g., Day, 2012). Occurrences of the UHP polymorph of rutile (TiO_2^{II}; α-PbO_2 structured TiO_2), supersilicic titanite, and/or K-bearing Cpx, and Arg + Mgs inclusions in garnet from microdiamond-bearing Kokchetav gneisses suggest subduction depths of ~190–280 km (e.g., see the review by Schertl and Sobolev, 2013). The recent interpretation of quartz pseudomorphs after stishovite in pelitic gneiss from western China suggests that some continental materials might have been exhumed from even greater depths (>350 km?) than commonly accepted (Liu et al., 2007, 2009). A comparable depth of subduction of ocean-floor, high Mn–Fe hydrothermally altered rocks reflected by the occurrence of relict diamond, majoritic garnet and possible ringwoodite has been suggested by Glassley et al. (2014) for an occurrence in West Greenland as described below.

1.4. Newly recognized UHP terranes and localities in collisional orogens

New UHP terranes have been documented based on the occurrences of index minerals such as coesite and microdiamond preserved in rigid minerals including Grt, Omp, Ky, Zrn, K-tourmaline (maruyamaite) and Ap (e.g., Chopin, 1984; Smith, 1984; Sobolev and Shatsky, 1990; Liu and Liou, 2011; Ruiz Cruz and Sanz de Galdeano, 2014), and decompression breakdown microstructures and/or exsolution microstructures. Many previously recognized key minerals including those suspected based on experimental mineral stabilities and microstructures in UHP rocks were summarized by Schertl and O'Brien (2013). Except for the Paleoproterozoic UHP terrane of West Greenland (Glassley et al., 2014), all such UHP rocks reside in orogens ranging from Neoproterozoic (640 Ma) in southwestern Brazil (Parkinson et al., 2001) to late Miocene (8–7 Ma) from Papua New Guinea (Baldwin et al., 2004, 2008, 2012). The lack of old UHP terranes may reflect the rarity of preservation of mineral assemblages that are thermodynamically unstable at upper crustal conditions, or due to an evolution of terrestrial P–T conditions toward higher-P/lower-T in younger subduction zones (Ernst, 1972; Maruyama and Liou, 1998; Tsujimori and Ernst, 2014). Petrological and geochemical characteristics of new UHP terranes discovered since 2010, and new findings of classic ones including the Alps and the Western Gneiss Region of Norway (Table 2) are briefly described below:

Table 2
New UHP terranes and localities since 2000 described in this review.

Terrane and locality	Mineralogical evidence	P–T conditions	Age of UHP metamorphism	Special features	References
West Greenland	1. Diamond relics; 2. Exsolution of Opx in Grt (majoritic), Rt in Opx, Cpx; Mag in Ol; 3. Qz needles in fayalite ("Ringwoodite")	P: ~7 GPa, T = ~970 °C	~1800 Ma	1. Fe- and Mn-rich oceanic rocks; 2. Preserved in undeformed rocks	Glassley et al. (2014)
Betic-Rif belt of NW Africa South Spain	1. Diamond inclusions in Grt & Ap; 2. Intergrowth of Dia + Coe, and Coe + Ph (after K-cymrite); 3. Exsolution textures of Grt	P > 4.3 GPa and T > 1100 °C	UHP stage: ~330 Ma, migmatization: ~265 Ma	Protolihs include felsic granulite, Grt peridotite; UHP stage overprinted by UHT and migmatization	Ruiz Cruz and Sanz de Galdeano (2012, 2013, 2014); El Atrassi et al. (2011)
Northern Bohemian Massif	1. Dia inclusions in Grt, Ky and Zrn; 2. Inclusion of Dia pseudomorph and Dia in Grt of Grt peridotite; 3. Px lamellae in Cr-spinel	UHP stage: ~5 GPa and 1100 °C	337 (core)–300 (rim) Ma	3 New UHP localities and Grt peridotite are more than >50 km apart; these together with previous UHP localities suggesting large UHP regions	Massonne et al. (2007a,b); Kotková et al. (2011); Naemura et al. (2011, 2013)
Lago di Cignana unit Italian Western Alps	Microdiamond inclusions in Mn-rich Grt	P: ~3.5 GPa, T = ~600 °C		Microdiamond inclusions in garnetite; Protolith: Oceanic Mn-rich nodules	Frezzotti et al. (2010, 2011); Groppo et al. (2009)
Eastern Alps	Coesite pseudomorph + Ky + Ph (3.5 Si) + Grt + Omp (~5% Eskola component)	P: 3.0–3.7 GPa, T: 710–940 °C	Late Cretaceous	UHP eclogite associated with UHP peridotite in pelites	Vrabec et al. (2012)
West Gneiss Region Northern Norway, Tromsø Nappe Caledonides	Microdiamond inclusions in Grt	P: 3.5 ± 0.5 GPa, T: 770 ± 50 °C			Janák et al. (2013b)
West Gneiss Region Northern Norway, island of Harøya	Coesite-bearing eclogite within migmatitic orthogneiss				Butler et al. (2013)
West Gneiss Region The Seve Nappe Complex northern Jämtland, central Sweden	Kyanite-bearing eclogite dike in garnet peridotite body; P–T estimate lies within the coesite stability field	P: ~3 GPa, T: 800 °C	Late Ordovician 460–445 Ma	New UHP locality in Sweden	Janák et al. (2013a)
West Gneiss Region Straumen	Diamond inclusions in eclogitic zircon	P: 3.75 ± 0.75 GPa, T: 750 ± 150 °C		New diamond locality in WGR	Smith and Godard (2013)
The North Qinling belt Central China	A single in-situ diamond inclusion in zircon of amphibolite	P: ~4.0 ± 0.5 GPa, T: 670–750 °C	490.4 ± 5.8 Ma	Two HP–UHP belts in the Qinling orogen (North Caledonia UHP and South Triassic HP belts)	Wang et al. (2014)

1.4.1. UHP terrane in West Greenland

In an E–W trending Paleoproterozoic (~1.8 Ga) collision belt more than 50 km long and 20 km wide in West Greenland, Glassley et al. (2014) reported relict UHP phases and numerous exsolution microstructures indicative of UHP metamorphism. Prior to this discovery, this orogen had been considered as a classic example of upper amphibolite- to granulite-facies Barrovian-type regional metamorphism (e.g., Davidson, 1979; Glassley and Sørensen, 1980). Mineralogical evidence of UHP metamorphism is well documented in four samples within a well-defined lithologic unit of metamafic and metasedimentary rocks of oceanic affinity. Phases include remnants of Opx exsolved from majoritic Grt, graphitized diamond, exsolution of rutile from garnet and pyroxene, exsolution of magnetite from olivine, and complex exsolution textures in ortho- and clinopyroxenes (including omphacite). Associated with these mineralogical features is an unusual occurrence of quartz needles that appear to have exsolved from fayalitic olivine, suggesting a possible remnant of ringwoodite; this phase has not been recorded previously in any collisional UHP terrane. P–T conditions inferred for the UHP episode are ~7 GPa and ~975 °C; the unusually low T recrystallization in "the forbidden zone" at a depth of about 210 km suggests very rapid subduction of oceanic lithosphere or unexpectedly cool mantle conditions at ~1.8 Ga. These UHP rocks have protoliths characterized by higher Fe and Mn contents that resulted from ocean-floor hydrothermal alteration compared to protoliths of both continental and oceanic affinity from other UHP terranes. They are relatively undeformed within highly deformed country rocks; the UHP assemblages are preserved due to exceptionally low H_2O activity and lack of deformation during exhumation. The existence of this terrane is exciting as it is by far the oldest UHP one worldwide, and contains a possible occurrence of ringwoodite in the Fe–Mn-rich oceanic rocks.

These West Greenland UHP rocks of unusual bulk-rock compositions are volumetrically trivial, relatively undeformed masses that have escaped elevated H_2O activity/infiltration, and have P–T estimates greatly exceeding those of the Paleoproterozoic upper amphibolite- to granulite-facies country rocks (e.g., Glassley et al., 2010). Although the postulated occurrence of reaction products from ringwoodite breakdown is speculative, such ringwoodite remnants may be present in other UHP regions in which Fe-rich assemblages occur.

1.4.2. UHP terrane in the Betic-Rif Cordillera, NW Africa and SE Spain

The Betic-Rif Cordilleras are part of the peri-Mediterranean Alpine orogenic system marking the Africa–Eurasia collision zone (e.g., Platt et al., 2013 and references therein). UHP minerals including coesite and microdiamond have been recently identified as inclusions in Grt and Ky from UHT felsic granulites of the Internal Zone of the Rif belt in NW Africa (Ruiz Cruz and Sanz de Galdeano, 2012, 2013) and SE Spain (Ruiz Cruz and Sanz de Galdeano, 2014). These UHP felsic rocks differ from the Alpine belt inasmuch as they record much higher estimates of P > 4.3 GPa and T > 1100 °C, topotaxial growth of diamond and coesite, lack of palisade quartz around relict coesite, and intergrowths of Coe and Ph possibly after K-cymrite. Ruiz Cruz and Sanz de Galdeano (2013) documented numerous exsolution microstructures and chemical

patterns in garnets from two UHP rocks from the Northern Rif, Ceuta, Spain. Some garnets contain primary inclusions of Ap, Qz, Coe, Rt and retrograded pyroxene, exsolution microstructures of Rt, high Ca- and low Mn contents, and high X_{Mg} [Mg/(Mg+Fe) atomic ratio], characteristic of growth at high P–T conditions below the solidus of felsic granulite. On the other hand, garnets from other samples contain exsolution microstructures of Qz, Coe, Ap and Rt, and inclusions formed from a melt at peak metamorphic conditions; these garnets contain high Mn and low Ca and have low X_{Mg}, characteristic of garnet formed at lower P–T.

Due to extensive low-P Hercynian melting, migmatization and melt migration, whole-rock compositions of UHP rocks could have been significantly modified, hence precise P–T estimates of the early UHP event are problematic. Nevertheless, Ruiz Cruz and Sanz de Galdeano (2013) suggested peak pressure conditions of UHP metamorphism on the order of 6–7 GPa based on observed apatite exsolution microstructures and experimental results on phosphorous solubility in garnet (Konzett and Frost, 2009; Konzett et al., 2012).

Ronda garnet peridotites with graphite pseudomorphs after diamond (El Atrassi et al., 2011) similar to those of the Bohemian Massif associated with UHP–UHT felsic rocks described below also occur at Ceuta. Ruiz Cruz and Sanz de Galdeano (2014) recently reported an integrated study of mineral inclusions in zoned garnets and U–Pb ages of zircons from granulites overlying the Ronda Massif. They found diamond inclusions in both Grt and Ap of UHP–UHT granulites and migmatites, and concluded that both peridotites and host continental rocks were subjected to coeval UHP metamorphism at ~330 Ma and UHT, and migmatization at ~265 Ma. Although HP conditions are considered to have been generated during the Eocene (~42 Ma) Alpine orogenic event (Platt et al., 2013), the UHP domain including garnet peridotites might represent a Hercynian domain similar to the Bohemian Massif and French Massif Central. However, Platt et al. (2006) and Gómez-Pugnaire et al. (2012) reported young garnet Lu–Hf (16–18 Ma) and zircon U–Pb (15–17 Ma) ages from the associated eclogites. Therefore further systematic study of zircon separates from diamond-bearing gneisses in combination with mineral inclusions and U–Pb dating for each zircon domain (e.g., Liu and Liou, 2011; McClelland and Lapen, 2013) is required to solve the regional geotectonic evolution.

1.4.3. New UHP terranes suggested by pseudosection analyses

Pseudosection analyses of P–T paths for HP–UHP rocks have been extensively used to constrain both subduction and exhumation paths for both Pacific- and Alpine-type metamorphic rocks (e.g., Powell and Holland, 2010; Massonne, 2013) over the past two decades. Applying internally consistent datasets and well con-strained bulk compositions, a new UHP terrane has been suggested by Massonne (2013) for Oman.

Massonne (2013) and Massonne et al. (2013) described minor metapelite interlayers in Late Cretaceous eclogite of the lower As Sifah unit, a slice of oceanic crust, located on the NE coast of Oman. The metapelite, originally a pelagic clay poor in SiO_2, contains abun-dant phengite (3.2–3.4 Si pfu) and millimeter-sized garnet (~25 vol%), with minor quartz, rutile, epidote, and sodic amphibole. Pseudomorphs of Pg + Ep and Ab + Mag after original lawsonite and Na-rich clinopyroxene, respectively, are enclosed in garnet. Pseudo-section modeling of the metapelite produces an abundance of diag-nostic mineral assemblages and demonstrates that pelitic rocks were subducted to mantle depths and subjected to UHP metamor-phism at around 2.75 GPa and 440 °C. As the Oman metapelites are too low in SiO_2 to produce coesite, the UHP assemblage of Ph + Na-rich   Cpx + Chl + Cld + Grt + Lws + Ilm + Rt + Hem/Mag,   formed according to Massonne's calculation, whereas only Ph, Grt, and oxide minerals are preserved in the rock today.

1.5. Recently documented diamond-bearing rocks in classical UHP terranes

Other well-documented occurrences of global UHP orogens reveal that microdiamond, coesite, and other UHP phases are more common than previously thought in both Alpine- and Pacific-type belts. Several new localities from five classical UHP terranes (Bohemia, the Alps, the Western Gneiss Region, Dabie-Sulu and Kokchetav) are described below:

1.5.1. UHP minerals in UHT granulites and garnet peridotites of the Northern Bohemian Massif

The Bohemian Massif consists of a Variscan metamorphic core and a collage of several smaller basement complexes differing in age and metamorphic evolution. Both eclogites and Grt peridotites have been extensively investigated but the widespread Bohemian Variscan rocks are best known for their HT–UHT granulite-facies pelitic and granitic protoliths. Coesite pseudomorphs have long been reported in eclogite from the Polish Sudetes (Bakun-Czubarow, 1991); UHP index minerals including coesite, diamond, and nano-sized grains of α-PbO$_2$-type TiO_2 (TiO_2^{II}) are restricted to minor pelitic gneisses of the central Erzgebirge in eastern Germany (Hwang et al., 2000; Nasdala and Massonne, 2000; Massonne, 2001). Microdiamonds and coesite inclusions were documented in Ky, Grt and Zrn grains of felsic and intermediate granulites in three widely separated localities (>50 km apart); they are at least 45 km from the Erzgebirge (e.g., Kotková et al., 2011). These felsic granulites are petrographically indistinguishable from those cover-ing thousands of square kilometers of the Variscan crystalline core, and may have been subjected to significantly higher pressures than can be recovered from the surviving minerals due to later high-T recrystallization and/or exsolution of UHP phases (e.g., Ti and P in garnet). Kotková et al. (2014) subsequently identified kumdykolite, a high-T analog of albite, from their earlier investigated UHP granulites and suggested that this phase and other feldspar modifications can be more common in felsic rocks as they are diffi-cult to be distinguished from plagioclase or K-felspar by optical microscopy or electron microprobe (EPMA).

These UHP rocks are intimately associated with garnet perido-tites throughout the Variscan belt. Minor occurrences of Grt peri-dotites are widespread and their diverse origins have been documented (e.g., Medaris et al., 2005; Naemura et al., 2009). Some Grt peridotites are mantle derived, and formed at 900–1200 °C, 3–5 GPa, whereas others represent lower P, high T (1000–1200 °C, ~2 GPa) subducted to much greater depths in the garnet stability field. For example, in the Moldanubian zone of the Bohe-mian Massif, lenticular Grt peridotite bodies occur within UHT fel-sic granulite/migmatitic gneiss (>1000 °C at P > 1.6 GPa) of the Gföhl Unit. Carswell and O'Brien (1993) showed that felsic- and mafic-granulite of the Gföhl Unit underwent regional UHT meta-morphism under relatively high pressures.

Perraki and Faryad (2014) recently identified inclusions of mic-rodiamond, coesite, Ti-rich phengite, kumdykolite, and moissanite in zircon and garnet from heavy mineral fractions and polished thin sections of kyanite-bearing Gföhl granlites. Most of these bodies are characterized by the presence of lenses and boudins of garnet peridotites, garnet pyoxenites and eclogite for which UHP conditions were obtained applying conventional geothermoba-rometry (e.g., Carswell, 1991; Nakamura et al., 2004; Faryad, 2009). These new mineralogic finding of UHP minerals constrain the UHP metamorphism at P > 4 GPa and T = 680 °C; this unit was subsequently subjected to granulite-facies recrystallization and partial melting at P < 2 GPa and T ~ 850–950 °C. The heat source for the UHT recrystallization of subducted crustal rocks has been suggested to be from the asthenospheric mantle (e.g., Medaris et al., 2003; Naemura et al., 2009). Naemura et al. (2011) first

documented inclusions of graphite pseudomorphs after diamond in garnet separated from the Plešovice garnet peridotite. They further documented topotaxial relations between pyroxene lamellae and host Cr-rich spinel, suggesting that the pyroxene lamellae had an exsolution origin, and in turn postulated a possible ultradeep origin for the garnet peridotite (>200 km).

Subsequently, Naemura et al. (2013) confirmed the presence of graphitized diamond inclusions in chromite, which in turn is surrounded by kelyphytized garnet. The diamonds occur as <2 μm grains in a multiphase solid inclusion consisting mostly of Dol + Ba-rich Phl + F-apatite + graphite. However, Naemura et al. (2013) preferred an earlier mantle origin for the diamond rather than due to Variscan continental subduction for two reasons: (1) the peak pressure of ~3 GPa for the Plešovice garnet peridotite during Variscan high-P metamorphism was in the graphite stability field; and (2) textural evidence indicates that the diamond was included in chromite which is surrounded by later Variscan high-pressure garnet.

1.5.2. Diamond and coesite in UHP rocks from the Alps

Frezzotti et al. (2011) reported the first occurrence of microdiamonds in Fe–Mn-rich garnetites in Mn-rich nodules from the Lago di Cignana meta-ophiolite, Italian Western Alps. Microdiamonds occur within spessartine-rich Grt as tiny euhedral inclusions (<2–30 μm) in syngenetic association with C–O–H fluid inclusions, Qz, and magnesite. Most diamonds are intergrown with, or coated by poorly crystalline graphite. In areas surrounding microdiamonds, spessartine-rich host Grt is strained and shows enrichment in Fe^{3+}. Conversely, Qz grains in contact with strain-free Grt show no evidence for transformation from Coe. The oxygen isotope composition of Qz ($\delta^{18}O$ values, +18.1 to +18.7‰) is not in equilibrium with Grt ($\delta^{18}O$ values, +17.4 to +17.9‰), confirming that the matrix Qz grew or recrystallized after the formation of Grt and diamond. The very heavy $\delta^{18}O$ values of Grt are consistent with an inherited low-T seafloor bulk-rock signature, whereas quartz values indicate an external fluid source, likely from adjacent mica schists during retrograde metamorphism at crustal depths. Subsequently, Frezzotti et al. (2014) identified additional occurrence of microdiamond and disordered diamond in water-rich fluid inclusions in spessartine garnets from these garnetites. Such occurrence provides evidence for carbon transport and precipitation of diamond in an oxidized H_2O-rich C–O–H crustal fluid, consistent with the earlier suggestion for the formation of Kokchetav microdiamonds (e.g., Ogasawara et al., 2000).

Vrabec et al. (2012) reported Late Cretaceous UHP Ky-bearing eclogites + associated UHP Grt peridotites embedded in metapelitic gneisses and mica schists in the Eastern Alps. The eclogites contain Grt + Omp (>5% of Ca-Eskola component) + Ky + Ph (~3.5 Si) and coesite pseudomorphs, and have P–T estimates of 3.0–3.7 GPa and 710–940 °C. Such high temperatures at peak P exceed those of UHP rocks of the Western Alps where mostly oceanic crust was subducted.

1.5.3. Diamond in the Tromsø Nappe, Caledonides of N. Norway

Janák et al. (2013a) reported the first finding of *in-situ* diamonds as inclusions in garnet from gneisses in the Tromsø Nappe. The rock is composed essentially of Grt, Bt, white mica, Qz and Pl, with minor Ky, Zo, Rt, Tur, Amp, Zrn, Ap and carbonates (Mgs, Dol and Cal). The microdiamond, as single grains or as composite diamond + carbonate inclusions, is cuboidal to octahedral and ranges from 5 to 50 μm in diameter; some diamonds are partially transformed to graphite. The calculated peak P–T conditions for diamond-bearing rocks are 3.5 ± 0.5 GPa and 770 ± 50 °C. Other reported occurrences of microdiamond in crustal rocks of the Western Gneiss Region (WGR) include concentrates of separated grains from a Ky + Grt-bearing gneiss at Fjørtoft

(Dobrzhinetskaya et al., 1995), and *in-situ* microdiamond in Grt peridotites at Bardane (van Roermund et al., 2002) and Svartberget (Vrijmoed et al., 2008). The fourth diamond locality in the WGR was reported from a mafic pod at Straumen, where microdiamond occurs as inclusions in zircons from a Ph–Ky–Coe–eclogite sample (Smith and Godard, 2013). This locality lies in the SW part of the WGR, close to the type locality where Coe and polycrystalline Qz after Coe were first described (Smith, 1984). Some diamond inclusions coexist with hematite and others have disordered structures; they all have partially retrogressed to graphite. The diamond-bearing eclogite has a minimum P constraint at 3.5 GPa.

Butler et al. (2013) reported the P–T history of a new Coe-bearing eclogite locality from the island of Harøya in the Nordøyane UHP domain, the most northerly occurrence yet documented in the WGR. The Coe–bearing eclogite occurs in migmatitic orthogneiss, interpreted as Baltica basement, and underwent multiple stages of deformation + partial melting during exhumation. This new UHP domain belongs to a large section of the WGR that has been buried to depths of >100 km during the Scandian subduction. Butler et al. summarized three UHP domains along the Norwegian coast—Nordfjord/Stadlandet, Sørøyane and Nordøyane—separated by Baltica basement gneisses that lack evidence of UHP metamorphism (Hacker et al., 2010). The earliest discovery of coesite in the WGR was made at Selje (Smith, 1984) in the Nordfjord/Stadlandet domain, where coesite is rather common (Wain, 1997; Cuthbert et al., 2000; Wain et al., 2000). Later discoveries of coesite and microdiamond (Dobrzhinetskaya et al., 1995; Terry et al., 2000; van Roermund et al., 2002; Carswell et al., 2003; Root et al., 2005) extended the UHP metamorphic regions over 100 km to the northeast, making the WGR one of the Earth's largest UHP terranes.

A new terrane in the Seve Nappe Complex of the Scandinavian Caledonides is based on P–T estimate of Ky-bearing eclogite occurring as a metadike within a garnet peridotite body in northern Jämtland, central Sweden (Janák et al., 2013b). Although UHP index minerals were not found, calculated UHP conditions of ~3 GPa and 800 °C are within the stability field of Coe based on inferred UHP minerals from microtextures, geothermobarometry and pseudosections modeling. A Late Ordovician (460–445 Ma) age of metamorphism was suggested for subduction of the Baltoscandian continental margin underneath an outboard terrane during the final stages of closure of the Iapetus Ocean. UHP rocks within the allochthonous units of the Scandinavian Caledonides indicate that Ordovician UHP events may have affected much wider parts of the orogen than previously thought, involving deep subduction of the continental crust prior to final Scandian collision between Baltica and Laurentia (Gee et al., 2010).

Partial melting may have played a critical role in exhumation of northern WGR (e.g., Sizova et al., 2012). The partial melting and mass transfer at UHP conditions related to the breakdown of the hydrous mineral phengite led to a significant change in the physical–chemical–rheological properties of deeply subduction crust (Zheng et al., 2011; Hermann et al., 2013). The partial melting attending UHP has been documented in several UHP terranes including the Kokchetav Massif (Ragozin et al., 2009), the Bohemia Massif (Nahodilová et al., 2011; Massonne, 2013), and the Betic-Rif (Ruiz Cruz and Sanz de Galdeano, 2013, 2014), or during decompression passing through the thermal stability limit of phengite documented in the Western Gneiss Region (e.g., Butler et al., 2013) and the Dabie-Sulu terranes (e.g., Liu et al., 2012; Chen et al., 2013b).

1.5.4. The Kokchetav Massif of northern Kazakhstan

The Kokchetav Massif of northern Kazakhstan, the type locality of metamorphic diamond (Sobolev and Shatsky, 1990), is part of one of the largest suture zones in Central Asia, and contains slices

of HP and UHP metamorphic rocks. A comprehensive review of UHP and new minerals in a large variety of lithologies such as calcsilicate rocks, eclogites, gneisses, schists, marbles of various compositions, Grt–Cpx–Qz rocks, and Grt peridotites was recently completed by Schertl and Sobolev (2013). Most diamond-bearing UHP rocks occur in the Kumdy Kol and Barchi Kol areas, whereas the Kulet region lacks diamond but contains coesite (e.g., Zhang et al., 2012). Most microdiamonds are less than 30 µm but some grains reach 200 µm; they show cuboid shapes and rare octahedral form. Microdiamonds contain highly potassic fluid inclusions, as well as solid inclusions of carbonate, silicate and sulfide, which support the idea of diamond formation from a C–O–H bearing fluid (e.g., Sobolev and Shatsky, 1990; Dobrzhinetskaya et al., 2001; Cartigny, 2005; Ogasawara, 2005).

Kokchetav diamonds are characterized by exceptionally light $\delta^{13}C$ values from -21.6 to $-10.4‰$ suggesting that the carbon was derived from recycled crustal materials (Sobolev and Sobolev, 1980; Cartigny et al., 2001). Several recent analyses of $\delta^{13}C$ and $\delta^{15}N$ values of diamonds from different rocks are summarized in Table 4. For example, some microdiamonds from dolomitic marbles possess clear differences in $\delta^{13}C$ between core and rim (Fig. 4A) (Imamura et al., 2012). The rim shows lower isotopic compositions ranging from -26.9 to $-17.2‰$, whereas the core is much higher, with $\delta^{13}C$ ranging from -13.0 to $-9.3‰$. Imamura et al. (2012) suggested a two-stage growth of Kokchetav microdiamonds; the core reflects the isotopic signature of carbonate rocks whereas the rim grew in the presence of infiltrated fluid of light carbon from the adjacent gneisses. Nitrogen isotope data and negative $\delta^{13}C$ values of Kokchetav diamonds indicate a metasedimentary origin (e.g., Schertl and Sobolev, 2013).

A number of unique mineralogical discoveries from Kokchetav UHP rocks have been reported. K-feldspar (+phengite) exsolutions in clinopyroxene (e.g., Katayama et al., 2002; Sakamaki and Ogasawara, 2013) demonstrate that potassium can be incorporated in the Cpx structure at upper mantle pressures. Other significant observations are (1) coesite exsolution and hydroxyls in titanite (Ogasawara et al., 2002; Sakamaki and Ogasawara, 2013), (2) quartz rods and phengite exsolution in Cpx (e.g., Katayama and Maruyama, 2009), (3) corundum, sapphirine and spinel in garnet rims and perovskite inclusions in forsterite from a layered calcsilicate rock (Schertl et al., 2004), (4) the occurrence of akdalaite (5Al$_2$O$_3$·H$_2$O) from a Kulet whiteschist (Hwang et al., 2006), (5) longsdaleite, the 2H hexagonal polytype of carbon, from a Grt–Bt gneiss (Dubinchuk et al., 2010), (6) hogbomite associated with spinel in diamond-free dolomite marble (Schertl and Sobolev, 2013), and (7) a host of high–Mg-bearing phases. Several new minerals

including kokchetavite (Hwang et al., 2004, 2013), a hexagonal polymorph of K-feldspar, and kumdykolite (Hwang et al., 2009), an orthorhombic polymorph of albite, have been reported. A new UHP K-tourmaline that contains diamond inclusions, named maruyamaite (Fig. 4B) has been approved by the IMA (Lussier et al., 2014).

1.5.5. The Dabie-Sulu UHP belt of East-central China

Zhang et al. (2009a) and Liou et al. (2012) provided summaries of extensive research on Dabie–Sulu UHP rocks including nearly continuous 5-km core samples recovered from the Chinese Continental Scientific Drilling (CCSD) project (also, see Ji and Xu, 2009; Zheng et al., 2009). This review describes many petrotectonic characteristics of the vast amount of UHP rocks previously studied. Earlier works defined at least three unusual features: (1) All UHP rocks have preserved three distinct stages of mineral parageneses and geochemical data in zircons (Late Proterozoic protoliths formed at 740–790 Ma, Permo-Triassic subduction at 225–245 Ma, and Late Triassic exhumation at 220–210 Ma). However, geochronological study of the North Sulu UHP belt indicated that some protoliths of coesite-bearing eclogites and their country rocks have Paleoproterozoic ages (Jahn et al., 1996; Xu, 2007) (Fig. 5). Therefore, although some Yangtze cratonal rocks have Paleoproterozoic ages (e.g., Zhang and Zheng, 2013), the North Sulu terrane is interpreted as a segment of the Sino-Korean craton margin that participated in the subduction of the Yangtze craton and underwent UHP metamorphism together with the descending slab (Xu, 2007). (2) Coesite and its pseudomorph are ubiquitous in many lithologies including eclogites in gneisses, quartzites, marbles and garnet peridotites; they occur as trace inclusions even in hydrous phases such as epidote and zoisite. They are most abundant as minute inclusions in these rocks (e.g., Liu and Liou, 2011). However, diamond is very rare, reflecting the oxidized nature of the protolith. (3) Limited fluid–rock interactions took place during the first two stages, hence this terrane preserves the most negative mineral $\delta^{18}O$ values (~ -10 to $-8‰$) among terrestrial metamorphic minerals in the world. Locally primary minerals, textures and structures of eclogitic protolith are preserved in the Yangkou metagabbro; rare intergranular coesite also occurs in this eclogite, one of the only two occurrences in UHP terranes worldwide (Fig. 6). A few North Sulu eclogitic rocks have extremely high ϵNd values (+160 to +170) and very low Nd concentrations (<1 µg/g); these isotopic features led Jahn et al. (1996) to argue for a lack of water activity during the entire processes of subduction and exhumation.

Since the reviews of Zhang et al. (2009a) and Liou et al. (2012), several petrochemical studies including pseudosection analyses
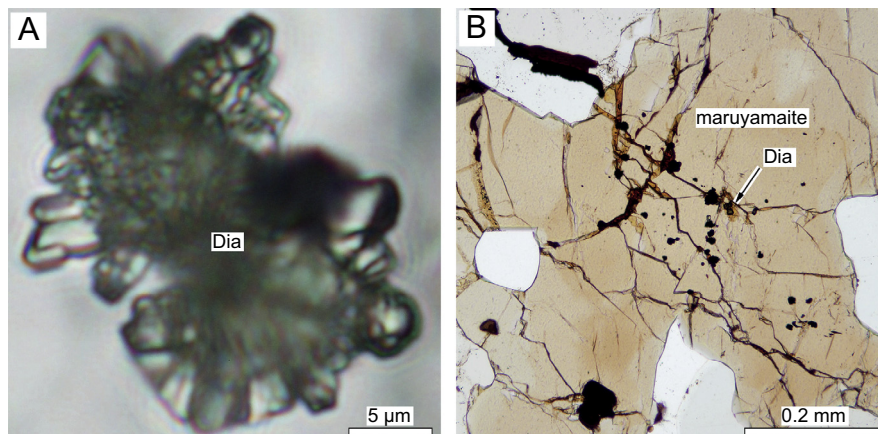
Fig. 4. Photomicrographs of (A) two-stage growth of star-shaped microdiamond inclusion with translucent core and transparent fine-grained polycrystalline rim in garnet of Kokchetav marble (Fig. 4D of Ogasawara, 2005), and (B) UHP K-tourmaine as a new name maruyamite that contains diamond inclusions (Lussier et al., 2014).
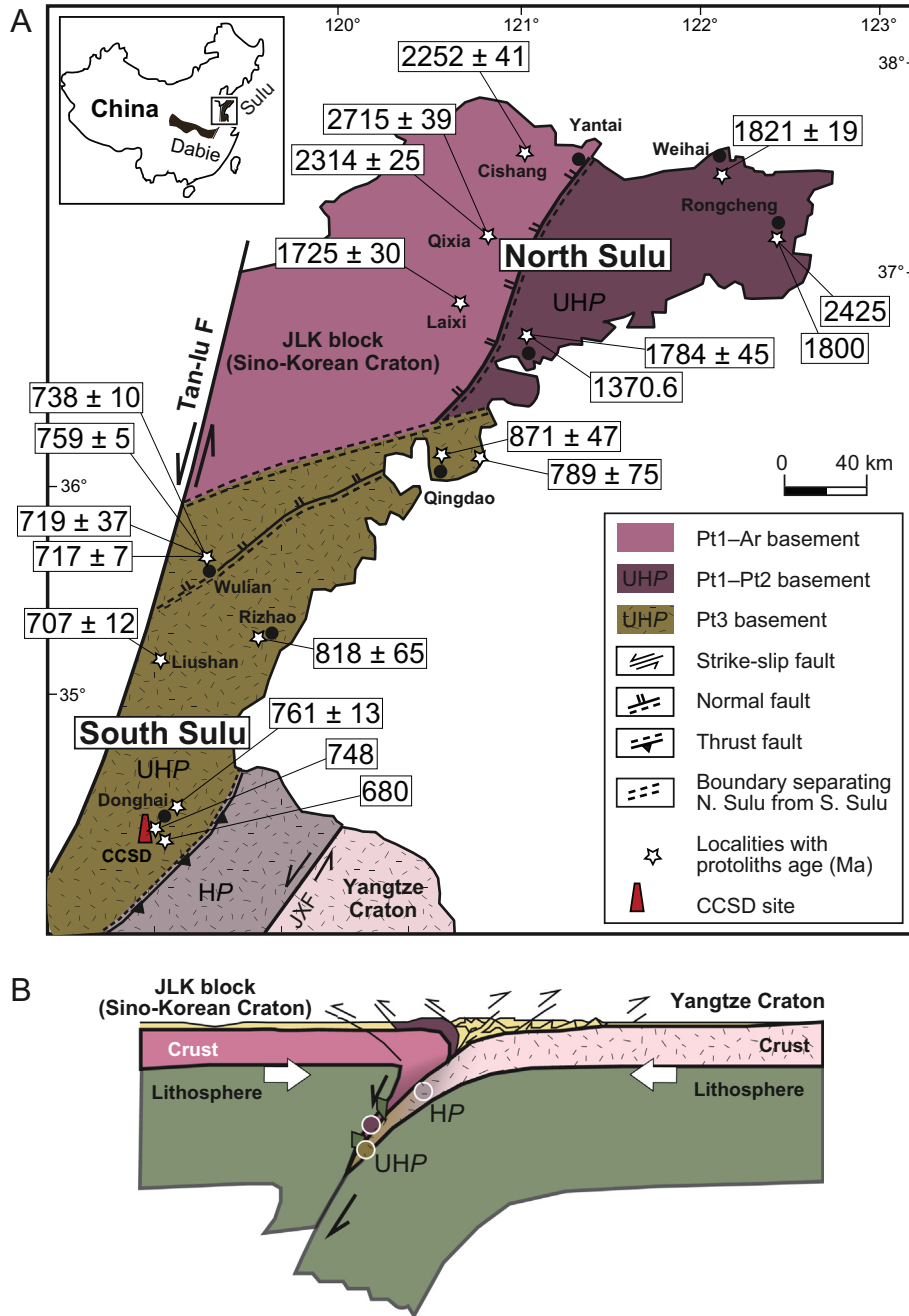
Fig. 5. (A) Simplified tectonic map of 2 Sulu UHP units in northeastern China showing the distinct difference in protolith ages of UHP rocks from the northern unit (Early Proterozoic) and the southern unit (Late Proterozoic). Age data and the subduction model are modified from Fig. 8 of Xu (2007). Those bounding faults for both UHP and HP belts involve both senses of reverse and normal motion. (B) A schematic model showing the concurrent subduction of the overriding Sino-Korean craton to mantle depths with the Triassic subduction of the Yangtze craton for UHP metamorphism. The exhumed North UHP unit contains protoliths of overriding plate, whereas the South Unit represents only exhumed protoliths of the Yangtze craton. The margin of the Sino-Korean craton as overriding plate decended during the Triassic subduction of the Yangtze craton.

have been conducted, providing better documented *P–T* paths of UHP rocks of various compositions (e.g., Chen et al., 2013a; Wei et al., 2013). Most Dabie–Sulu UHP rocks have passed through the lawsonite eclogite facies conditions inasmuch as relict lawsonite and its pseudomorphs were identified as inclusions in Grt and Omp of Mg-rich eclogites (e.g., Guo et al., 2013; Wei et al., 2013). *P–T* estimates from conventional and pseudo-section calculations lie within the *P–T* forbidden zone and yield the peak UHP recrystallization within the diamond stability field (e.g., Liou et al., 2000, 2012). The rarity of diamond is due to the occurrence of oxidized protoliths evidently produced through intense

meteoric water–rock interactions during Neoproterozoic snowball Earth conditions.

1.5.6. The Qinling orogen UHP–HP belts

The Qinling orogen of central China consists of two fault-bounded HP–UHP belts (e.g., Hacker et al., 2004; Yang et al., 2003a, 2005; Wang et al., 2014 and references therein). The Triassic South HP belt is a western extension of the coeval HP–UHP Tongbai–Dabie–Sulu belt, whereas the Paleozoic North belt contains poorly exposed amphibolite and eclogite blocks in gneissic rocks. Hu et al. (1995) first petrographically recognized a

Fig. 6. Photomicrographs of intergranular (matrix) coesite from two UH*P* terranes: (A) Yangkuo eclogite of the Sulu terrane (Zhang and Liou, 1997), and (B) Parigi coesitite of the Dora Maira Massif (Chopin, 1984).

pseudomorph after coesite in eclogitic garnet but did not provide corresponding Raman data to confirm the existence of any relict coesite. Subsequently, microdiamond inclusions in zircon crystals from both eclogite and gneiss were reported by Yang et al. (2003a). Since the 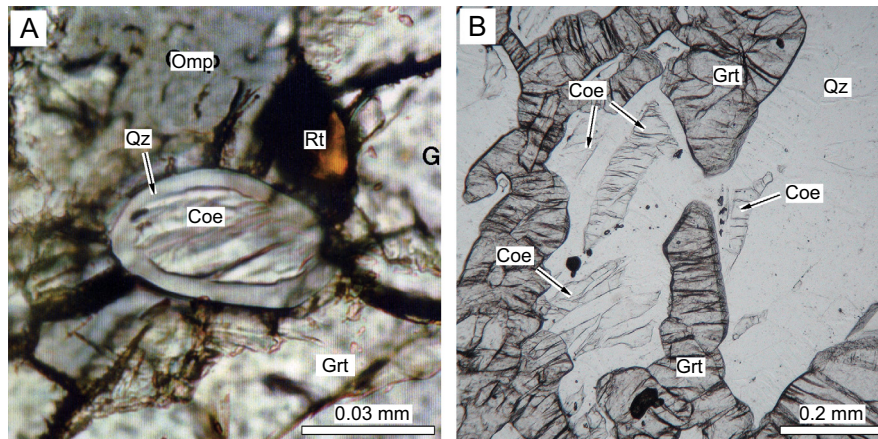report of microdiamond in 2003, extensive search for microdiamond by Chinese investigators failed to confirm its presence (Liou et al., 2009b).

Recently, a single *in-situ* diamond inclusion in a zircon separate from an amphibolite sample in the North Qinling belt was identified by Raman spectroscopy (Wang et al., 2014). The crystal ~15 × 30 μm in size occurs beneath the surface of the host zircon, is bright, grayish-white, and multifaceted; it possesses distinctive characteristics similar to polycrystalline diamond of the UH*P* Erzgebirge described by Dobrzhinetskaya et al. (2013b). The zircon host exhibits typical metamorphic growth zoning + geochemical features and has a weighted mean U–Pb age of 490.4 ± 5.8 Ma for the peak UH*P* metamorphism. However, diamond inclusions in zircons from most other UH*P* terranes such as Kokchetav, Western Alps, and Bohemian Massif mentioned above are micro-sized and more abundant. The report of a single *in-situ* diamond in the North Qinling amphibolite remains to be confirmed. If it is verified, this would further confirm that the North Qinling microcontinent was subducted to mantle depths long before Triassic subduction/accretion of the South China craton that formed the South Qinling–Tongbai–Dabie–Sulu orogen. The near-absence of diamond in these UH*P* rocks may be due to its complete transformation to graphite during retrograde recrystallization and/or to a very low concentration of CO_2 ($XCO_2 < 0.01$) that would preclude diamond crystallization (e.g., Ogasawara et al., 2000; Dobrzhinetskaya et al., 2006a,b).

1.6. Discussion

1.6.1. Contamination of microdiamonds attending sample preparation
The danger of contamination by industrial diamonds (cutting saw, polishing paste, etc.) during sample preparation is serious as exemplified by a recent paper (Dobrzhinetskaya et al., 2014a). For instance, Menneken et al. (2007) reported diamonds as inclusions in 45 detrital zircon grains (~4.2 to ~3.0 Ga) from the Archean Jack Hills conglomerate complex of Western Australia; the conglomerates were deposited at about 3.0 Ga (Spaggiari et al., 2007) and the diamond inclusions were characterized by low $\delta^{13}C$ values ranging from −58 to −5‰ (Nemchin et al., 2008). Such surprising findings of tiny diamonds in the oldest Earth materials challenged the existing interpretation of the Jack Hills zircons derived from granitic rocks that were crystallized at depths of <10 km (e.g., Hopkins

et al., 2010). Dobrzhinetskaya et al. (2014a) showed that many of these diamonds lie below the polished surface and randomly occur in zircon domains of different ages. However, the zircons were polished employing diamond abrasive paste, implying that the reported diamonds could have been introduced by sample preparation. Thus contamination was suspected and intensive search of a very large sample of Jack Hills zircons (>400 grains) failed to confirm the occurrence of diamond (e.g., Hopkins et al., 2008, 2010, 2012); new *P–T* data support earlier interpretation of a shallow crustal origin of the zircons. Dobrzhinetskaya et al. (2014a) reexamined the diamonds in the Menneken et al. (2007) and Nemchin et al. (2008) papers and found that the reported diamonds are not in direct contact with the host zircons. Dobrzhinetskaya et al. (2014a) also reinvestigated the original Jack Hills occurrences, and failed to find indigenous diamonds; FIB–TEM techniques (TEM observations of thin films extracted by focused ion beam (FIB) milling demonstrated that the zircon hosts contain low-*P* phases including Qz, graphite, Ap and other common granitic minerals. Hence, Dobrzhinetskaya et al. (2014a) concluded that the reported diamonds in the Jack Hills zircons were contaminated by diamond polishing paste.

In general, polishing mineral surfaces using industrial diamonds can insert them into cracks and pores of the sample, along with polishing dust (minerals, resins, organic matter, etc.). Because optical microscopes have a resolution of about 1 μm, it is difficult to identify whether industrial diamond grains (<~1 μm) filling small pores of a polished surface lie below the surface or not. SEMs with a conventional (tungsten filament-type) electron gun also imperfectly characterize submicron size particles. Amorphous carbon shows Raman peaks at ~1350 cm^{-1} (the D_1 band; sp^2-bonded carbon) and ~1580 cm^{-1} (the *G* band; sp^2-bonded carbon). Although the *D* peak is broader than the diamond peak (C–C bonding of sp^3-bonded carbon) at 1332 cm^{-1}, it might easily be misidentified as partially graphitized diamond.

Hence, to avoid false positives we recommend using a high-resolution SEM with field-emission type electron gun for surface observations in addition to Raman study. Moreover, as Dobrzhinetskaya et al. (2014a) demonstrated, FIB–TEM techniques are crucial to prove contact relationship between diamond inclusions (especially inclusions smaller than ~5 μm) and host minerals.

1.6.2. Recycling of crustal materials including fluids through UHP minerals
Numerous hydrous and carbonate phases in equilibrium with UH*P* metamorphic assemblages have been described (Liou et al., 1998; Zhang et al., 2010). These phases include but are not limited to OH-rich topaz (Zhang et al., 2002), kokchetavite (Hwang et al.,

2004), K-cymrite (Zhang et al., 2009b), phengitic mica, Ep, nyböite (Hirajima et al., 1992), Gln, Tlc, Phl, Ti-clinohumite, Lws (e.g., Tsujimori and Ernst, 2014), maruyamaite (Shimizu and Ogasawara, 2005, 2013), guyanaite (Schulze et al., 2014), and apatite (Ruiz Cruz and Sanz de Galdeano, 2014). Such occurrences together with hydroxyl-bearing anhydrous phases (e.g., Cpx, Katayama et al., 2002; Katayama and Nakashima, 2003; Sakamaki and Ogasawara, 2013) suggest that many rocks including gneisses, pelites, marbles, eclogites, and garnet peridotites retained minor fluids during UHP metamorphism. These phases transport substantial amounts of H_2O ± other fluids and transform into other dense hydrous magnesian silicates at greater mantle depths. The subduction channel provides direct transport of fluid into the deeper Earth (e.g., Zheng, 2012a,b); hence the mantle transition zone could be hydrous and store abundant H_2O (e.g., Pearson et al., 2014).

An especially important hydrous mineral is lawsonite that is common in most HP and some UHP terranes (cf. Tsujimori et al., 2006; Tsujimori and Ernst, 2014). Vitale Brovarone et al. (2014) recently discovered the widespread occurrence of HP hybrid rocks including metasomatic lawsonitite and Chl–Tlc–Amp-rich (±carbonate) rocks that formed by chemical and mechanical mixing of mafic, ultramafic and sedimentary protoliths in the HP terrane of Alpine Corsica. Lawsonitites, consisting of more than 70 vol% lawsonite, have compositions close to the system $CaO–Al_2O_3–SiO_2–H_2O$ (CASH) and have higher trace element, Cr and Ti contents than most mafic blueschists and eclogites. Thermodynamic calculations by Vitale Brovarone and Beyssac (2014) show that lawsonitite is stable at much higher pressures than the experimental P-limit for lawsonite-bearing HP–UHP rocks of MORB composition (e.g., Okamoto and Maruyama, 1999). Metasomatic lawsonitite contains the highest H_2O content (>7.5 wt%) compared to all major subducted rock-types, including metasedimentary, mafic and ultramafic rocks at UHP conditions (e.g., 4 GPa and 550–800 °C). Chlorite-rich hybrid rocks also display very high water contents, but may have a much shallower stability field compared to lawsonitites. The presence of such hybrid rocks in Alpine-type terranes and numerical calculation led Vitale Brovarone and Beyssac (2014) to conclude that these lithologies may transfer volatiles to great depths along the subduction channel, with implications for cycling of water and crustal minerals to the mantle. Furthermore, metasomatic hydrous phases associated with ultramafics are common in UHP rocks; in addition to antigorite, chlorite, Ti-clinohumite, phlogopite, and magnesite, other trace but unusual phases including a recently documented guyanaite (β-CrOOH) have been documented (e.g., Zhang et al., 2009a,b; Schulze et al., 2014). These may well be important in transporting water to great mantle depths where hydrous ringwoodite (Pearson et al., 2014) is stable.

Experimental data on trace element partition coefficients for lawsonite show a preference for LREE/HREE and Be; consequently the observed decrease of B/Be ratio in Phanerozoic arc magmas with increasing distance away from the trench can be explained by progressive lawsonite breakdown (Martin et al., 2011, 2014). After decomposition, the remaining trace elements inherited from the precursor lawsonite in some UHP phases may return to the Earth's surface via a deep-seated mantle plume, or may be accidentally trapped as peculiar UHP phases such as LREE-rich CaTiSi perovskites inclusions within Group-2 Brazilian diamonds (Bulanova et al., 2010) and/or chromitites in the mantle transition zone.

1.6.3. UHP phases in deeply subducted continental rocks

Large continental masses have been subducted to mantle depths >90–100 km and subjected to UHP metamorphism; some were subsequently exhumed to crustal depths and underwent mid- to upper crustal HT–UHT granulite- to amphibolite facies recrystallization. Due to the K-feldspar-rich nature of granite,

future study may reveal preserved UHP minerals so far undiscovered and known only from laboratory experiments or extraterrestrial materials (e.g., K-wadeite: Harlow and Davies, 2004; K-hollandite (libermannite: Ma et al., 2014): Yagi et al. 1994); this would allow further insights into the ultimate fate of deeply subducted granitic continental crust (e.g., Yamamoto et al., 2009a).

Most UHP rocks contain minor accessory minerals including apatite, zircon, rutile, and titanite. These phases, as illustrated above, preserve coesite and microdiamond inclusions, exhibit UHP polymorphs (e.g., TiO_2^{II}) or have exsolved coesite lamellae (e.g., titanite with coesite lamellae). Through the combination of careful petrographic examination for reaction textures, calculated simple petrogenetic grids and the application of geothermometry involving these small grains of Ti- and Zr-bearing accessory minerals becomes an indispensible tool when reconstructing subduction and exhumation history of continental rocks (for details, see Tropper, 2014; Proyer et al., 2014).

1.6.4. Temporal distribution of HP–UHP metamorphic rocks

UHP metamorphic rocks document the subduction of continental crust along a cold geothermal gradient to depths of at least 90–100 km, and in many cases, considerably deeper. The geological record of blueschist-facies and UHP metamorphism appear to reflect a secular change in thermal regimes of subduction zones since the late Neoproterozoic (e.g., Ernst, 1972; Maruyama et al., 1996; Maruyama and Liou, 1998). In fact, except for the Paleoproterozoic UHP rocks in West Greenland (Glassley et al., 2014), all UHP rocks date from late Neoproterozoic to Pliocene and are coeval with blueschists and glaucophane-bearing eclogites (Tsujimori and Ernst, 2014) (Fig. 7). However, the secular trend of 31 UHP metamorphic terranes shows three apparent hiatuses, during the Ediacaran (latest Neoproterozoic), Permian, and Jurassic-to-Early Cretaceous. The Permian UHP hiatus overlaps the global lawsonite hiatus, which is a robust indication of relatively warm subduction-zone thermal regimes (Tsujimori and Ernst, 2014). Moreover, the Jurassic-to-Early Cretaceous stasis is well known as the Tethyan duration of high ophiolite production (Dilek, 2003). Although the recognition of UHP terranes in continent–continent and arc–continent collision zones is highly dependent on the preservation of UHP index minerals from post-collisional Barrovian type metamorphism and/or regional migmatization, the absence of recognized UHP metamorphic rocks in the early Earth may be related to plate tectonics and global heat production. Presumably sea-floor spreading is a continuous event, therefore, so is subduction. However, return of subducted slabs need not be continuous, and is more likely episodic—accounting for some of the apparent periods of reduced or no plate underflow.

1.6.5. Formation and exhumation of HP–UHP terranes

Numerical modeling of continental subduction/collision and exhumation is less abundant than that of Pacific-type plate underflow, but new studies are becoming more numerous (e.g., Warren et al., 2008a,b; Burov and Yamato, 2008; Gerya et al., 2008; Gerya, 2011; Butler et al., 2011; Li et al., 2011). High-quality data from natural UHP occurrences provide tight boundary conditions for modeling simulation. For instance, Gerya et al. (2008) proposed a "hot channel" model in which deeply subducted continental crust achieves temperatures of 700–900 °C by intense viscous shear + radiogenic heating; consequently, the high-T causes buoyancy-driven upward extrusion of the UHP slab due to melting. Warren et al. (2008a,b) addressed importance of "plunger-expulsion" as an exhumation mechanism, following the early-stage buoyancy-derived exhumation; strong crust of the overlying plate acts as a plunger that expels weaker UHP materials. In some cases, of course, a segment of the overlying lithospheric plate fails maintain its stress guide behavior, and instead decouples and descends
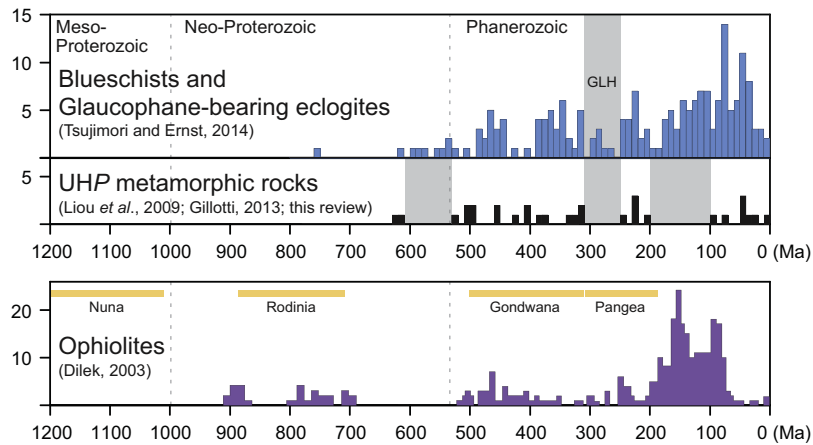
Fig. 7. Age-histogram for distributions of UHP terranes, ophiolites and lawsonite-eclogites (modified from Fig. 3 of Tsujimori and Ernst, 2014). GLH: Global lawsonite hiatus; age distribution of ophiolites are based on Dilek (2003).

with the subducting lithosphere (e.g., Western Alps, Eastern Green-land) as described by Hacker et al. (2013). The elegant results of numerical modeling of continental subduction/collision help us to understand petrological, structural, and geochronological data from natural UHP rocks.

Hacker et al. (2013) has also drawn attention to the contribution of protoliths of UHP rocks through erosion of the overriding plate and insertion into subduction channels, hence not all UHP terranes need be derived from the subducting slab. In fact, the UHP terrane of NE Greenland (Gilotti and McClelland, 2011; Gilotti et al, 2014) is an example of subduction and UHP metamorphism of the overriding plate. The Laurentian continent, far from the suture with Baltica, the upper plate of the Caledonides, experienced UHP metamorphism late in the collision. The large Sulu terrane of NE China shown in Fig. 5 is another example; it consists of the North Sulu UHP Unit with protoliths of the hanging wall Sino-Korean margin with Early Prote-rozoic ages of ~1400 to ~2400 Ma, descending with the underlying South Sulu UHP Unit with Middle Neoproterozoic Yangtze protoliths of ~650 to ~880 Ma (cf Xu, 2007). Moreover, supracrustal rocks of the North Sulu terrane are characterized by what appear to be typi-cal "Sino-Korean craton style" sediments; specifically, these rocks are well correlated with coeval sequences from the Liaodong Penin-sula, as both lack O₃-D (Upper Ordovician to Devonian) sediments (Xu Zhi-Qin, personal communication, August, 2014). In any case, the speculative model of Fig. 5 requires further detailed geochrono-logic investigations of Sulu UHP rocks and Yangtze cratonic rocks to better constrain the ages and affinity of the protoliths for the North Sulu UHP Unit (e.g., Zhang and Zheng, 2013).

2. UHP and crustal minerals in chromitites and harzburgites associated with ophiolitic complexes

2.1. Introduction for ophiolites and chromitites

As shown in Fig. 1, ophiolites occur along sutures between con-tinental terranes and represent ancient oceanic crust formed in a variety of spreading environments, including oceanic ridge, back-arc basin, and supra-subduction zone (SSZ), and subsequently were emplaced onto continental margins (e.g., Coleman, 1977; Dilek and Newcomb, 2003; Metcalf and Shervais, 2008; Dilek and Furnes, 2011, 2014). They show significant variations in their internal structures, geochemical fingerprints, and emplacement mecha-nisms depending on their proximity to their formation at a ridge, back-arc basin, or trench. Depending on rate of influx of ascending asthenosphere, spreading rate of the oceanic lithosphere, and mechanism of emplacement, ophiolites may consist of plutonic

and/or extrusive sequences resulting from multiple magmatic pulses; most are later dismembered.

Dilek and Furnes (2014) grouped the mechanism of ophiolite formation into subduction-unrelated (e.g., spreading ridges) and subduction-related (e.g., SSZ and volcanic arc types) ophiolites. Despite the different settings for their formation, the general mechanism by which a complete ophiolite succession forms is rea-sonably well understood and agreed upon. In extensional environ-ments, heat flow is high due to rising asthenospheric mantle. As pressure decreases in the ascending asthenosphere beneath mid-ocean ridges (MOR) or back-arc basins, undepleted lherzolites par-tially melt to form basaltic magma. The melts collect in a chamber (or chambers) at depths about 4–6 km, and undergo fractional crystallization. Some magma rises as dikes, forming a sheeted-dike complex, and/or is extruded as pillow lavas in the axial rift on the sea floor. The remaining magma within the chamber continues dif-ferentiating upon cooling to form the layered and massive rocks of the plutonic sequence. Fractional crystallization gives rise locally to diorite and plagiogranite. Petrologic and chemical data indicate that the lavas, dikes, gabbros, and underlying depleted harzburgite are all cogenetic; harzburgite represents a crystalline residue from partial melting in the mantle that produced the overlying igneous rocks. Many mantle peridotites, however, contain high SiO_2 and high ratios of LREE/HREE that are inconsistent with an origin as the residuum of partial melting of primitive mantle. These occur-rences instead may represent the metasomatic products of mantle lithosphere and ascending melt (Kelemen et al., 1992).

Ophiolite formation ages may be obtained by direct U–Pb dating of zircon from comagmatic diorite or plagiogranite of the plutonic sequence. They are also constrained by the ages of radiolarian fossils in overlying pelagic chert. Ophiolites are rather abundant in Phan-erozoic orogenic belts and their peak times of genesis and emplace-ment in Earth history coincide with collisional events (see Fig. 7 and the recent compilation of age distribution in Fig. 4 of Dilek and Furnes, 2011, 2014). Inasmuch as MOR-generated oceanic litho-sphere has been extensively subducted, such ophiolites are rela-tively rare compared to other ophiolite types. Age gaps between the deposition of pelagic sediments and ophiolite emplacement in continental margins and/or island arcs are commonly less than 25 Myr (Coleman, 1977; Dilek and Furnes, 2011). Such a short dura-tion is consistent with the life span of a back-arc basin (less than 20 Myr) and indicates that obduction of many ophiolites occurred soon after their creation. Such ophiolites consequently represent young oceanic lithosphere that was detached while still hot.

In short, ophiolites provide the best opportunity for geologists to walk across the ocean floor on land; they also offer vertical

sections in addition to horizontal distributions. Moreover, ophiolite formations record the ages of oceanic fragments that escaped disappearance into subduction zones. In a conventional view, all components including podiform chromite mentioned below are formed in low-*P* extensional tectonic settings with high heat flow; they represent a cross-section of newly formed oceanic crust/upper mantle. However, recent petrological and geochemical studies of ophiolites and the spatially associated chromitites containing UH*P* minerals to be described below provide new challenges for the conventional hypothesis; some harzburgites and their chromitites lying directly beneath ophiolites have experienced multi-stage deformation and crystallization–recrystallization including H*P*–UH*P* metamorphism (e.g., Zhou et al., 1996; Arai, 2013; González-Jiménez et al., 2014; Huang et al., 2014).

2.2. Ophiolitic podiform chromitites

A typical ophiolitic sequence consists of podiform chromite deposits associated mainly with dunite rather than with harzburgite or pyroxenites. Numerous schemes for classifying chromitites have been proposed (e.g., for recent reviews, see Arai, 2013; González-Jiménez et al., 2014). In an early study, Coleman (1977) described two types of chromite deposits: The first type exhibits a nonsystematic distribution of the podiform deposits within metamorphic peridotites with no relationship between the size of the deposit and its enclosing dunite. The second type is closely associated with layered gabbro and peridotite; the chromite bodies are randomly distributed within metamorphic peridotites.

Arai (2010, 2013) classified high-*P* (concordant) recycled chromitites and low-*P* (discordant) podiform chromitites based on structural criteria and the presence of inclusions of H*P*–UH*P* minerals. Those conventionally recognized chromitites by Coleman (1977) are low-*P* chromites; they contain low-*P* phases including Na-rich pargasite, Na-rich phlogopite and pyroxenes (e.g., Borisova et al., 2012). The occurrence of such low-*P* hydrous phase inclusions suggests the shallow mantle origins for the host chromitites. Nodular chromitites with minute primary inclusions of hydrous minerals and pyroxenes have been considered to be low-*P* igneous features (Cassard et al., 1981). On the other hand, Arai (2010) interpreted Luobusa nodular chromitites as a distinct H*P* type recrystallized at mantle conditions where hydrous minerals were unstable. High-*P* chromitites from several Tibetan ophiolites as well as from the Ray-Iz massif, the Polar Urals (e.g., Robinson et al., 2004; Yang et al., 2007, 2014b; Yamamoto et al., 2009b; Xu et al., 2009; Huang et al., 2014) contain UH*P* mineral inclusions. The UH*P* podiform chromitites are similar in petrography and mineral chemistry to "ordinary" podiform chromitites, and mainly comprise chromite and olivine. Arai (2013) proposed the possibility of a deep recycling origin for these UH*P* chromitites. Low-*P* chromites were initially crystallized and have inclusions of hydrous phases in spinels: these chromites were subducted to mantle depths and recrystallized at H*P*–UH*P* conditions and subsequently were exhumed to a rift setting to be included as parts of an ophiolitic complex. Indeed, such suggestion of transformation of low-*P* to high-*P* chromites was later substantiated by finding of relict hydrous phases in chromite of Tibetan chromitites (e.g., Huang et al., 2014).

2.3. Historical advance in the study of UHP minerals in chromitites associated with ophiolites

2.3.1. Early findings of UHP minerals in mineral separates and sediments from Tibetan ophiolites

Prior to the initial investigation of UH*P* minerals and their host chromitites and harzburgites from Tibetan ophiolites by western scientists including Paul Robinson and his students/postdocs at Dalhousie University in the 1990s (Zhou, 1995; Hu, 1999), most petrological and mineralogical studies of minerals and rocks of Tibetan ophiolites were carried out by Chinese scientists including Bai Wen-Ji, Fang Qing-Song and others from the Institute of Geology, Chinese Academy of Geological Sciences (IGCAGS, 1981). Exciting findings of coarse-grained diamonds in heavy mineral separates and placer sediments in Tibet led to numerous follow-up search for occurrences of diamond and other UH*P* minerals in several ophiolite bodies; the results of Chinese efforts in the early 1980s are best summarized in Bai et al. (1993) and Robinson et al. (2004).

Large, ton-sized samples of Tibetan chromite ores and associated ultramafics were collected from the ore bodies; they were washed, air dried and transported to the Institute of Multipurpose Utilization of Mineral Resources at Zhengzhou, China for mineral separations. Other samples were independently processed in different laboratories. Many precautions were taken both in the field and in the laboratories in order to eliminate possible sources of contamination for diamonds, native elements, and alloys described below. All equipment was dismantled and cleaned before the samples were processed. For example, a 200-kg granitic sample was processed first as a blank to check for contamination; the results yield only Qz, Kfs, Pl, Bt, Zrn and Ap in the residues of granitic samples (Bai et al., 1993). Mineral separations were carried out using a combination of vibration, magnetic, flotation by heavy liquids, and electrical conductivity techniques. Diamond and other UH*P* minerals were handpicked from heavy-mineral separates, examined by binocular microscope prior to further laboratory determination including XRD and laser Raman spectroscopy. Identical procedures for collections and mineral separations were independently carried out at different laboratories in order to ensure the nature of these unusual minerals and their *in-situ* natures. Most of the UH*P* minerals recovered from the chromitites are black, dark gray or brightly colored; had contamination taken place, they would have been easily recognized in granite residues through identical mineral separation procedures.

A number of unusual minerals, including diamond, moissanite, graphite, native chromium, Ni–Fe alloy and Cr^{2+}-bearing chromite were found in mineral separates during the study of two major Tibetan ophiolite belt suture zones bordering the Lhasa block: the Yarlung–Zangbo suture on the south between the Indian continent and the Lhasa block and the Bangong–Nujiang suture on the north between the Lhasa block and the South Qingtang block. Such findings were mainly described in local journals in Chinese (e.g., IGCAGS, 1981; Fang and Bai, 1986; Yan et al., 1986). Regional tectonic settings of the Yarlung–Zangbo suture in Tibet and its adjacent region together with location and lithologic units of the Luobusa and other ophiolite bodies are shown in Fig. 8.

Several coarse diamond grains were first recognized in heavy mineral separates of ophiolitic chromitites from Donqiao, about 300 km north of Lhasa by Bai Wen-Ji (IGCAGS, 1981). Following the confirmation of diamonds in chromitite residues of the Dongiao ophiolite, placer diamonds were discovered in stream sediments and alluvial fans on the south side of the Donqiao massif. Later, geologists of the Tibetan Geological Bureau independently found diamonds in podiform chromitites of the Luobusa ophiolite along the Yarlung–Zangbo suture, about 200 km southeast of Lhasa. More than 100 diamond grains were recovered from chromitites and harzburgites of these two massifs. Of these, 20 are from Luobusa, 6 from mafic and ultramafic minerals suggesting that they were derived from the ophiolites. Later study of chromitites and harzburgites of these two ophiolite bodies confirmed the presence of moissanite, graphite, native Cr, Ni–Fe alloys and other minerals.

A few examples of ophiolite-type diamond separates are shown in Fig. 9A (after Fig. 2 of Yang et al., 2014a). Most diamond grains
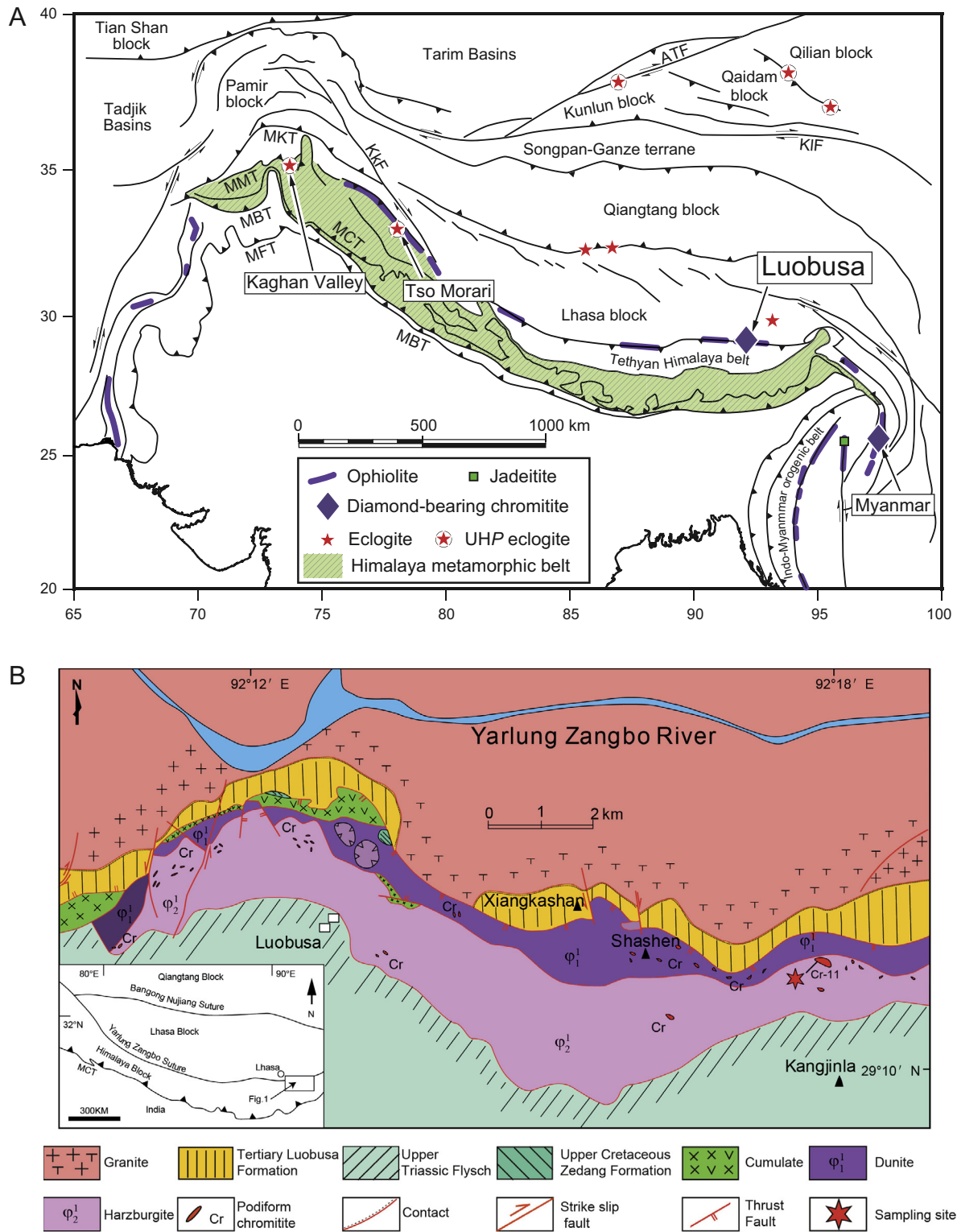
Fig. 8. Maps showing the tectonic setting and geological map of the Luobusa ophiolite: (A) Schematic map showing (a) major tectonic units, (b) localities of eclogites and ophiolite, and diamond-bearing chromitite associated with ophiolite, and (c) the 2000 km long Yarlung–Zangbo suture and the Himalaya metamorphic belt between the Indian–Eurasian continents (modified after Liou et al., 2004); (B) location and distribution of geologic and lithologic units of the Luobusa ophiolitie (after Xu et al., 2009).

are 0.1–0.2 mm in diameter; some exceed 0.5 mm. The largest one is 0.7 × 0.6 × 0.6 mm. Similar to those diamond grains from the Ray-lz chromitite of the Polar Urals, Russia shown in Fig. 9A, Luobusa diamonds are colorless and transparent; many are euhedral forms with octahedral, dodecahedral, or cubo-octahedral forms. Some exhibit evidence of plastic deformation. They contain numerous dark micro-inclusions (Yan et al., 1986).

Many grains of Os–Ir and octahedral silicates are either enclosed in or attached to, chromite grains, leaving no question as to their natural origin (Bai et al., 2000). Thus, the Chinese scientists were confident that the reported UHP minerals are naturally occurring grains in the Tibetan chromitites. Other early findings in Tibetan chromitites include but were not limited to a new octahedral pseudomorph of lizardite included in and attached to chromite grains
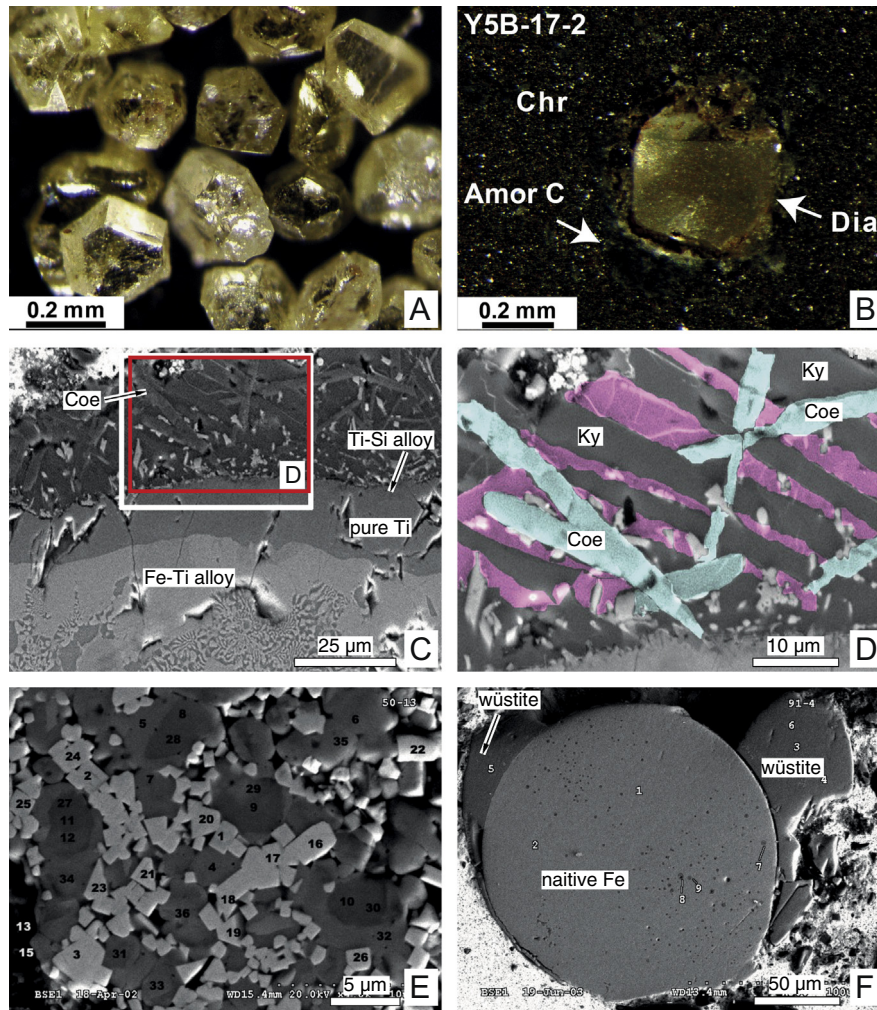
Fig. 9. Representative photos of diamond and other UHP minerals from ophiolite complex: (A) Coarse-grained diamond separates from chromititie of the Ray-Iz ophiolite (Yang et al., 2014b); (B) *in-situ* diamond occurring as an inclusion in chromite of the Ray-Iz ophiolite (Yang et al., 2014b); (C) backscattered electron images of Fe–Ti alloy rimmed by coesite and kyanite from chromitite of the Luobusa ophiolite; the alloy exhibits 3 distinct 3 zones from the inner nearly pure Ti rimmed by darker Ti–Si alloys and the outer silicate materials enlarged in (D) (Yang et al., 2007); (D) detailed morphology of prismatic crystals of coesite (gray color) intergrown with unknown amorphous material in pink, and crosscutting Ky crystals in blue (Yang et al., 2007); (E) backscattered electron image for qusongite (1–3, and 16–26) intergrown with W–Ti alloys (4–7), (Ti,W) C (32–35, 8–12 and 27–31), chlorite (13), and calcite (15) (Fang et al., 2009); (F) backscattered electron image of a well-rounded native Fe (1, 2) and wüstite (3–9) (Yang et al., 2008).

(Yang et al., 1981). These octahedral forms of lizardite have been subsequently considered to be hydrated "ringwoodite" with olivine composition as described below (Robinson et al., 2004).

Abundant PGE and base-metal alloys are enclosed in chromite grains from Luobusa (Bai et al., 2000). They are anhedral to subhedral, equidimensional grains up to 0.5 mm in diameter and span a wide range of compositions; most contain less than 10% Ru and are classified as osmium and iridium. Many are compositionally zoned, typically with cores of osmium and rims of iridium. The Os–Ir ratios in these alloys range from approximately 2:1 to 1:1. A few Os–Ir alloys contain small spherical silicate inclusions about 5–50 μm across, and have sharp boundaries. Energy-dispersive analyses indicate that they are Ca–A1–Fe–Mg silicates tentatively identified as silicon spinel. The Pt–Fe alloys occur as single subrounded to tabular grains 0.1–0.4 mm in diameter or as intergrowths with Os–Ir–Ru alloys. They consist chiefly of Pt and Fe with up to 10% Rh and small amounts of Ni, Co, and Cu. Only one grain has a composition close to isoferroplatinum (Pt_3Fe). Small inclusions of Os–Ir–Ru alloy are present in some Pt–Fe grains. The Ir–Ni–Fe alloys occur as single grains or as coliform intergrowths with Os–Ir–Ru alloys. These alloys have relatively

constant Fe (15–25 at.%) but vary widely in Ir and Ni contents. Some grains also contain small amounts of Ru, Os and Cu.

2.3.2. Study of UHP minerals from Luobusa chromitite separates by Robinson et al. (2004)

In the early 1990s, Paul Robinson led his former students and postdoctoral fellows (e.g., Zhou MF, Yang JS, Hu XF) together with Chinese (Bai WJ, Fang QS) and other colleagues to collect more samples from the Luobusa chromitites, applying similar approaches for mineral separations. They handpicked UHP and other minerals from residues and identified minerals by XRD, laser Raman, IR, and other crystallographic techniques. Selected grains were mounted in epoxy, polished, and then analyzed using EPMA and SEM–EDAX. U–Pb ages of some zircon separates were dated by ion microprobe. They recovered an additional 25 diamond grains of similar morphologies and grain sizes as those previously reported (Robinson et al., 2004). Several other phases including native elements, carbides, PGE and base-metal alloys, sulfides, silicates and oxides were found in the new chromitite samples. The compositional and morphological characteristics of these phases are described below.

2.3.3. Findings of Luobusa in-situ UHP minerals by Yang et al. (2007 to present)

Recent study and discovery of numerous UHP unusual phases in Luobusa and several other ophiolitic bodies in Tibet and elsewhere are credited to Yang Jingsui and his co-workers. They used modern analytical tools to examine polished sections of mineral separates and several newly collected large samples, positively identifying numerous UHP minerals ranging from nano- to micro-scales as *in-situ* occurrences, exsolutions and other textures as described below. The initial publication (Yang et al., 2007) exemplified their first conclusive findings of diamond as an inclusion in Os–Ir alloy and coesite as part of a silicate assemblage rimming a grain of Fe–Ti alloy extracted from the Luobusa chromitites. Subsequent studies by Yang associates and collaborators yielded many other unusual minerals (Dobrzhinetskaya et al., 2009, 2014b); at least eight new minerals were first documented from Luobusa. Furthermore, many new localities of similar UHP mineral occurrences have since been discovered (Xu et al., 2009, 2014; Yang et al., 2013, 2014a,b).

Yang et al. (2007) described a chromitite fragment that comprises three zones: (1) a core of Fe–Ti alloy about 500 μm across, mantled by (2) an inner zone 1090 μm thick of native Ti, which in turn is partially mantled by (3) an outer zone of aluminosilicate minerals 30–60 μm thick. A very narrow zone (<1 μm) of Si–Al alloy ($Si_{78}Al_{20}Ti_2$) borders the native Ti adjacent to the aluminosilicate zone, which consists of ~45 model% coesite, ~15% kyanite and ~40% of other phases, largely amorphous aluminosilicate with significant Ti, Mg and alkalis. Minor phases include native Fe, TiO_2^{II}, boron carbide of unknown stoichiometry, amorphous carbon, osbornite (TiN), and qingsongite (see next section for details) as well as Ti–Si–O and Ti–Al–Si–O grains that are too tiny to be identified. Coesite forms prisms several tens of μm long, but is polycrystalline, and is interpreted to be pseudomorphic after stishovite, similar to synthetic stishovite crystallized at $T = 900\,°C$ and $P = 10\,GPa$ (Dobrzhinetskaya and Green, 2007). Because these pioneering findings are so important, a few photos of this paper are reproduced in Fig. 9. Based on these findings, Yang et al. (2007) proposed that the UHP minerals likely were incorporated into the chromitites in the deep mantle.

2.3.4. Finding of coesite lamellae in chromite by Yamamoto et al. (2009b)

S. Maruyama, JS Yang, and associates conducted field investigations of the Luobusa ophiolite complex and its overlying flysch unit (H. Yamamoto et al., 2007a); they also collected large chromitite samples and conducted nearly identical mineral separation processes in China as described above. They documented structures and compositions of nano-size exsolution lamellae of both diopside and coesite in chromite employing TEM data (Yamamoto et al., 2009b). These authors also described different modes of chromite occurrence; some are of ultra-deep origin whereas others are of low-P magmatic origin at the mid-oceanic ridge.

2.3.5. Finding of nano-size nitrites and other UHP minerals by Dobrzhinetskaya et al. (2009 to present)

Employing several state-of-the-art analytical tools, Dobrzhinetskaya et al. (2009, 2014b) discovered numerous unusual oxides, nitrites and coesite–kyanite + other silicate phases. These include osbornite (TiN), qinsongite (c-BN), the high-pressure TiO_2^{II} phase, and native Fe occurring as submicroscopic inclusions (50–200 μm) together with Ky + Coe pseudomorphs after stishovite (Yang et al. (2007) (Fig. 9C and D). The characteristic features of these and other new phases will be detailed in the next section.

2.3.6. Findings of similar UHP minerals in other Chinese ophiolites and elsewhere (Yang et al., 2012 to present)

Using the same approach and analytical tools, Yang and colleagues described similar findings of UHP minerals in other Tibetan ophiolites in the Yarlung–Zangbo suture zone, including Zedang, Xigaze, Dangqiong, Purang and Dongbo (Yang et al., 2014a,b; Xu et al., 2009, 2014) and in ophiolites from Sartohai, NW China, Ray-Iz from the Polar Urals, Russia and the Myitkyina region of Myanmar (see Fig. 1 of Yang et al., 2014b).

The Paleozoic Ray-Iz ophiolite consists mainly of lherzolite–harzburgite and minor dunite and is regarded as formed in a mantle wedge above a subduction zone. Yang et al. (2014b) report more than 1000 diamond grain in mineral separates from ~1500 kg of chromitite collected from two ore bodies. These small (ca. 0.2–0.5 mm) diamonds are colorless, transparent and euhedral, with well-developed crystal forms (see Fig. 9A and B); some are polycrystalline aggregates. Many diamond grains also contain micro-inclusions of $Ni_{70}Mn_{20}Co_5$ alloy and Mn-rich silicates. In addition, more than 60 other mineral species were identified, grouped as: (1) native elements: Cr, W, Ni, Co, Si, Al and Ta; (2) carbides: SiC and WC; (3) alloys: Cr–Fe, Si–Al–Fe, Ni–Cu, Ag–Au, Ag–Sn, Fe–Si, Fe–P, and Ag–Zn–Sn; (4) oxides: wüstite, periclase, eskolaite, TiO_2^{II}, baddeleyite, Ilm, Crn, chromite, NiO and SnO_2; (5) silicates: kyanite, pseudomorphs of octahedral olivine, zircon, garnet, feldspar, and quartz; (6) Fe, Ni, Cu, Mo, Pb, Ab, As–Fe, Fe–Ni, Cu–Zn, and Co–Fe–Ni sulfides; and (7) native Fe, FeO, and Fe_2O_3.

Diamonds from Tibetan and other ophiolites show similarities in morphology, carbon isotopes and mineral inclusions, but all are distinctly different from diamonds occurring in kimberlites and UHP metamorphic rocks. They have LREE-enriched trace-element patterns similar to those of some kimberlitic fibrous diamonds, but are characterized by strong negative anomalies in Sr, Sm, Eu and Yb. Trace element patterns are clearly distinct from those of synthetic diamonds and show striking differences from the cratonic diamonds described below. Hence, Yang et al. (2014a) proposed a new class for ophiolite-hosted diamonds to differentiate their origin from those in kimberlites and UHP belts. Ophiolite-hosted diamonds and associated phases may have formed in a profoundly deep mantle environment; such diamonds may be present in other ophiolitic bodies as well as in the oceanic mantle.

2.3.7. SinoProbe-05 continental scientific drilling at Luobusa (Yang, JS)

An on-going mega-government-funded Earth-science SinoProbe Program projects initiated in 2008 is Project #5 led by J.S. Yang. It includes continental scientific drilling (CSD) to sample and chart UHP rock profiles in several ophiolitic bodies for investigation of compositions, structures and fluids from the deep mantle. The Luobusa pilot-hole drilling (LSD-1) (2009–2010) was selected as the first hole reflecting the unusual mineral group discovered in the *in-situ* diamond-bearing chromitites. It was drilled to a depth of 1479 m with an average core recovery rate of 93.6%. SIMS analysis shows that the ophiolite-hosted diamond has a distinctively light $\delta^{13}C$ isotopic composition, compatible with the ophiolite-hosted moissanite ($\delta^{13}C$ from −35 to −18‰, $n = 36$); both are much lower than the main carbon reservoir in the upper mantle ($\delta^{13}C$ near −5‰). Compiled data from moissanite from kimberlites and other mantle settings share this characteristic of light $\delta^{13}C$ isotopic compositions. These data suggest that both diamond and moissanite originated from a separate carbon reservoir in the mantle, or that its formation involved strong isotopic fractionation, and may have formed in the lower mantle.

2.4. Description of Luobusa unusual minerals

As noted above, >60 discrete phases have been reported from chromitites and peridotites associated with ophiolites; except for specific citations, most compositional and textural features are from Robinson et al. (2004) and are briefly summarized below:

2.4.1. Native carbon: diamond and graphite

Most diamond crystals from mineral separates (Fang and Bai, 1986; Robinson et al., 2004) are colorless, euhedral octahedra ranging in size from 0.2 to 0.7 mm; irregular grains and broken fragments have also been recovered. Some grains contain small inclusions of clinoenstatite with somewhat higher SiO_2. The diamond inclusions in Os–Ir alloy discovered by Yang et al. (2007) are micro-size (6 μm across) and intergrown with an unidentified Mg–Al silicate phase (possible a highly aluminous enstatite or a high-P polymorph of enstatite). Analyzed diamonds have total N contents of 20–700 μg/g and N aggregation states of up to 75%.

Graphite is common in Luobusa chromitites and occurs as gray, tabular prisms and irregular grains, 0.1–0.7 mm long; most grains have rounded corners, but their hexagonal morphology is apparent. None of the graphite grains have diamond morphology, hence may not be the retrograde product mentioned above.

Yang et al. (2014a,b) identified numerous micro- and nano-inclusions of previously subducted crustal materials in some Tibetan diamonds; these include Ni–Mn–Co alloys, galaxies (Al–Mn spinel), tephroite (Mn olivine), spessartine, Mn-oxide and native Mn. Diamonds and moissanite in southern Tibet and the Polar Urals have extremely light $\delta^{13}C$-values (-29 to $-18‰$), much lower than most kimberlitic diamonds (-10 to $-5‰$). As the diamonds occur not only in mineral separates but also in-situ as micro-scale inclusions in chromites from both chromitites and peridotites in at least six ophiolitic bodies worldwide and are associated with unusual, extremely reduced phases (e.g., Xu et al., 2011), Yang et al. (2014a,b) proposed a unique type of ophiolite-hosted diamonds having a distinct deep mantle origin.

2.4.2. Moissanite, native silicon

Moissanite (α-SiC) 0.1–1.1 mm in size recovered from mineral separates (e.g., IGCAGS, 1981; Fang and Bai, 1986) occurs as either single rounded or pinacoidal idiomorphic crystals and fragments. Some show color zonings from dark-blue to grayish-blue to nearly colorless, or from pale green to yellow to yellowish-blue to bluish green caused by small amounts of impurities such as nitrogen and aluminum. A few euhedral moissanite crystals contain small inclusions of probable gehlenite ($Ca_2Al_2SiO_7$); other crystals contain minute oval or needle-like opaque inclusions of native Si. Native Si, nearly pure Si with minor Fe, occurs as irregular inclusions in moissanite and Fe-silicides; the grains are subcircular in shape, up to about 0.25 mm across, and have sharp boundaries with the host material.

2.4.3. TiO_2^{II} phase and silicon rutile

Trace amount of nano-size TiO_2^{II} has been identified as isolated inclusions in host coesite of chromititie fragments from both Luobusa, and Ray-Iz. Its occurrence suggests that the host chromitites formed at 10 GPa within the stability of stishovite. The Luobusa TiO_2^{II} is associated with coesite laths after stishovite (Yang et al., 2007; Dobrzhinetskaya et al., 2009). Both TiO_2^{II} and coesite lack any sign of retrogression to low-P phases. Preservation in such a pristine state in ophiolite reflects extraordinarily reduced, anhydrous conditions indicated by the coexisting phases. Such a feature is in marked contrast to the TiO_2^{II} in UHP rocks from the Erzgebirge (Hwang et al., 2000) and the Dabie belt (Wu et al., 2005) where it is preserved only along a single twin boundary of a retrograde rutile crystal. The presence of TiO_2^{II} by itself confirms the high-minimum pressure necessary to stabilize stishovite because at 1300 °C, certainly a minimum temperature for a mantle upwelling at 300 km, rutile is stable to 10 GPa (Withers et al., 2003).

One grain of silicon rutile reported by Yang et al. (2003b) has a prismatic shape, weak cleavage, and is about $50 \times 50 \times 200$ mm. X-ray diffraction data yield a tetragonal lattice and is isostructural with stishovite. An average composition is: SiO_2 = 13.8 wt%, TiO_2 = 85.9 wt% and Cr_2O_3 = 0.3 wt%. The Si substitutes for Ti in the sixfold coordination position, indicating formation under UHP conditions at depths equivalent to the mantle transition zone or the lower mantle (Yang et al., 2003b). Ren et al. (2009) reported experimental results on the SiO_2 solubility in rutile up to 23 GPa and 2000 °C; the SiO_2 solubility at constant T of 1800 °C increases from 1.5 wt% SiO_2 at 10 GPa to 3.8 wt% SiO_2 at 23 GPa and at constant pressure of 18 GPa, the solubility increases from 0.5 wt% SiO_2 at 1500 °C to 4.5 wt% SiO_2 at 2000 °C. On the other hand, the solubility of TiO_2 in coesite or stishovite is very limited, with an average of 0.6 wt% TiO_2 over the experimental P–T ranges.

2.4.4. Wüstite (FeO), and native iron (Fe)

In Luobusa, wüstite occurs as light-gray, sub-rounded grains 0.1–1.5 mm in diameter commonly hosting spherical inclusions of native Fe. Robinson et al. (2004) reported some wüstite compositions. Most grains are nearly pure FeO with small amounts of Mn or Ti; a few contain high MnO and a few wt% each of SiO_2 and Al_2O_3 and traces of Cr_2O_3 and MgO. One prismatic grain about 0.3 mm long appears to be an intergrowth of SiO_2 and FeO and has compositional zoning with Si replacing by Fe from rim to core.

Native Fe is common and occurs as small round globular inclusions 50–100 μm in diameter in wüstite (Fig. 9F) or rarely as irregular clusters of acicular grains (Bai et al., 2000). These grains are pure Fe; a few contain minor amounts of Mn, Si and Al, up to a total of about 4 wt%. The well-round Fe inclusions have sharp contacts with host wüstite; they were probably immiscible liquids from a molten melt. Robinson et al. (2004) further described small round inclusion of an Fe–Mn silicate 1–7 μm in diameter in globular native Fe. SEM photographs of the inclusions reveal small, irregular dark patches within a homogeneous, lighter gray phase of an Fe-rich silicate (approximately 69–74 wt% FeO and 17.5–22 wt% SiO_2), whereas the small dark patches contain lower FeO and SiO_2, higher MnO (up to ~20 wt%) and TiO_2 and small quantities of Al_2O_3. The Raman spectrum of these inclusions does not match any known mineral, but grains are similar in composition to Mn-rich fayalite. Likewise, the composition of the lighter gray, high-FeO, low-SiO_2 background material could be Si-rich wüstite. These nano-size phases and several other unusual opaque minerals remain to be investigated and may be new UHP phases.

2.4.5. Ni–Fe–Cr–C alloys

These carbide alloys are compositionally variable but fall into three main groups: Cr–C, Fe–Ni–C and Ni–Fe–Cr–C based on their atomic proportions. The Cr–C alloy occurs as steel-gray, acicular crystals with well-developed crystal faces and contain mainly C and Cr with small amounts of Fe and Ni and traces of Ti. Native Cr has also been reported from the Luobusa chromitites (IGCAGS, 1981; Zhang et al., 1996). The Ni–Fe–Cr–C alloys occur as sub-rounded grains ~200 μm across, with a silver white, metallic luster; some have distinct compositional bands or zones, and many are light-gray material with many small irregular patches or blebs of dark material scattered through the grains. The light-gray areas and bands are higher in both Fe and Ni but lower in Cr than the dark bands; they represent the products of exsolution or intergrowths of different composition. Ni–Fe–C alloys form grayish-white, granular grains, 200–300 μm across, with strong metallic luster and form two compositional group, Fe-rich and Ni-rich. Fe-rich varieties lack Ni and have atomic proportions close to $Fe_{0.5}C_{0.5}$ whereas the Ni-rich

grains have variable amounts of Fe and C. Most Fe–Ni–C grains are optically homogeneous and show little compositional variation.

2.4.6. PGE alloys

In previous studies on other ophiolitic complexes, Dick (1974) described many base-metal alloys that occur along cracks and fractures in ophiolitic chromite associated with serpentinization, and considered them to be secondary. However, abundant PGE and base-metal alloys from the Luobusa chromitites described by Bai et al. (2000) are completely enclosed in chromite grains, so are probably primary. These Os–Ir–Ru, Pt–Fe and Ir–Fe–Ni alloys are anhedral to subhedral, equidimensional grains up to 0.5 mm in diameter. The Ir–Fe–Ni alloys occur as single grains or as colliform intergrowths with Os–Ir–Ru alloys. These Ir–Fe–Ni alloys have constant Fe (15–25 mol%) but vary widely in Ir and Ni. Some grains also contain small amounts of Ru, Os and Cu.

The Os–Ir–Ru alloys span a wide range of composition; most contain less than 10% Ru and are classified as osmium and iridium (Bai et al., 2000). Many are compositionally zoned, typically with cores of osmium and rims of iridium. The Os–Ir ratios in these alloys range from approximately 2:1 to 1:3. A few Os–Ir alloys contain small spherical silicate inclusions about 5–50 μm across with sharp boundaries. Energy-dispersive analyses indicate that the inclusions are Ca–Al–Fe–Mg silicates tentatively identified as silicon spinel.

Pt–Fe alloys occur as single subrounded to tabular grains 0.1–0.4 mm across or as intergrowths with Os–Ir–Ru alloys. They consist mainly of Pt and Fe with up to 10% Rh and small amounts of Ni, Co, and Cu (Bai et al., 2000). Only one analyzed grain has a composition close to isoferroplatinum (Pt_3Fe). Small inclusions of Os–Ir–Ru alloy are present in some Pt–Fe grains.

2.4.7. Silicate minerals

In addition to the Coe and Ky pseudomorphs after stishovite inclusions in Ir–Fe alloys of the Luobusa chromitite fragment described by Yang et al. (2007) (Fig. 9C and D), a variety of other silicate minerals, including Ol, Opx, Cr–Di, and minor Phl, Srp and Chl occur as inclusions in other minerals or as discrete crystals. Yang et al. (1981) first reported a new octahedral pseudomorph of lizardite grains 0.2–0.7 mm across included in and attached to Luobusa chromite. Subsequently, several hundred grains recovered from mineral separates were reported by Robinson et al. (2004); most consist of serpentine. X-ray diffraction data indicate that the serpentine grain has a spinel crystal structure with a cubic, face-centered lattice (space group Fd-$3m$) with dimensions $a = 8.277$ Å and $V = 567.1$ Å^3. Refinement of the crystallographic data yields a best fit with the composition $Fo_{90}Fa_{10}$. An energy-dispersive spectrum confirms that the octahedral grain consists of nearly pure Mg silicate containing a small amount of iron. The morphology, structure and composition of the octahedral grain strongly suggest that it was high-pressure form of olivine, possibly ringwoodite (Robinson et al., 2004).

2.4.8. Oxides and nitrides

Dobrzhinetskaya et al. (2009, 2014a,b) reported numerous unusual oxides and nitrites including osbornite (TiN), qinsongite (c-BN), TiO_2^{II}, and native Fe from a Ky–Coe-bearing silicate assemblage (e.g., see Fig. 2 of Yang et al., 2007). Nano-size osbornite (TiN) (50–200 nm) inclusions are abundant within coesite and are accompanied by qinsongite and less-abundant crystals of native Fe, sporadic inclusions of TiO_2^{II}, and boron carbide of unknown stoichiometry. Isotopic compositions of $\delta^{15}N = -10 \pm 3.0‰$ and $\delta^{13}C = 5 \pm 7‰$ were obtained for osbornite. No variations in N and C isotope compositions were detected. Natural osbornite is very rare on the Earth (Tatarintsev et al., 1987), but it is rather common in meteorites, especially iron meteorites. Those in a Ca–Al-rich

inclusion from a carbonaceous chondrite were suggested to have formed by gas–solid condensation in a high-T ($\sim$2000 K) region of the solar nebula instead of having a high-pressure origin (Meibom et al., 2007).

Qinsongite is a cubic boron nitride (cBN); this new mineral was named by Dobrzhinetskaya et al. (2009, 2014b) for Qingsong Fang (1939–2010), who found the first diamond in the Luobusa chromitite. Qingsongite forms isolated anhedral single crystals from 100 nm up to 1 μm in size. This mineral contains 48.54 ± 0.65 wt% B and 51.46 ± 0.65 wt% N with a structural formula corresponding to $B_{1.113}N_{0.887}$ to $B_{1.087}N_{0.913}$ maximum and minimum B contents, respectively. The presence of qinsongite is significant not only because of its association with coesite pseudomorphs after stishovite, but also reflecting the rare source of N and B. The only B concentrations exceeding 1 μg/g in minerals from mantle depths are blue diamonds (1–8 μg/g B, N < 5–10 μg/g, Gaillou et al., 2012), and B in diamonds could have been sourced from the crust. On the other hand, nitrogen is widespread in kimberlitic/lamproitic diamonds and varies greatly depending on the source of the diamond (e.g., a few parts per million to over 1000 μg/g, Palot et al., 2012). Diamonds from UHP metamorphic terrains (e.g., Kokchetav) contain up to 11,000 μg/g N (De Corte et al., 1998). Based on geochemical characteristics of qinsongite and its association with reduced UHP silicates and nitrides, Dobrzhinetskaya et al. (2014a,b) suggested that formation of qingsongite required a pelitic rock that was subducted to mid-mantle depths where crustal B originally present in mica or clay combined with mantle N ($\delta^{15}N = -10.4 \pm 3‰$ in osbornite) and subsequently was exhumed by entrainment in chromitite. The Luobusa qinsongite-bearing silicate fragment thus had a hybrid crustal + mantle origin. Its occurrence implies the recycling of crustal material into the mantle since boron, an essential constituent of qingsongite, is potentially an ideal tracer of material from the Earth's surface.

2.4.9. Fe-silicide

Fe-silicides of various Fe and Si stoichiometries (+minor Ti and P) are present in mineral separates and in-situ as inclusions in other minerals of the Luobusa chromitites (e.g., Bai et al., 2002, 2003, 2004; Robinson et al., 2004; Li et al., 2007b; Yang et al., 2014a,b). They occur as gray, irregular grains up to about 1.5 mm across. Most individual grains are chemically uniform; some contain small inclusions of native Si. Based on their compositions, several new minerals have been identified: these include luobusaite, $Fe_{0.8}Si_{0.2}$ (Bai et al., 2006; Li et al., 2007a), qusongite, $W_{1.006}Cr_{0.02}C_{0.992}$ (Fang et al., 2009), yarlongite (Cr,Fe,Ni)$_9C_4$ (Shi et al., 2009), zangboite, $TiFeSi_2$ (Li et al., 2009) and naquite, FeSi (IMA2010-010), and linzhiite, $FeSi_2$ (Li et al., 2012), titanium, Ti (Fang et al., 2013), and qingsongite, $B_{1.1}N_{0.9}$ (Dobrzhinetskaya et al., 2014b). Two other phases, xifengite, (Fe_5Si_3), first identified from the Yanshan, China meteorite by Yu (1984), and gubeiite (Fe_3Si) also occur. These phases possess high symmetry and small cell volumes with closest packed crystal structures. Characteristics of these and other unusual Luobusa minerals are listed in Table 3.

Among them, qusongite (WC) is a new mineral named from the type locality, Qusong County; it was discovered as angular grains in heavy mineral separates, associated with chromian chlorite, calcite, (W,Ti)C and (Ti,W)C alloys, and chromite (Fang et al., 2009). Qusongite contains mainly W (92.07–94.48 wt%) and C (6.01–6.16 wt%) with minor Cr ($\sim$0.04 wt%), and has a formula $W_{1.006}Cr_{0.02}C_{0.992}$ close to end-member WC (Fig. 9E).

Among iron-silicide intermetallic compounds, the new mineral linzhiite ($FeSi_2$) is the most common, and is named after the Linzhi Prefecture (Li et al., 2012). The typical composition is close to the ideal formula, with minor Al and Mn. Synthetic $FeSi_2$ has two polymorphs: tetragonal $P4/mmm$ space group and orthorhombic $Cmca$ space-group, linzhiite and luobusaite ($Fe_{0.8}Si_{0.2}$–$FeSi_2$),

Table 3
Crystallogrphic and compositional characteristics of new minerals from Luobusa chromitites, Tibet.

Name of minerals	Luobushaite	Zangboite	Linzhiite	Naquite	Qinsongite	Qusongite	Yarlongite	Titanium
Formula	$Fe_{0.84}Si_{0.2}$	$TiFeSi_2$	$FeSi_2$	$FeSi$	$B_{1.1}N_{0.9}$	$W_{1.006}Cr_{0.02}C_{0.992}$	$Cr_4Fe_4NiC_4$	Ti
Crystal system	Orthorhombic	Orthorhombic	Tetragonal	Cubic	Cubic	Hexagonal	Hexagonal	Hexagonal
Unit-cell parameters	$a = 9.874 (14)$ [Å]	$a = 8.605 (10)$	$a = 2.696 (1)$	$a = 4.486 (4)$	$a = 3.61 \pm 0.045$	$a = 2.902 (1)$	$a = 13.839 (2)$	$a = 2.950 (2)$
	$b = 7.784 (5)$ [Å]	$b = 9.5211 (11)$	$b = 2.696 (1)$	$V = 90.28$		$c = 2.831 (1)$	$b = 13.839 (2)$	$c = 4.686 (1)$
	$c = 7.829 (7)$ [Å]	$c = 7.6436 (9)$	$c = 5.147 (6)$			$V = 20.05 (1)$	$c = 4.4960 (9)$	$V = 35.32 (5)$
	$V = 601.7(8)$ [Å³]	$V = 626.25 (13)$	$V = 37.41 (14)$				$V = 745.7 (2)$	
Z	16	12	1	4	4	1	6	2
Space group	Cmca	Pbam	P4/mmm	$P2_13$	$F\bar{4}3m$	P6m2	$P6_3/mc$	$P6_3/mmc$
Chemical composition (electron probe)								
Si	54.58 (8)	35.13	50.00 (60)	32.57				
Fe	45.40 (8)	34.92	49.09 (64)	65.65			40.6	
Ni							8.54	
Mn			0.28 (11)					
Al			0.64 (28)	1.78				
Ti		29.95						99.32–100
C						6.07	9.22	
Cr							41.38	
W						93.44		
B					48.54 ± 0.65			
N					51.46 ± 0.65			
Total	99.87		100.01				99.74	
Location	Orebody 31, Luobusa mining district, Qusong County, Tibet (29°5′N 92°5′E)							
IMA no.	IMA2005-052a	IMA2007-036	IMA2010-011	IMA2010-010	IMA2013-030	IMA2007-034	IMA2007-035	IMA2010-044
References	Bai et al. (2006)	Li et al. (2009)	Li et al. (2012)	Shi et al. (2012)	Dobrzhinetskaya et al. (2014a,b)	Fang et al. (2009)	Shi et al. (2009)	Fang et al. (2013)

respectively. Intergrowths between $FeSi_2$, zangboite ($TiFeSi_2$), and native silicon also occur. Zangboite named after the Yarlung Zangbo River, was first found in heavy-mineral separates derived from a 1500 kg sample of chromitite collected from Luobusa (Li et al., 2009). Most grains are between 0.002 and 0.15 mm across; some are 0.08×0.15 mm in size. Finer grains were also discovered as inclusions in Fe–Si phases; native Si forms a rim around the zangboite crystals. Zangboite has an ideal composition of Ti 29.95, Fe 34.92, Si 35.13 wt% and contain traces of Cr, Mn, Zr and Al. Zangboite has been synthesized by reaction of ilmenite ore with molten Si at ambient pressure (Saito et al., 2005). Hence, its presence alone does not necessarily imply a high-P environment.

Linzhiite and other intermetallic compounds may have crystallized from the melt that formed the Luobusa chromitites. Compositions and mineral parageneses indicate that they formed under a strongly reducing environment. Thus they are likely xenocrysts derived from mantle sources, transported upward by a plume and incorporated in the ophiolite during seafloor spreading. Blocks of the mantle containing exotic minerals were presumably picked up by later boninitic melts from which the chromitites precipitated, were transported to a shallow depth and partially digested in the melt, with insoluble residues incorporated in the chromitite (Robinson et al., 2004; Yang et al., 2007, 2014a,b).

2.4.10. Exsolution lamellae of coesite and pyroxene in chromite

Yamamoto et al. (2009b) documented nano-size exsolution lamellae of both diopside and coesite in chromite. The presence of these lamellae, coupled with topotaxial crystallographic relations with the host chromite, and abundant micro-inclusions of clinopyroxene, requires high solubility of Si and Ca in the chromite. In fact, the high-P polymorphic phase transformation of chromite to $CaFe_2O_4$ (CF)-type structure at 12.5 GPa and further to $CaTi_2O_4$ (CT)-type structure above 20 GPa at 2000 °C has been experimentally documented, and the UHP chromite accommodates

substantial amounts of Ca, Si, Ti, and Fe as $CaFe_2O_4$ and $CaTi_2O_4$ solid solutions (Chen et al., 2003). These UHP $MgCr_2O_4$-rich CF and CT phases could be the precursors of chromite stable at P > 12.5 GPa (~380 km depth).

Such nano-scale observations and geological occurrence indicate that the mantle peridotite/chromitite may have been transported from the deep mantle by convection. It implies that the root of mantle upwelling has a much deeper origin than previously believed. As chromite is a highly refractory mineral, the petrological UHP evidence and geochemical signatures can be preserved in spite of its long history. In fact, thin lamellae of pyroxene in chromite, similar to those in UHP chromitites from Tibet, have also been documented in concordant podiform chromitites in the Ballantrae Complex ophiolite, SW Scotland (Yamamoto et al., 2007b) and in the northern Oman ophiolite (Miura et al., 2012).

2.5. Host chromitites and peridotites of the Luobusa ophiolites

As UHP minerals are most concentrated in host chromitites and depleted harzburgites from Luobusa, these ultramafic rocks have received the most intensive study (e.g., Zhou et al., 1996, 1998, 2005; Arai et al., 2009; Huang et al., 2014). Recent drilling to nearly 1475 m at Luobusa have recovered continuous fresh core samples of residual peridotites, cumulus dunites, +gabbros and podiform chromitites.

Luobusa chromitites can be divided into three types: massive, nodular, and disseminated. Based on petrographic and geochemical data, Zhou et al. (1996) suggested that the podiform chromitites formed by crystallization of boninitic melts that were probably produced by a second-stage melting above a subduction zone. This hypothesis, however, does not explain the presence of UHP minerals in the chromite. Robinson et al. (2004) suggested that the Tibetan chromitites crystallized near the top of the mantle transition zone, and were then transported in mantle peridotites

to shallow levels. Based on its geochemistry as typical of suprasubduction zone ophiolitic chromitites and their host rocks as old as Archean (Shi et al., 2007), González-Jiménez et al. (2014) postulated that the Luobusa ophiolites developed from thinned continental lithospheric mantle, then was subducted to great depths; buoyancy of ancient SCLM would enable its rapid exhumation when compression was replaced by extension.

Recent investigation of parageneses and compositions of minerals and P–T paths of crystallization/recrystallization of Luobusa chormitites and harzburgites by Huang et al. (2014) yields a different interpretation. These rocks apparently underwent five different stages of crystallization and metamorphism. (1) The nodular chromite and olivine grains, and their "melt inclusions", indicate a high-T, high-P magmatic crystallization, most likely in the deep upper mantle. (2) Serpentinization and low-T metasomatic alteration are indicated by the occurrence of inclusions of relict uvarovitic garnet, magnetite and low-T hydrous phases. These hydrous minerals include lizardite, brucite, Chl, Tlc, and Act in metamorphic disseminated chromite and olivine, suggesting that they formed at shallow-crustal levels under near-surface conditions similar to the mineral parageneses in some Alpine peridotites (Trommsdorff and Evans, 1972; Evans, 1977). (3) High-pressure metamorphism and fragmentations of magmatic nodular olivine and chromite grains occurred at upper mantle depths at about 2 GPa with the main assemblage of chromite + Opx + Ol. At such depths, these rocks recrystallized to depleted harzburgite, dunite and chromitite with relict serpentine mineral inclusions in peridotite minerals. (4) Upwelling of these rocks allowed formation of the ophiolitic components of oceanic crust at rifting settings (e.g., MOR). (5) Interaction of seawater and ophiolitic rocks and serpentinization took place during their emplacement at shallow crustal depths. The calculated P–T path of the studied harzburgite does not enter the coesite or diamond stability fields (Fig. 14 of Huang et al., 2014). Instead, they suggested that UHP metamorphism was not coeval with the late chromitite formation but occurred earlier as an independent event. Their investigated chromitite and its ultramafic wall rocks are similar to eclogites and peridotites in the Alps and other UHP terranes described in the previous sections (e.g., Biino and Compagnoni, 1992; Zhang and Liou, 1997). In the Alps, HP–UHP metamorphism of emplaced oceanic crustal rocks (e.g., eclogitic pillow basalts) including rodingites is well known (e.g., Cortesogno et al., 1977; Evans and Trommsdorff, 1987). Many HP–UHP metamorphic rocks preserved primary minerals, textures and structures in spite of prolonged tectonic evolution (e.g., Zhang and Liou, 1997). Ultramafics of the subcontinental lithospheric mantle evidently preserve depleted harzburgite. Based on lead and osmium isotopic data of sulfides from oceanic abyssal peridotites, Warren and Shirey (2012) suggested that the mantle contains volumetrically significant reservoirs of ultra-depleted material, probably derived from recycled oceanic lithospheric mantle. These depleted reservoirs contribute only small amounts to oceanic crust generation, both due to a limited ability to melt and to the dilution of any melt by more enriched melts during crust formation. Such depleted ultramafics could be included and associated with younger ophiolitic components formed at spreading centers.

Some Chinese authors (Yang et al., 1981, 2008; Bai et al., 2001) have suggested that serpentine inclusions with octahedral shapes reflect former ringwoodite, transformed into serpentine due to fluid infiltration at low pressure. Robinson et al. (2004) interpreted the "octahedral-shaped" inclusion with an olivine composition in chromite to be lower-mantle ringwoodite. However, Huang et al. (2014) speculated that "octahedral shapes" of the serpentine inclusions simply could be the negative crystal facets of chromite crystals. There is no reason that the "ringwoodite" inside the diamond would have retrogressed to serpentine whereas the diamond host was not graphitized. Moreover, the observed widespread

occurrence of lizardite (a serpentine mineral stable only at <350 °C) inclusions in HP minerals shows that all serpentine inclusions are likely prograde mineral inclusions formed at shallow subduction depths. Apparently, the Luobusa chromitite/harzburgite may have originally crystallized in the upper mantle (spinel-facies lherzolite/harzburgite) from a Cr-rich melt (Zhou et al., 1996) and later was serpentinized prior to UHP metamorphism and recrystallization at mantle depths.

2.6. Occurrences of low-P crustal mineral inclusions in zircons

Independent studies by Robinson et al. (2014) and Yamamoto et al. (2013) on U–Pb age and mineral inclusions of zircons separated from podiform chromitites from the Luobusa ophiolite reached the same conclusion. Employing laser Raman spectroscopy, they identified low-P crustal inclusions, such as Qz, Kfs, Rt, Ilm and Ap, but a lack of mantle minerals (e.g., olivine, pyroxene, and chromite) in zircons, suggesting that the zircons are crustal in origin. Spot analyses with LA-ICPMS, assisted by cathodoluminescence images gave a wide age range, from the Cretaceous to the Late Archean (ca. 100–2700 Ma). The minimum ages of ca. 100 Ma, plotted on the concordia curve, are slightly younger than the ophiolite magmatic event in the suprasubduction zone (120 ± 10 Ma), suggesting that the zircons underwent minor Pb-loss. However, most zircon ages are much older than the formation ages of both the chromitite and the ophiolite. Thus the crustal zircons are xenocrystic origin and resided in mantle peridotite for a long time before being enclosed by chromitite formation; the mantle peridotite beneath the Neo-Tethys Ocean clearly was contaminated by crustal materials. This suggestion is consistent with previous reports that mid-oceanic ridge basalts of the Indian Ocean have isotopic signature of crustal material contamination (e.g., Ingle et al., 2002).

Robinson et al. (2014) described zircon, corundum, Pl, Kfs, Grt, Ky, andalusite, Qz and Rt in podiform chromitites from the ophiolites of Tibet, Oman, and the Polar Urals. Separated zircons are rounded grains, contain low-P mineral inclusions, and have much older age ranges than the host ophiolites. These features suggest that crustal low-P minerals were mixed with subduction-origin UHP and highly reduced phases in the ophiolitic chromitites. Apparently, some ancient zircons in podiform chromitites provide evidence of crustal material being recycled through the upper mantle; subducted crustal relics may be widespread in the mantle and may account for much of the mantle heterogeneity.

2.7. Tectonic model for genesis of UHP and LP minerals – recycling of crustal materials

Tectonic models attempting to account for the unusual petrotectonic–geochemical–mineralogical characteristics described above must consider the following observations: (1) lithologic components of ophiolites have formed in low-P rifting settings (e.g., MOR, back-arc or SSZ); (2) high-P chromitites beneath some ophiolites have undergone multiple tectonic events from low-P through deep subduction to mantle upwelling; (3) HP chromitites contain xenolithic minerals included in old crustal zircons; (4) diamonds, moissanite, coesite pseudomorphs after stishovite, possible ringwoodite and many other phases including native elements, oxides, silicates, nitrides evidently formed at great depths under highly reducing conditions.

Thus far, several models explaining the intimate association of crustal materials with mantle minerals have been proposed. Robinson et al. (2004) pointed out that ophiolites along the Indus–Yarlung–Zangbo suture zone are variable in age and may represent the remnants of numerous small collapsed oceanic basins that accreted at ca 126 Ma as a result of intraoceanic subduction. Three stages were suggested: In stage 1, during early

Mesozoic formation of Neo-Tethys, lithospheric subduction carries continental/oceanic materials into the deep upper mantle; convection brings mantle UHP minerals and rocks to shallow levels. In stage 2 at ca 175 Ma, sea-floor spreading produces the MORB-like crust, which makes up the bulk of the Luobusa ophiolite. In stage 3 at ca 126 Ma, a subduction zone descends through this weakly depleted mantle; hydrous melting in the overlying mantle wedge produces boninitic melts, which rise upward and undergo fractional crystallization to form podiform chromitites.

The model of Yamamoto et al. (2013) with four discrete stages is simplified in Fig. 10: (1). From >∼500 Ma: Consolidation of Gondwana caused contamination of subcontinental lithospheric mantle by subducted crustal materials. (2) At ca 170 Ma: after Gondwana breakup, the Luobusa ophiolite was generated above the 'contaminated/polluted' mantle in the Neo-Tethys between the Lhasa block and the Indian continent. About the same time the podiform chromitites formed and assimilated recycled crustal zircons from the polluted upper mantle during melt–mantle interaction at a mid-oceanic ridge; many isotopically unusual UHP and reduced minerals may have formed in the lower mantle and subsequently were brought up after the formation of the Neo-Tethys Ocean through mantle upwelling (3) At ca 120 Ma: the Luobusa ophiolite was affected by supra-subduction zone magmatism and metasomatism; and (4) At_ca 50 Ma: the Indian continent containing the 80–90 Ma obducted Luobusa ophiolite collided with the Eurasia continent. The accretion formed the Indus–Yarlung–Zangbo suture zone as well as the Himalayan UHP terrane.

J.S. Yang and his co-workers have been working on the UHP and LP minerals associated with ophiolitic rocks for more than two decades, and have proposed numerous tectonic models to account for the observed field and analytical data. The latest version is duplicated in Fig. 11 (Yang et al., 2014a,b, Fig. 3). This model

accounts for the facts described above and explains the following events: (1). The similarity of mineralogical and geochemical characteristics of diamonds + associated reduced + UHP minerals from ophiolites of various regions and ages (early Paleozoic to Cretaceous) indicate that most phases likely formed at mantle depths of 150–300 km or deeper. (2) The occurrence of low-P silicate minerals, such as zircon, corundum, andalusite, kyanite, and rutile in ophiolitic chromitites and peridotites document the recycling of crustal materials including various fluid species such as phlogopite, lawsonite, glaucophane, nominally anhydrous phases via subduction into the mantle transition zone (>300 km depth). These crustal contaminates must have been introduced into the deep mantle by subduction, long before the formation of ophiolitic magmas at shallow depths. (3) Ophiolite-type diamonds crystallize from supercritical C–O–H fluids prior to inclusion in chromites. (4) On the upwelling of fluid/melt-charged asthenosphere, UHP chromite grew and encapsulated diamonds, moissanite, and other highly reduced phases. (5) With continued ascent to upper mantle depths, coesite exsolves from chromite and stishovite is replaced by coesite, whereas the diamonds and other phases are preserved as inclusions in chromite grains. (6) The rising asthenosphere with inclusions of diamond and associated phases + crustal contaminates of various ages is brought to the suprasubduction zone mantle wedge where the ophiolitic melts evolve.

3. UHP–UHT crustal materials from kimberlite and lamproite pipes

3.1. Introduction

Diamondiferous ultramafic and eclogitic xenoliths and xenocrystic diamonds in kimberlite and lamproite pipes as old as 3.2 Ga
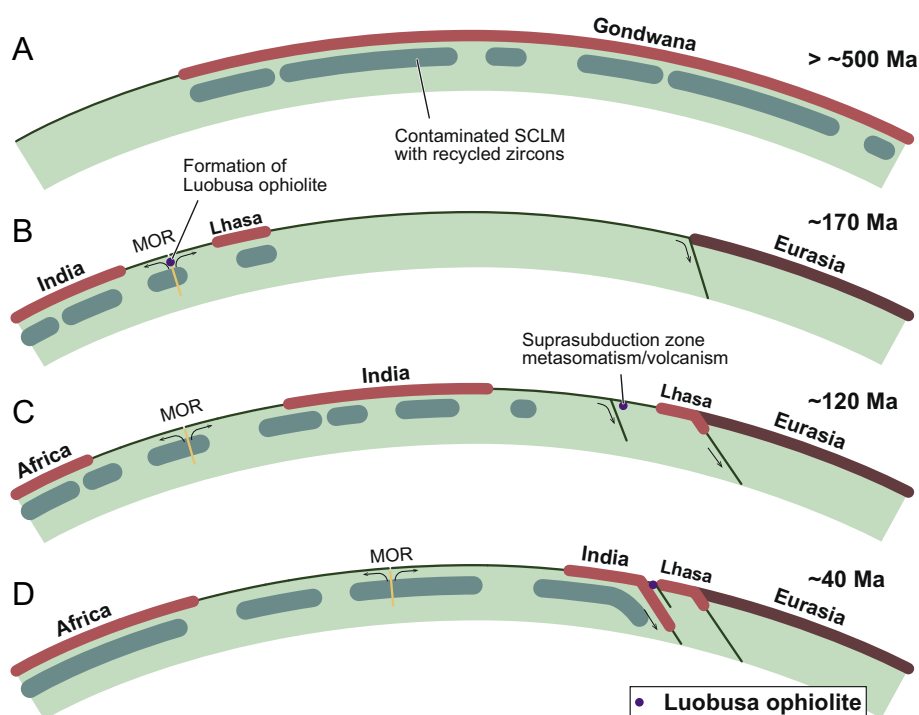

Fig. 10. Schematic diagrams showing the tectonic evolution of the Luobusa ophiolite and the Neo-Tethys Ocean (modified after Yamamoto et al., 2013). (A) >∼500 Ma: During the consolidation of Gondwana, subduction of crustal materials were brought into—and mixed with—UHP minerals in the upper mantle. The Lhasa block and Indian continent were in the northern part of Gondwana, and at ca 500 Ma it started to break up. (B) At ca 170 Ma the Luobusa ophiolite was generated in the Neo-Tethys Ocean overlying the 'polluted' upper mantle. (C) At ca 120 Ma the Luobusa ophiolite was affected by secondary magmatism (metasomatism) in a suprasubduction zone setting. (D) At ca 40 Ma, the Luobusa ophiolite was obducted onto the edge of the Indian continent prior to the collision of India with Eurasia, now occurring in the suture zone.
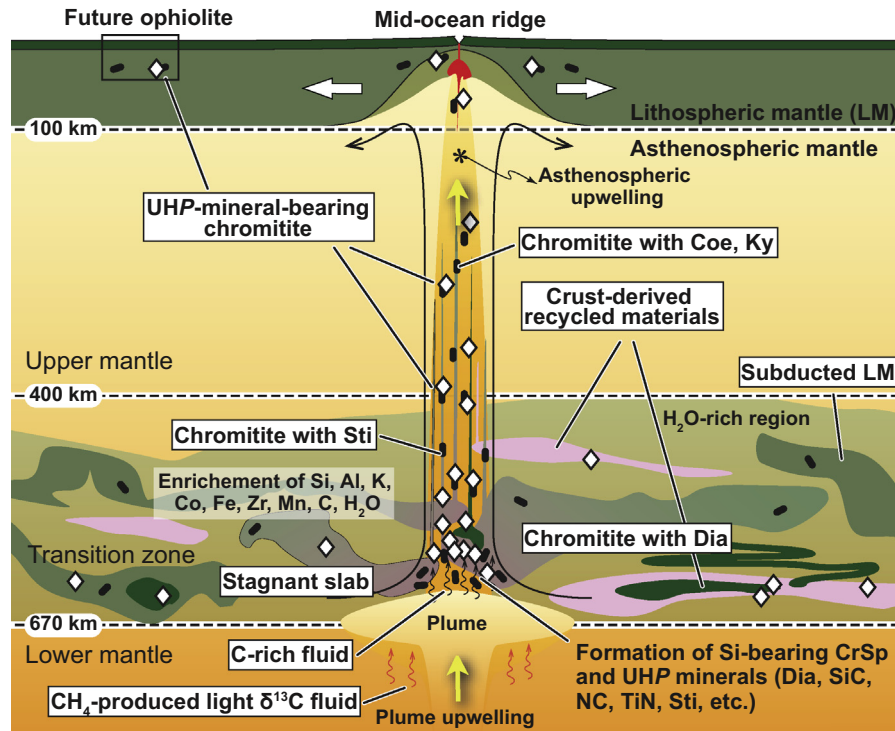
Fig. 11. A conceptual model of Yang et al. (2014a,b) for the formation and occurrence of diamonds and associated UHP and low-P minerals in the oceanic mantle (Fig. 3 of Yang et al., 2014a,b). See text for discussion.

have been extensively studied and have advanced our understanding of the Earth's mantle (e.g., Taylor and Anand, 2004; Shirey et al., 2013). Mineral inclusions in diamonds are the oldest, deepest, and most pristine samples of the Earth's mantle. They provide age and chemical information over a 3.2 Gyr span that includes continental crustal growth, atmospheric evolution, and an evolution toward the current style of plate tectonics. Shirey and Richardson (2011) compiled isotopic and bulk chemical data of silicate and sulfide inclusions in diamonds from kimberlitic xenoliths worldwide and reported that a compositional change occurred at 3.2–3.0 Ga. Before 3.2 Ga, only diamonds with peridotitic inclusions formed, whereas after 3.0 Ga, eclogitic diamonds also became prevalent. This transition was suggested to have resulted from the capture of eclogite and diamond-forming fluids in SCLM via subduction and continental collision, marking the onset of the modern Wilson cycle of petrotectonics. For an alternative scenario involving the Hadean onset of primitive plate tectonic crust–mantle circulation attending a gradual thermal relaxation of the planet, see Ernst (1991, 2009).

The UHP–UHT mineral inclusions in diamond crystals from kimberlite and lamproite pipes offer a unique opportunity to explore petrogenesis and material recycling beneath the cratonic mantle. Depending on the nature of the host xenoliths, Sobolev (1974) classified diamonds as 'eclogitic' E-type in mafic eclogites and 'peridotitic' P-type (or 'ultramafic' U-type) in peridotites and other ultramafics (see Taylor and Anand, 2004 for summary). To differentiate these mantle-produced diamonds in xenoliths from analogues in UHP rocks formed by subduction of crustal materials, the terms "cratonic" vs "crustal" diamonds have also been used (e.g., Helmstaedt, 2013). Mineral inclusions are mostly silicates, oxides, sulfides and rarely carbonates and metals. Syngenetic silicate mineral inclusions trapped in E-type diamonds attest to the recycling of crustal materials in the Earth's mantle. Mineral inclusions in both E- and P-type diamonds have been reviewed in special issues, books, conference proceedings on kimberlites, diamond, high-pressure

experiments, and diamond exploration (e.g., Meyer, 1985; Taylor and Anand, 2004; Harte, 2010, 2011; Kaminsky, 2012). Therefore, we focus mainly on recent topics of 'super-deep' mineral inclusions and also some important observations related to the recycling of crustal materials preserved as inclusions in diamonds.

3.2. 'Super-deep' mineral inclusions in cratonic diamonds

Thus far, deep-seated mantle minerals have been reported from diamond crystals in kimberlites from Brazil, Guinea, South Africa, South Australia, and Canada (e.g., Harte et al., 1999; Stachel et al., 2000, 2005; Davies et al., 2004; Tappert et al., 2005; Walter et al., 2011). Harte (2010) grouped phase assemblages and inclusion associations in diamond with depth, and proposed seven depth zones based on the natural parageneses and experimental stabilities of minerals. These zones in P-type diamonds with increasing depth are: (1) garnet peridotite [Ol + Opx + Grt + Cpx + Chr], (2) majorite peridotite, (3) majorite–'wadsleyite–peridotite', (4) majorite–'ringwoodite–peridotite', (5) upper/lower mantle boundary (mantle transition zone) [Mg_2SiO_4 + MgSi-perovskite (Mg,Fe)SiO_3 + ferropericlase (Mg,Fe)O + tetragonal almandine-pyrope phase (TAPP) + CaSi perovskite], (6) ferropericlase and MgSi-perovskite [MgSi perovskite + ferropericlase + TAPP + CaSi-perovskite $CaSiO_3$], and (7) ferropericlase + Al-rich MgSi-perovskite [Al-rich Mg–Si perovskite + ferropericlase + Ca-Si perovskite]. Thus far, principal mineral inclusions of zones (2), (3), (4) and (5) have not been identified. Similarly, seven depth zones are suggested for E-type diamonds: (1) eclogite [Grt + Cpx + Coe/Qz + Ky], (2) Cpx–majorite [Maj + Cpx], (3) majorite, (4) CaSi perovskite + Maj, (5) upper/lower mantle boundary association [Maj + TAPP], (6) CaSi perovskite majorite [TAPP + Ca-Si perovskite + Maj + Sti], and (7) Al-rich MgSi-perovskite + CaSi perovskite [+Crn + stishovite]. It is important to note that majoritic garnets (>3.05 Si apfu per 12 oxygen) are common in both E-type and P-type diamonds (e.g., Sobolev et al., 2004); these diamond hosts are typically characterized by

very light $\delta^{13}C$ values (e.g. -24 to $-10‰$). However, negative Eu anomalies in majoritic garnets in P-type diamonds with light $\delta^{13}C$ values ($\sim-20‰$) from the Jagersfontein kimberlite (South Africa) suggest a possible source of deeply subducted oceanic crust and mantle lithosphere (Tappert et al., 2005).

Kaminsky (2012) divided mineral inclusions in diamonds into three groups based on their host rocks (ultramafic, eclogitic, and carbonatitic); some inclusions may have been derived from the D" layer. The 'super-deep' phases of ultramafic associations are fer-ropericlase, Mg–Si-perovskite, Ca–Si-perovskite, Ca–Ti-perovskite, TAPP, Mg_2SiO_4, spinel, mangano-ilmenite, titanite, native nickel, native iron, an unidentified Si–Mg phase, majorite garnet and moissanite. The 'super-deep' phases of eclogitic associations include phase 'Egg' ($AlSiO_3OH$) + stishovite occurring in the Rio Soriso, Juina area, Brazil (Wirth et al., 2007) and are characterized by negative Eu-anomalies in CaSi-perovskite and majoritic garnet. The carbonatitic association of minerals includes calcite, dolomite, nyerereite [$Na_2Ca(CO_3)_2$], nahcolite ($NaHCO_3$), halides ($CaCl_2$), TiO_2^{II}, wollastonite-II ($CaSiO_3$), cuspidine ($Ca_4Si_2O_7F_2$), monticellite ($CaMgSiO_4$), and apatite. Peculiar mineral associations of wüs-tite + periclase (possibly a former ferropericlase that is stable at P exceeding 85 GPa) and iron carbides + native iron in diamonds of carbonatitic association were considered by Kaminsky to have been derived from the D" layer.

Brazilian diamonds are the focus of recent attention as a locality of 'super-deep' minerals; these kimberlitic diamonds are charac-terized by light $\delta^{13}C$ values (-25 to $-14‰$) and by the occurrence of numerous micro- to nano-size inclusions (20–30 nm in size) (Wirth et al., 2007, 2009; Kaminsky et al., 2009; Walter et al., 2011). These inclusions include, but are not limited to Egg + stish-ovite, spinel + nepheline-kalsilite phase, wüstite + ferropericlase, native iron + magnesite, TiO_2^{II}, wollastonite-II, cuspidine, TAPP, and various halides; some of these phases had precursor phases stable at depths >700 km. Walter et al. (2011) also identified two new minerals (NAL, a "new aluminus" phase and CF, a "calcium ferrite" phase) previously only known from the laboratory; the NAL transforms to CF phase at ~40 GPa (Kawai and Tsuchiya, 2012). Pearson et al. (2014) discovered an inclusion of ringwoodite in a diamond; this HP polymorph of olivine is the first terrestrial occurrence on the Earth. FT–IR measurement on the ringwoodite yielded a minimum of 1.4–1.5 wt% H_2O. This exciting new finding supports the conjecture that the mantle transition zone may store substantial amounts of H_2O (e.g., Bercovici and Karato, 2003; Ohtani et al., 2004; Huang et al., 2005; Schulze et al., 2014). This suggestion is further substantiated by recent UHP experiments on the transition of hydrous ringwoodite to perovskite and (Mg,Fe)O to produce intergranular melt; the hydration of a large region of the transition zone and dehydration melting may act to trap H_2O in the transition zone (Schmandt et al., 2014).

3.3. Hydrous silicate inclusions

Hydrous silicates are extremely rare as syngenetic inclusions in diamond. However, Daniels et al. (1996) discovered a Fe-rich stau-rolite inclusion in a graphite-bearing diamond from the Dokolwayo kimberlite, Swaziland, East Africa. Although the host diamond has a $\delta^{13}C$ mantle value of $-5‰$, the presence of Fe-rich staurolite and relative abundance of coesite in the same pipe suggest incorpora-tion of crustal material into the mantle. On the other hand, epige-netic inclusions have been found as replacements of "syngenetic" primary inclusions and infillings of fractures. For instance, Banas et al. (2007) reported serpentine, calcite, dolomite and biotite that have replaced primary inclusions in diamonds. Anand et al. (2004) described calcite and chlorite inclusions in diamond; calcite is con-sidered as primary but chlorite is a secondary phase related to fluid infiltration along fractures.

3.4. Diamondiferous eclogite xenoliths with oceanic crustal protoliths

Eclogitic xenoliths are volumetrically minor (5–20%) in most kimberlite pipes (Taylor and Anand, 2004). In many localities, dia-mondiferous eclogite xenoliths exhibit geochemical and isotopic characteristics including trace-element, REE, Sr, Pb, C, O and N iso-topes for diamond + its mineral inclusions and in the host eclogite bulk rock. These data are consistent with low-T seawater alteration of oceanic crust, suggesting subduction-zone high-pressure recrys-tallization. In fact, systematic X-ray 3D tomographic images of 17 Siberian eclogite xenoliths yield intimate spatial relations of dia-monds with their host silicates (Howarth et al., 2014, in press). These CL images together with nitrogen-defect aggregation states and stable isotopes (C and N) of diamonds reveal intergrowth zones and discrete diamond crystallization stages. For example, diamond was found in different textural settings in these eclogite xenoliths, representing three temporally distinct diamond growth events: (1) completely enclosed in garnet, (2) associated with highly embayed silicate grain boundaries, and (3) contained within distinct metasomatic 'plumbing-systems'. The common occurrence of diamond in association with embayed garnets suggests diamond growth at the expense of the hosting silicate protolith. In addition, the spatial associations of diamonds with metasomatic pathways, which are generally interpreted to result from late-stage proto-kimberlitic fluid percolation, indicate a period of diamond growth occurring close to but prior to the time of kimberlite emplacement. Based on geochemical data, Howarth et al. (2014, in press) further concluded that most mantle eclogites and their contained dia-monds were derived from materials having a crustal origin and suggested that some mantle peridotites, including diamondiferous ones as well as inclusions in P-type diamonds, also may have had crustal protoliths.

Diamondiferous eclogite xenoliths from Siberian kimberlite pipes have been intensively studied (e.g., Jacob et al., 1994; Snyder et al., 1995, 1997; Jacob and Foley, 1999; Howarth et al., in press); isotopic compositions ($\delta^{18}O$, $\delta^{13}C$, $\delta^{15}N$, $^{87}Sr/^{86}Sr$, $^{143}Nd/^{144}Nd$ ratios) indicates their origin as hydrothermally-altered plagioclase-bearing intrusive rocks of the Archean oceanic crust. Heavy $\delta^{18}O$ (up to +9.7‰) and trace-element compositions are major evidence supporting a model of ancient subducted oce-anic crust stacking beneath the Archean subcratonal lithosphere (Spetsius et al., 2008; Riches et al., 2010). Recent study of garnets in diamondiferous eclogite xenoliths also led Pernet-Fisher et al. (2014) to conclude that the protoliths were oceanic crust; such garnets do not show Eu anomalies and have heavy $\delta^{18}O$ values, whereas those in eclogites with oceanic gabbro (cumulate) affini-ties possess Eu anomalies and $\delta^{18}O$ (+5‰ to +6‰) mantle values. Carmody et al. (2011) proposed that heavy $\delta^{18}O$ isotope signatures in eclogite and pyroxenite xenoliths from Siberian kimberlites are attributable to low-T (<350 °C) seawater–basalt interactions.

Schulze et al. (2013) studied coesite-bearing E-type diamonds from Venezuela, Western Australia and Botswana, and found a negative correlation between $\delta^{13}C$ of E-type diamonds and $\delta^{18}O$ of their coesite and garnet inclusions; all diamonds with lighter $\delta^{13}C$ values contain heavier $\delta^{18}O$ values, suggesting the recycling of continental crustal materials.

Paleoproterozoic eclogite xenoliths from the Jericho and Muskox kimberlites of the northern Slave craton, western Canada, display geochemical and isotopic evidence of a recycled oceanic lithosphere origin (see Smit et al., 2014 and references therein). The eclogites comprise a diverse suite of kyanite–diamond-bearing and bi-mineralic xenoliths that have wide range of geochemical compositions. Recent study of diamond inclusions support a recycled oceanic crust origin owing to the presence of hallmark geochemical signatures such as Eu positive anomalies, non-mantle' $\delta^{18}O$ signatures of Pl-bearing, seawater-altered oceanic basaltic

and gabbroic protoliths (e.g., Schulze et al., 2003; Spetsius et al., 2009; Smit et al., 2014). Some Jericho high-Mg diamond-bearing eclogites with high concentrations of incompatible trace elements and radiogenic Sr and Pb isotopic compositions suggest a complex, multi-stage petrogenesis (Smart et al., 2009). Garnet and clinopyroxene inclusions in diamonds from such high-MgO eclogites have lower MgO and higher Na_2O contents than the same phases of the host eclogites; this indicates that post-diamond growth secondary processes were significant. Diamonds of the high-MgO eclogites have the lightest diamond $\delta^{13}C$ values reported to date ($-41‰$). Smart et al. (2011) proposed that the carbon source for these highly $\delta^{13}C$ depleted diamonds was ancient subducted organic matter.

Nanocrystalline diamonds as discrete phases and polycrystalline aggregates were first discovered in melt inclusions from a mantle-derived garnet pyroxenite xenolith from Salt Lake Crater, Oahu, Hawaii by Wirth and Rocholl (2003). The inclusions consist of a C–Cl–S-rich basaltic glass together with other nanocrystalline phases including native Fe and Cu, FeS, FeS_2, ZnS, AgS and several Ti, Nb, Zr, Ir, Pd-rich phases of unknown compositions. All these reduced phases stable at mantle depths >180 km apparently were transported by ascending basaltic magma in a mantle plume; this scenario raises numerous questions pointed out by the authors. These include: (1) how could diamond survive in such a "low-P" environment at $T > 1000\,°C$? (2) What is genetic relationship between silicate melt, carbonate, CO_2 and diamond? (3) What was the source and evolution of the diamond-bearing low-degree partial melt? Did melts and diamonds originate from the Hawaiian plume or from the depleted upper mantle? In fact, these reduced phases including microdiamonds are similar to those in ophiolitic chromitites described in previous sections. Analyses of $\delta^{13}C$ and N contents of nano-size diamonds and geochemical characteristics of other native elements + alloys will be required to clarifying these problems.

3.5. SiO$_2$ phase-bearing UHP eclogites in kimberlite and lamproite pipes

3.5.1. Coesite–sanidine eclogites

Grospydite is an abbreviated name for a special type of eclogite containing grossularite, pyroxene and disthene and was first discovered in Siberian kimberlites by Bobrievich et al. (1960). Subsequently full compositional ranges of the Mg–Ca garnets were described in a continuous series of kyanite eclogites and grospydites (Sobolev et al., 1968). Both matrix (intergranular) and coesite inclusions in garnet in a grospydite xenolith from the Roberts Victor kimberlite, South Africa were first described by Smyth (1977) and Smyth and Hatton (1977). The mineral assemblage Grt + Omp + Ky + San + Coe formed at $P > 2.9$ GPa and $T = \sim900\,°C$. Smyth and Hatton (1977) further described a heavy $\delta^{18}O$ value +7.7‰ for the rock and suggested that the protolith was altered oceanic basalt (Sharp et al., 1992). Similar occurrences of intergranular coesite have been described in eclogites from the unique UHP locality in Yangkou, eastern Sulu terrane of China (Liou and Zhang, 1996); its occurrence suggests lack of fluid during UHP metamorphism supported by the preservation of primary gabbroic minerals and textures of protoliths (see Liou et al., 2009a,b, 2012).

Based on $\delta^{13}C$ values of 92 kimberlitic diamonds from which inclusions were extracted, Sobolev et al. (1979) concluded that most P-type diamonds have mantle values in the range -9 to $-2‰$; however about 40% from E-type diamonds yield anomalous both light and heavy $\delta^{13}C$ compositions in the range -34.4 to $+0.5‰$. Such differences were substantiated by Cartigny (2005) based upon several thousand analyses. The wide range of $\delta^{13}C$ for E-type diamonds (-15 to $+5‰$) suggests crustal histories including near-surface biogenic input (Taylor and Anand, 2004).

Coesite-bearing eclogitic parageneses also occur as inclusions in E-type diamonds from the Siberian kimberlites (Sobolev et al., 1976). Since these initial findings, inclusions of coesite and its pseudomorph have been reported in several diamondiferous eclogite xenoliths and E-type diamonds from South Africa, Siberia, Venezuela, and South Australia (e.g., Schulze and Helmstaedt, 1988; Jaques et al., 1989; Sobolev et al., 1998; Schulze et al., 2000, 2003; Tomilenko et al., 2009).

3.5.2. Coesite-bearing lawsonite eclogite xenoliths from Colorado

Navajo diatremes of the Colorado Plateau, USA occur as very unusual ca 30 Ma kimberlitic pipes that contain Lws- and Coe-bearing eclogite xenoliths (Watson and Morton, 1969; Helmstaedt and Doig, 1975; Usui et al., 2006) together with antigorite peridotite, chlorite harzburgite, Cr-magnetite dunite and other ultramafic rock fragments (Smith, 2010). The eclogites containing lawsonite and phengite as hydrous phases together with Grt + Omp + Rt have a Phanerozoic Re–Os mantle extraction age for the protoliths (Ruiz et al., 1998) and 81–30 Ma U–Pb zircon ages for UHP eclogite-facies metamorphism (Usui et al., 2003). The inferred P–T trajectory for the Coe-bearing Lws eclogite xenoliths follows a relatively cool subduction path into the UHP part of the Lws eclogite stability field. Usui et al. (2003) provide conclusive evidence that the eclogites were derived from the subducted Farallon plate based on the Cretaceous U–Pb age and the lawsonite- and jadeite-bearing mineral assemblages similar to those of Franciscan HP rocks (Fig. 12). Helmstaedt (2013) recently provided a schematic tectonic model for emplacement of the UHP Lws eclogite xenoliths due to a change in subduction geometry from relatively steep slab descent to shallow-angle underflow, allowing the Farallon plate to maintain contact with the subcontinental lithosphere of the overriding plate (see Fig. 16 of Smith, 2010; Fig. 5 of Helmstaedt, 2013). Transport of the xenoliths to the surface by the Oligocene Navajo diatremes evidently was related to the upwelling of hot material from the upper mantle below the slab that in turn was caused by tearing and sinking of the Farallon plate.

Those ultramafic fragments are viewed as part of the serpentinitized mélange of the Farallon plate; they underwent multi-stage metasomatism and recrystallization, hence pyropic Grt, Ol ($Fo_{98–92}$) and Alpine-type peridotie assemblages formed (Smith, 2010). Moreover, Schulze et al. (2014) recently identified guyanaite (β-CrOOH) as a dominant phase in small clusters of accessory minerals intergrown with Cr-rich Omp, Zn-rich chromite, eskolaite (Cr_2O_3) and carmichaelite ($Ti_{0.6}Cr_{0.2}Fe^{2+}_{0.1}O_{1.5}(OH)_{0.5}$) in a xenolith of Cr-rich omphacitite from the Moses Rock diatreme in the Navajo Volcanic Field. Carmichaelite, an OH-bearing titanite, also occurs in the Navajo diatremes of nearby Garnet Ridge (Wang et al., 2000). This unusual assemblage is interpreted as the result of metasomatism of chromite-bearing serpentinite by slab-derived fluids during subduction of the Farallon plate. At the time of xenolith entrainment, the rock was undergoing prograde metamorphism, with guyanaite dehydrating to eskolaite + water. This reaction and the coeval dehydration of the inferred accompanying host serpentinites may have provided water for hydration of the subcontinental upper mantle, contributing to uplift of the Colorado Plateau.

3.6. Alluvial and detrital diamonds

Alluvial diamonds with no apparent sources are well known from many localities: Myanmar, southern Thailand (Phuket), Sumatra, Kalimantan, eastern Australia, Russian Far East, Algeria, and northern California (Kopf et al., 1990; Davies et al., 1999; Heylmun, 1999; Wina et al., 2001; Spencer et al., 2008; Shcheka et al., 2006; Smith et al., 2009; Tappert et al., 2009; Kahoui et al., 2012). At the world-class jadeitite locality of Myanmar (e.g., Tsujimori and Harlow, 2012; Harlow et al., in press), alluvial
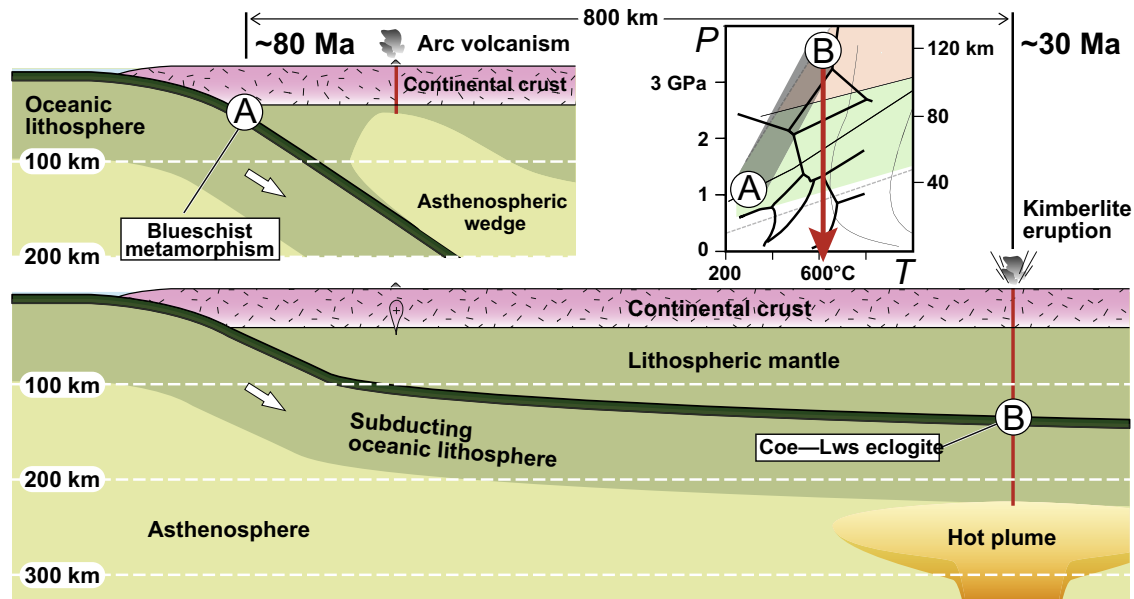
Fig. 12. Classical Pacific-type active margin in California: (A) At about 175–80 Ma, subduction of the Fallon plate beneath the North American continent to form the Franciscan blueschist-facies metamorphic complex and the Sierra Nevada Arc volcanism-magmatic belt; (B) the shallow subduction of the Fallon plate under the SCLM and overlying Colorado Plateau to form coesite lawsonite eclogite that was brought to the surface by Navajo diatreme at about 40 Ma. An insert diagram showing *P–T*–time path of the coesite-bearing lawsonite eclogite xenolith is modified from Fig. 2 of Usui et al. (2003).

diamonds contain inclusion assemblages of peridotitic and rare eclogitic parageneses (Wina et al., 2001). Similar alluvial diamonds have been recovered from several Quaternary to recent alluvial deposits in Kalimantan, Indonesia (Spencer et al., 2008). Study of 872 diamonds by Smith et al. (2009) confirmed that 68% were ultramafic (P-type) and 32% were eclogitic (E-type). They identified inclusions of Ol, Grt, Opx, chromite, and pentlandite from P-type diamonds, and Rt + Ky + Coe from E-type diamonds; they suggested that the mineral inclusions formed at T = 930–1250 °C and P = 4.2–6 GPa, conditions appropriate to the lithospheric keel. Alluvial diamonds with light $\delta^{13}C$ values (-21 to $-10‰$) in Sikhote Alin, Russian Far East contain mineral inclusions of K-bearing omphacite (0.5 wt% K_2O), corundum, Ti-rich kaersutite (4 wt% TiO_2), Mg-rich ilmenite (8 wt% MgO), titanomagnetite, and churchite (hydrated phosphate) (Shcheka et al., 2006). Kaersutite occurs in the core of polycrystalline diamonds with fractures, suggesting an epigenetic origin.

In the Phanerozoic New England fold belt of eastern Australia, about 2 million diamonds have been mined from Tertiary alluvial deposits >1500 km from the nearest craton (Davies et al., 1999; Barron et al., 2005). Sobolev et al. (1984) was among the first to have identified Coe + grossular and Coe + Omp inclusions in these diamonds and reported unusually heavy $\delta^{13}C$ values (-3.3 to $+2.4‰$), indicating their deep mantle origin. Davies et al. (2002) distinguished two diamond groups: one with low to moderate N concentrations and high defect aggregation states, resembling diamonds from kimberlites and lamproites, but showing signs of a long recycling history. Other diamonds with high N concentrations, low defect aggregation states and morphological characteristics are consistent with an origin in a Paleozoic subduction environments similar to those of subducted alluvial diamonds proposed by Barron et al. (2005). Unlike diamonds from ancient cratons, subduction-type diamonds contain unique inclusions of Phanerozoic eclogitic rocks. Some garnets exhibit unusual chemical characteristics and microstructures (oriented exsolution lamellae of Rt/Ap/Ilm); Barron et al. (2008) later identified rare mineral inclusions of Coe, Grt, Omp, anatase, and calcite in alluvial diamonds from the Bingara-Copeton area, and suggested

the possible existence of an unexposed UH*P* metamorphic terrane in eastern Australia.

Detrital diamonds (>0.5 mm) containing inclusions of P-type mineral parageneses occur in Neoarchean metaconglomerate from the southern Superior province, Canada (Kopylova et al., 2011; Miller et al., 2012); the metasediments also contain detrital Cr-rich (6 wt% Cr_2O_3) pyrope and picro-ilmenite that likely originated from diamondiferous kimberlites. This is promising because Chinese identification of coarse-grained placer diamonds led to the discovery of new ophiolite-type diamonds from Tibet, the Polar Urals and Myanmar, as described in Part II (e.g., Yang et al., 2014a,b). Moreover the recent finding of many diamond crystals (50–200 μm) from arc-basalt lavas and pyroclastics from an active volcano in Kamchatka (Gordeev et al., 2014) suggests that diamond is highly resistant to short-term heating. Its stability in the deep upper mantle (>120 km) and high resistance to weathering/corrosion under near-surface conditions might cause unexpected geological inheritance and/or contamination.

3.7. Summary of carbon isotopic characteristics of the three types of diamond

Both cratonic and crustal diamonds have unique occurrences, morphologies, mineral inclusions, and characteristic geochemical and isotopic signatures (Cartigny, 2005; Ogasawara, 2005; Dobrzhinetskaya, 2012; Helmstaedt, 2013; Shirey et al., 2013). From carbon isotope analyses of cratonic diamonds obtained in the 1970s by Sobolev et al. (1979), Sobolev and Sobolev (1980) first proposed that most E-type diamonds formed from crustal carbon recycled into the mantle by subduction, whereas the more abundant P-type diamonds formed from deep-seated mantle. More recent stable isotope studies of nitrogen, oxygen, and sulfur, as well as carbon, combined with studies of mineral inclusions within cratonic diamonds, have significantly modified the early proposal (Fig. 13). One major achievement in our understanding of diamond formation both in the Earth's mantle and in UH*P* metamorphic rocks is the increasing evidence for its formation from a C-bearing fluid, commonly referred to as "C–O–H-bearing fluid or melt". The

mantle recycling of crustal materials including such supercritical fluids through subduction channels led to the conclusion that the vast majority of E-type diamonds could have been derived from a crustal carbon reservoir apparently isolated from mantle carbon. The crustal source of carbon is evident from the association of diamonds with meta-sedimentary protoliths, the unusual chemical composition of their fluids and their high-N content (up to 1 wt%) or heavy $\delta^{15}N$ (Cartigny, 2005) that are not found among cratonic diamonds. These fluid phases give diamond the remarkable ability to track carbon mobility in the deep mantle, as well as mantle mineralogy and mantle redox state (e.g., Malkovets et al., 2007; Stagno et al., 2013), and hence follow the path and history of the carbon from which cratonic diamond crystallized. However, recycled sediments also contain light C produced by organisms at or near the surface. Thus, whether or not the light C was mobilized by an aqueous fluid, it had to be present as organic condensed C anyway. Aqueous fluid may well have been present, but the carbon isotopes do not necessarily require it.

It should be noted the early reviews were confined to cratonic and crustal diamond studies as shown in the comparative histograms of Cartigny (2005, Fig. 2) and Shirey et al. (2013, Fig. 7). These reviews provide several key conclusions from the distributions: (1) Worldwide samples cover a large carbon isotopic composition ($\delta^{13}C$) ranging from −41 to +5‰. (2) Approximately 72% are contained within a narrower interval of −8 to −2‰ centered on a value of −5‰ to the range displayed by other mantle-derived rocks such as MORB, OIB, carbonatites, and kimberlites. (3) The $\delta^{13}C$ distributions are significantly different between E- and P-type diamonds. P-type diamonds cover a narrower range of $\delta^{13}C$ values (−26.4 to +0.2‰) than E-type diamonds (−41.3 to +2.7‰); the distribution is continuous with a clear decrease in frequency on either side of mantle $\delta^{13}C$ values of about −5‰. (4) E-type diamonds from the transition zone and lower mantle have variable abundances of negative or positive $\delta^{13}C$ values (mostly below −1.0‰), (5) Metamorphic diamonds in UHP rocks have $\delta^{13}C$ values ranging from −30‰ to −3‰ (Table 4).

In this review, we have included an additional terrestrial type of ophiolite-type diamond occurrence. As well known, ophiolite complexes form by decompressional partial melting of rising asthenospheric mantle at depths of ~30–40 km. However, ophiolite-type diamonds from numerous regions (China, Russia, Myanmar) and Phanerozoic ages were documented in Part II; some diamonds coexist with stishovite, moissanite and many other native elements, alloys, and nitrides, and formed under extremely reducing environments at depths of 150–300 km or ~~even~~ deeper. These ophiolite-type diamonds show many similarities in their morphology, carbon isotopes ($\delta^{13}C$ = −28 to −18‰), trace elements, and mineral inclusions, but are different in these respects from most diamonds occurring in kimberlites, UHP metamorphic belts, and impact craters (e.g., Griffin et al., 2013; Helmstaedt, 2013; Shirey et al., 2013). Many grains also contain micro-inclusions of Ni_{70}-$Mn_{20}Co_5$ alloy and Mn-rich silicates not found in other diamonds. It is clear that the partial melting of decompressing asthenospheric mantle at ~1.0 GPa produced the ophiolitic association of mafic + ultramafic rock type, whereas the subjacent chromatites containing diamond and other UHP phases are relict mantle assemblages previously generated in the deep Earth (some containing recycled continental materials), then transported to the base of the much younger ophiolitic complexes.

4. Epilogue: recycling the Earth's crust

In summary, we have described many eclogite xenoliths and E-type diamonds from kimberlites that show geochemical and isotopic signatures compatible with an origin by subduction of oceanic crustal rocks; they cover both Precambrian and Phanerozoic UHP metamorphic ages. On the other hand, most UHP orogenic belts lie on opposite ends of the geological age spectrum; continental subduction and UHP metamorphism is considered to be a Neoproterozoic or younger process that was not possible in a much hotter early Earth. The Archean underflow and return of oceanic litho-

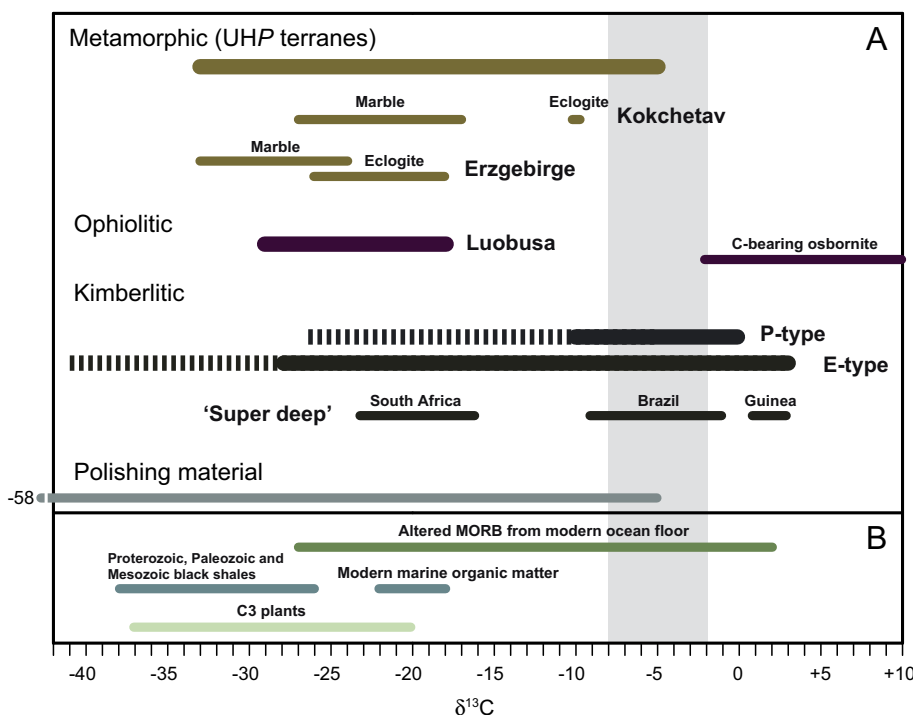**Fig. 13.** (A) $\delta^{13}C$ values of diamonds for metamorphic (UHP), ophiolitic and kimberlitic origins (Table 4). For comparisons, $\delta^{13}C$ values of altered MORB from modern ocean floor, modern marine organic matter, black shales (Phanerozoic, Paleozoic, and Mesozoic ages) and C3 plants are shown (range of values are after Kohn, 2010 and Meyers, 2014).

Table 4
δ^{13}C and δ^{15}N values of UH*P* diamonds from orogens, ophiolitic chromitites and kimberlitic xenoliths.

	Rock type	δ^{13}C	δ^{15}N	N contents	Reference
Orogens					
1. Kokchetav	Grt–Cpx rock	−10.5‰	+5.9‰		De Corte et al. (2000)
	Grt–Cpx rock	−10.5‰ (mean)	+5.9‰ (mean)		Cartigny et al. (2001)
	Marble	−10.2‰	+8.5‰		De Corte et al. (2000)
	Marble	−10.19‰ (mean)	+8.5‰ (mean)		Cartigny (2005)
	Marble	−26.9 to −17.2‰			Imamura et al. (2012)
	Marble (cores)	−13 to −9.3‰			Imamura et al. (2012)
2. Erzgebirge	Ky–Grt–Ph rock	−33 to −24‰			Massonne and Tu (2007)
	Ky–Grt–Ph rock	−25.5 to −17.8‰		740–3377 µg/g	Dobrzhinetskaya et al. (2010)
3. Worldwide	UH*P* metamorphic rocks	−3 to −30‰	−1.8 to +12.4‰		Cartigny (2005)
Kimberlitic xenoliths	E-type	−26.4 to +0.2‰	−12.4 to +18‰	Average ∼300 µg/g	Cartigny (2005)
	P-type	−38.5 to +2.7‰	−20 to +12‰	Average ∼200 µg/g	Cartigny (2005)
			∼−5‰		Imamura et al. (2012)
Ophiolitic chromitite	Chromitite	−28 to −18‰		20–670 µg/g	Yang et al. (2013a)

sphere to the deep mantle undoubtedly took place, but large tracts of continental crust may have been nearly unsubductable. Studies of UH*P* rocks have been dominately carried out on continental supracrustal lithologies. Their return to the Earth's surface attended tectonic exhumation as the result of continental collision. However, subduction of oceanic crust must have preceded continental underflow; in fact, immense volumes of oceanic materials subducted prior to collisions are expected to undergo UH*P* metamorphism after descending to depths >90–100 km. The petrological–geochemical evidence described in this review are consistent with a model that diamond- and coesite-bearing UH*P* orogens and diamond/coesite mantle eclogite xenoliths are complementary end products of subduction-zone metamorphism. The former represent low-density supracrustal assemblages that are tectonically exhumed during continental collision. The latter are parts of the oceanic slabs that were subducted prior to continental collision and were accreted to the lithospheric roots of pre-existing cratons or cratonic nuclei.

Since the subduction of the oceanic lithosphere began about 3.0 Ga (Shirey and Richardson, 2011; Shirey et al., 2013), or perhaps much earlier (Ernst, 1991, 2009), abundant oceanic and minor continental materials have been returned to the deep mantle; some relics have been preserved metastably as inclusions in rigid minerals such as zircon, garnet and chromite. Others were metamorphosed to eclogite-facies, and resided long enough in the diamond stability field for carbon or C–O–H fluid to crystallize as cratonic or ophiolite-type diamond with well-aggregated nitrogen before exhumation in younger igneous rocks, such as chromitites, harzburgites, kimberlites or lamproites.

The presence of UH*P* minerals within ophiolitic chromitites has long been considered "forbidden" by conventional concepts of ophiolite genesis under high-*T* and low-*P* conditions in mid-oceanic ridges or back-arc spreading realms. These new, unexpected findings should renew interest in the exploration for UH*P* minerals and rocks in both ophiolitic and granulite terranes. The isotopic and inclusion characteristics of kimberlitic diamonds provide compelling evidence for deep subduction of oceanic lithosphere, injection of surface 'organic' carbon into the lower mantle, and eventual return to the Earth surface through ascent of deep mantle plumes. Diamonds and moissanite from ophiolitic chromitites in southern Tibet and the Polar Urals have extremely light δ^{13}C values, −29 to −18‰, much lighter than most kimberlitic diamonds, −10 to −5‰. Although the origin of such low isotopic composition in diamonds remains under debate, numerous studies of carbon isotopic compositions of 'super deep' kimberlitic diamonds from Brazil suggest that they, too, were derived from deep mantle recycling of oceanic crust (e.g. Taylor and Anand, 2004; Wirth et al., 2009; Walter et al., 2011). Investigations of composite mineral inclusions in Brazilian diamonds indicate that these

diamonds crystallized under lower mantle *P–T* conditions; for example, inclusions of tetragonal almandine pyrope phase was suggested to be a retrograde phase of Mg-perovskite stable at *P* > 30 GPa (Armstrong and Walter, 2012).

Over the last decade, global mantle seismic tomography has provided images of slab stagnation (e.g. Fukao et al., 2009). The presence of recycled materials in the peridotitic mantle and the entire subduction/mantle plume cycle is also supported by abundant geochemical evidence (e.g. Sobolev et al., 2007). Isotope geochemistry of orogenic peridotites implies that primary isotope signatures of oceanic residual mantle can be retained in the mantle for at least 1 Gyr without being homogenized by global mantle convection (Malaviarachichi et al., 2008, 2010). Crust-derived quartz-bearing zircons occur as inclusions in garnet peridotite xenoliths from the Tran-North China orogenic belt (Liu et al., 2010). Abundant crust-derived recycled zircons were also described in orogenic peridotite (dunite) from the Ural Mountains (Bea et al., 2001). Moreover, xenolithic eclogites with heavy δ^{18}O values in garnet from diamondiferous kimberlites were also considered as indicators of an ancient subducted oceanic crust rather than having a magmatic origin (e.g. Spetsius et al., 2008).

5. Final remarks

Much of this paper has involved an exhaustive listing and description of a wide range of prior studies by many workers on rocks and especially on mineral inclusions in host lithologies that unambiguously document the introduction of crustal phases into the deep mantle. Such crustal relics have been incorporated as trace assemblages in subsequently exhumed UH*P* metamorphic complexes, sub-ophiolitic chromitites, and ultramafic diatrimes—transporting media of vastly contrasting genesis. These relict phases and rocks document not only the recycling of crustal lithosphere into the deep Earth, but also yield a glimpse of an evident compositional heterogeneity of the thermally driven, dynamically circulating mantle.

References

Anand, M., Taylora, L.A., Misraa, K.C., Carlson, W.D., Sobolev, N.V., 2004. Nature of diamonds in Yakutian eclogites: views from eclogite tomography and mineral inclusions in diamonds. Lithos 77, 333–348.

Arai, S., 2010. Possible recycled origin for ultrahigh-pressure chromites in ophiolites. J. Petrol. Mineral. Sci. 105, 280–285.

Arai, S., 2013. Conversion of low-pressure chromitites to ultrahigh-pressure chromitites by deep recycling: a good inference. Earth Planet. Sci. Lett. 379, 81–87.

Armstrong, L.S., Walter, M.J., 2012. Tetragonal almandine pyrope phase (TAPP): retrograde Mg-perovskite from subducted oceanic crust? Eur. J. Mineral. 24, 587–597.

Bai, W.J., Zhou, M.F., Robinson, P.T., 1993. Possible diamond-bearing mantle peridotites and chromitites in the Luobusa and Dongiao ophiolites, Tibet. Can. J. Earth Sci. 30, 1650–1659.

Bai, W.J., Robinson, P.T., Fang, Q.S., Yang, J.S., Yan, B., Zhang, Z., Hu, X.-F., Zhou, M.-F., Malpas, J., 2000. The PGE and base-metal alloys in the podiform chromitites of the Luobusha ophiolite, southern Tibet. Can. Mineral. 38, 585–598.

Bai, W.J., Yang, J.S., Fang, Q.S., Yan, B.S., Zhang, Z.M., 2001. Explosion of ultrahigh pressure minerals in the mantle. Acta Geosci. Sin. 22, 385–390.

Bai, W., Shi, N., Fang, Q.S., Li, G., Xiong, M., Yang, J.S., Rong, H., 2006. Luobusaite, a new mineral. Acta Geosci. Sin. 80, 656–659.

Bakun-Czubarow, N., 1991. On the possibility of occurrence of quartz pseudomorphs after coesite in the eclogite-granulite rock series of the Zlote Mountains in the Sudetes, SW Poland. Arch. Mineral. 48, 3–25.

Baldwin, S.L., Monteleone, B., Webb, L.E., Fitzgerald, G., Grove, M., Hill, E.J., 2004. Pliocene eclogite exhumation at plate tectonic rates in eastern Papua New Guinea. Nature 431, 263–267.

Baldwin, S.L., Webb, L.E., Monteleone, B., 2008. Late Miocene coesite-bearing eclogite exhumed in the Woodlark Rift. Geology 36, 735–738.

Baldwin, S.L., Fitzgerald, P.G., Webb, L.E., 2012. Tectonics of the New Guinea region. Annu. Rev. Earth Planet. Sci. 40, 495–520.

Banas, A., Stachel, T., Muehlenbachs, K., McCandless, T.E., 2007. Diamonds from the Buffalo Head Hills, Alberta: formation in a non-conventional setting. Lithos 93, 199–213.

Barron, B.J., Barron, L.M., Dungan, G., 2005. Eclogitic and ultrahigh-pressure crustal garnets and their relationship to Phaneroozoic subduction diamonds, Bingara Area, New England Fold belt, eastern Australia. Econ. Geol. 100, 1565–1582.

Barron, L.M., Barron, B.J., Mernagh, T.P., Birch, W.D., 2008. Ultrahigh pressure macro diamonds from Copeton (New South Wales, Australia), based on Raman spectroscopy of inclusions. Ore Geol. Rev. 34, 76–86.

Bea, F., Fershtater, G.B., Montero, P., Whitehouse, M., Levin, V.Y., Scarrow, J.H., Austrheim, H., Pushkariev, E.V., 2001. Recycling of continental crust into the mantle as revealed by Kytlym dunite zircons, Ural Mts, Russia. Terra Nova 13, 407–412.

Bercovici, D., Karato, S., 2003. Whole-mantle convection and the transition-zone water filter. Nature 425, 39–44.

Biino, G., Compagnoni, R., 1992. Very-high pressure metamorphism of the Brossasco coronite meta-granite, southern Dora Maira Massif, Western Alps. Schweiz. Mineral. Petrogr. Mitt. 72, 347–363.

Bobrievich, A.P., Smirnov, G.I., Sobolev, V.S., 1960. On the mineralogy of xenoliths of grossular-pyroxene-disthene rock from Yakutian kimberlites. Geol. Geofiz. 1, 18–24.

Borisova, A., Ceuleneer, G., Kamenetsky, V., Arai, S., Bejina, F., Bindeman, I., Polve, M., Deprseval, P., Aigouy, T., Pokrovski, G., 2012. A new view on the petrogenesis of the Oman ophiolite chromitites from microanalyses of chromite-hosted inclusions. J. Petrol. 53, 2411–2440.

Brown, M., 2007. Metamorphic conditions in orogenic belts: a record of secular change. Int. Geol. Rev. 49, 193–234.

Bulanova, G.P., Walter, M.J., Smith, C.B., Kohn, S.C., Armstrong, L.S., Blundy, J., Gobbo, L., 2010. Mineral inclusions in sublithospheric diamonds from Collier 4 kimberlite pipe, Juina, Brazil: subducted protoliths, carbonated melts and primary kimberlite magmatism. Contrib. Miner. Petrol. 160, 489–510.

Burov, E., Yamato, P., 2008. Continental plate collision, P–T–t–z conditions and unstable vs. stable plate dynamics: insights from thermo-mechanical modelling. Lithos 25, 178–204.

Butler, J.P., Beaumont, C., Jamieson, R.A., 2011. Crustal emplacement of exhuming (ultra)high-pressure rocks: will that be pro- or retro-side? Geology 39, 635–638.

Butler, J.P., Jamieson, R.A., Steenkamp, H., Robinson, P., 2013. Discovery of coesite–eclogite from the Nordøyane UHP domain, Western Gneiss Region, Norway: field relations, metamorphic history, and tectonic significance. J. Metamorph. Geol. 31, 147–163.

Carmody, L., Barry, P.H., Shervais, J.W., Kluesner, J.W., Taylor, L.A., 2011. Oxygen isotopes in subducted oceanic crust: a new perspective from Siberian diamondiferous eclogites. Geochem. Geophys. Geosyst. 14, 3479–3493.

Carswell, D.A., 1990. Eclogite and the eclogite facies: definitions and classification. In: Carswell, D.A. (Ed.), Eclogite Facies Rocks. Blackie, New York, pp. 1–13.

Carswell, D.A., 1991. Variscan high P–T metamorphism and uplift history in the Moldanubian Zone of the Bohemian Massif in lower Austria. Eur. J. Mineral. 3, 323–342.

Carswell, D.A., O'Brien, P.J., 1993. Thermobarometry and geotectonic significance of high-pressure granulites: examples from the Moldanubian Zone of the Bohemian Massif in Lower Austria. J. Petrol. 34, 427–459.

Carswell, D.A., Brueckner, H.K., Cuthbert, S.J., Mehta, K., O'Brien, P.J., 2003. The timing of stabilisation and the exhumation rate for ultra-high pressure rocks in the Western Gneiss Region. J. Metamorph. Geol. 21, 601–612.

Cartigny, P., 2005. Stable isotopes and the origin of diamond. Elements 1, 79–84.

Cartigny, P., De Corte, K., Shatsky, V.S., Ader, M., De Paepe, P., Sobolev, N.V., Javoy, M., 2001. The origin and formation of metamorphic microdiamonds from the Kokchetav massif, Kazakhstan: a nitrogen and carbon isotopic study. Chem. Geol. 176, 265–281.

Cassard, D., Nicolas, A., Rabinovitch, M., Moutte, J., LEeblanc, M., Prinzhofer, A., 1981. Structural classification of chromite pods in southern New Caledonia. Econ. Geol. 76, 805–831.

Chen, M., Shu, J., Mao, H.K., Hemley, R.J., 2003. Natural occurrence and synthesis of two new postspinel polymorphs of chromite. Proc. Natl. Acad. Sci. 100, 14651–14654.

Chen, Y.-X., Ye, K., Wu, T.F., Guo, S., 2013a. Exhumation of oceanic eclogites: thermodynamic constraints on pressure, temperature, bulk composition and density. J. Metamorph. Geol. 31, 549–570.

Chen, Y.-X., Zheng, Y.-F., Hu, Z., 2013b. Petrological and zircon evidence for anatexis of UHP quartzite during continental collision in the Sulu orogen. J. Metamorph. Geol. 31, 389–413.

Chopin, C., 1984. Coesite and pure pyrope in high-grade blueschists of the Western Alps: a first record and some consequences. Contrib. Miner. Petrol. 86, 107–118.

Coleman, R.G., 1977. Ophiolites—Ancient Oceanic Lithosphere? Springer-Verlag, Berlin, Heidelberg, New York, 229 pp.

Coleman, R.G., Lee, D.E., Beatty, L.B., Brannock, W.W., 1965. Eclogites and eclogites: their differences and similarities. Geol. Soc. Am. Bull. 76, 483–508.

Cortesogno, L., Ernst, W.G., Galli, M., Messiga, B., Pedemonte, G.M., Piccardo, G.P., 1977. Chemical petrology of eclogitic lenses in serpentinite, Gruppo di Voltri, Ligurian Alps. J. Geol. 85, 255–277.

Cuthbert, S., Carswell, D.A., Krogh Ravna, E.J., Wain, A., 2000. Eclogites and eclogites in the Western Gneiss Region, Norwegian Caledonides. Lithos 52, 165–195.

Daniels, L.R., Gurney, J.J., Harte, B., 1996. A crustal mineral in a mantle diamond. Nature 379, 153–156.

Davidson, L.M., 1979. Nagssugtoqidian granulite facies metamorphism in the Holsteinsborg region, West Greenland. Grønl. Geol. Undersøgelse Rapport 89, 97–108.

Davies, R.M., O'Reilly, S.Y., Griffin, W.L., 1999. Diamonds from Wellington, NSW: insights into the origin of eastern Australian diamonds. Mineral. Mag. 63, 447–471.

Davies, R.M., O'Reilly, S.Y., Griffin, W.L., 2002. Multiple origins of alluvial diamonds from New South Wales, Australia. Econ. Geol. 97, 109–123.

Davies, R.M., Griffin, W.L., O'Reilly, S.Y., Doyle, B.J., 2004. Mineral inclusions and geochemical characteristics of microdiamonds from the DO27, A154, A21, A418, DO18, DD17 and Ranch Lake kimberlites at Lac de Gras, Slave Craton, Canada. Lithos 77, 39–55.

Day, H., 2012. A revised diamond-graphite transition curve. Am. Mineral. 97, 52–62.

De Corte, K., Cartigny, P., Shatsky, V.S., Sobolev, N.V., Javoy, M., 1998. First evidence of fluid inclusions in metamorphic microdiamonds from the Kokchetav Massif, Northern Kazakhstan. Geochim. Cosmochim. Acta 62, 3765–3773.

De Corte, K., Korsakov, A., Taylor, W.R., Cartigny, P., Ader, M., De Paepe, P., 2000. Diamond growth during ultrahigh-pressure metamorphism of the Kokchetav Massif, northern Kazakhstan. Island Arc. 9, 428–438.

Dick, H., 1974. Terrestrial nickel-iron from the Josephine peridotite, its geologic occurrence, associations and origin. Earth Planet. Sci. Lett. 224, 291–298.

Dilek, Y., 2003. Ophiolite concept and its evolution. Geol. Soc. Am. Spec. Pap. 373, 1–16.

Dilek, Y., Furnes, H., 2011. Ophiolite genesis and global tectonics: geochemical and tectonic fingerprinting of ancient oceanic lithosphere. Geol. Soc. Am. Bull. 123, 387–411.

Dilek, Y., Furnes, H., 2014. Ophiolites and their origins. Elements 10, 2–9.

Dilek, Y., Newcomb, S., 2003. Ophiolite Concept and the Evolution of Geological Thought. Geological Society of American Special Paper 373, 504 pp.

Dobrzhinetskaya, L.F., 2012. Microdiamonds-frontier of ultrahigh-pressure metamorphism: a review. Gondwana Res. 21, 207–223.

Dobrzhinetskaya, L.F., Faryad, S.W., 2011. Frontiers of ultrahigh-pressure metamorphism: view from field and laboratory. In: Dobrzhinetskaya, L.F., Faryad, S.W., Wallis, S., Cuthbert, S. (Eds.), e-Book UHP Metamorphism, 25 years after Findings of Coesite and Diamond. Elsevier, pp. 1–40.

Dobrzhinetskaya, L.F., Green, H.W., 2007. Experimental studies of mineralogical assemblages of metasedimentary rocks at Earth's mantle transition zone conditions. J. Metamorph. Geol. 25, 83–96.

Dobrzhinetskaya, L.F., Eide, E.A., Larsen, R.B., Sturt, B.A., Tronnes, R.G., Smith, D.C., Taylor, W.R., Posukhova, T., 1995. Microdiamond in high-grade metamorphic rocks of the Western Gneiss region, Norway. Geology 23, 597–600.

Dobrzhinetskaya, L.F., Green, H.W., Mitchell, T.E., Dickerson, R.M., 2001. Metamorphic diamonds: mechanism of growth and inclusion of oxides. Geology 29, 263–266.

Dobrzhinetskaya, L.F., Wirth, R., Green, H.W., 2006a. Nanometric inclusions of carbonates in Kokchetav diamonds from Kazakhstan: a new constraint for the depth of metamorphic diamond crystallization. Earth Planet. Sci. Lett. 243, 85–93.

Dobrzhinetskaya, L.F., Liu, Z.X., Cartigny, P., Zhang, Z.F., Tchkhetia, D., Hemley, R.J., Green, H.W., 2006b. Synchrotron infrared and Raman spectroscopy of microdiamonds from Erzgebirge, Germany. Earth Planet. Sci. Lett. 248, 340–349.

Dobrzhinetskaya, L.F., Wirth, R., Yang, J.S., Hutcheon, I.D., Weber, P.K., Green, H.W., 2009. High-pressure highly reduced nitrides and oxides from chromitite of a Tibetan ophiolite. Proc. Natl. Acad. Sci. 106, 19233–19238.

Dobrzhinetskaya, L.F., Green, H.W., Takahata, N., Sano, Y., Shirai, K., 2010. Crustal signature of $\delta^{13}C$ and nitrogen content in microdiamonds from Erzgebirge, Germany: ion microprobe studies. J. Earth Sci. 21, 623–634.

Dobrzhinetskaya, L.F., Faryad, S.W., Hoinkes, G., 2013a. Mineral transformations in HP–UHP metamorphic terranes: experiments and observations. J. Metamorph. Geol. 31, 3–4.

Dobrzhinetskaya, L.F., Wirth, R., Green, H.W., Schreiber, A., O'Bannon, E., 2013b. First find of polycrystalline diamond in ultrahigh-pressure metamorphic terrane of Erzgebirge, Germany. J. Metamorph. Geol. 31, 5–18.

Dobrzhinetskaya, L., Wirth, R., Green, H., 2014a. Diamonds in Earth's oldest zircons from Jack Hills conglomerate, Australia, are contamination. Earth Planet. Sci. Lett. 387, 212–218.

Dobrzhinetskaya, L.F., Wirth, R., Yang, J.S., Green, H.W., Hutcheon, I.D., Weber, P.K., Grew, E.S., 2014b. Qingsongite, natural cubic boron nitride: the first boron mineral from the Earth's mantle. Am. Mineral. 99, 764–772.

Dubinchuk, V.T., Simakov, S.K., Pechnikov, V.A., 2010. Lonsdaleite in diamond-bearing metamorphic rocks of the Kokchetav Massif. Dokl. Earth Sci. 430, 40–42.

El Atrassi, F., Brunet, F., Bouybaouene, M., Chopin, C., Chazot, G., 2011. Melting textures and microdiamonds preserved in graphite pseudomorphs from the Beni Bousera peridotite massif, Morocco. Eur. J. Mineral. 23, 157–168.

Ernst, W.G., 1970. Tectonic contact between the Franciscan melange and the Great Valley sequence, crustal expression of a Late Mesozoic Benioff zone. J. Geophys. Res. 75, 886–901.

Ernst, W.G., 1972. Occurrence and mineralogical evolution of blueschist belts with time. Am. J. Sci. 272, 657–668.

Ernst, W.G., 1973. Blueschist metamorphism and P–T regimes in active subduction zone. Tectonophysics 17, 255–272.

Ernst, W.G., 1991. Evolution of the lithosphere, and inferred increasing size of mantle convection cells over geologic time. In: Purchuk, L.L. (Ed.), Korzhinskii Volume, Progress in Metamorphic and Magmatic Petrology. Cambridge University Press, Cambridge, UK, pp. 369–386.

Ernst, W.G., 2005. Alpine and Pacific styles of Phanerozoic mountain building: subduction-zone petrogenesis of continental crust. Terra Nova 17, 165–188.

Ernst, W.G., 2009. Archean plate tectonics, rise of Proterozoic supercontinentality and onset of regional, episodic stagnant-lid behavior. Gondwana Res. 15, 243–253.

Evans, B.W., 1977. Metamorphism of alpine peridotite and serpentinite. Annu. Rev. Earth Planet. Sci. 5, 397–447.

Fang, Q.-S., Bai, W.J., 1986. Characteristics of diamond and diamond-bearing ultramafic rocks in Qiaoxi and Hongqu, Xizang. Inst. Geol. Bull. Chin. Acad. Geol. Sci. 14, 62–125 (in Chinese).

Fang, Q.-S., Bai, W.J., Yang, J.S., Xu, X.Z., Li, G.W., Shi, N.C., Xiong, M., Rong, H., 2009. Qusongite (WC): a new mineral. Am. Mineral. 94, 387–390.

Fang, Q.S., Bai, W.J., Yang, J.S., Rong, H., Shi, N.C., Li, G.W., Xiong, M., Ma, Z.S., 2013. Titanium, Ti, a new mineral species from Luobusha, Tibet China. Acta Geol. Sini. 87, 1275–1280.

Faryad, S.W., 2009. The Kutna Hora Complex (Moldanubian zone, Bohemian Massif): a composite of crustal and mantle rocks subducted to HP/UHP conditions. Lithos 109, 193–208.

Faryad, S.W., Dobrzhinetskaya, L.F., Hoinkes, G., Zhang, J.G., 2013. Ultrahigh-pressure and high-pressure metamorphic terranes in orogenic belts: reactions, fluids and geological processes: preface. Gondwana Res. 23, 841–843.

Frezzotti, M.L., Selverstone, J., Sharp, Z.D., Compagnoni, R., 2011. Carbonate dissolution during subduction revealed by diamond-bearing rocks from the Alps. Nat. Geosci. 4, 703–706.

Frezzotti, M.F., Huizenga, J.M., Compagnoni, R., Selverstone, J., 2014. Diamond formation by carbon saturation in C–O–H fluids during cold subduction of oceanic lithosphere. Geochem. Cosmochimi. Ac,. http://dx.doi.org/10.1016/j.gca.2013.12.022.

Fukao, Y., Obayashi, M., Nakakuki, T. The Deep Slab Project Group, 2009. Stagnant slab: a review. Annu. Rev. Earth Planet. Sci. 37, 19–46.

Gaillou, E., Post, J.E., Butler, J.E., 2012. Boron in natural type IIb blue diamonds: chemical and spectroscopic measurements. Am. Mineral. 97, 1–18.

Gee, D.G., Juhlin, C., Pascal, C., Robinson, P., 2010. Collisional orogeny in the Scandinavian caledonides (COSC). GFF 132, 29–44.

Gerya, T., 2011. Future directions in subduction modeling. J. Geodyn. 52, 344–378.

Gerya, T.V., Perchuk, L.L., Burg, J.P., 2008. Transient hot channels: perpetrating and regurgitating ultrahigh-pressure, high-temperature crust–mantle associations in collision belts. Lithos 103, 236–256.

Gilotti, J.A., 2013. The realm of ultrahigh-pressure metamorphism. Elements 9, 255–260.

Gilotti, J.A., McClelland, W.C., 2011. Geochemical and geochronological evidence that the North-East Greenland ultrahigh-pressure terrane is Laurentian crust. J. Geol. 119, 439–456.

Gilotti, J.A., McClelland, W.C., Wooden, J.L., 2014. Zircon captures exhumation of an ultrahigh-pressure terrane, North-East Greenland Caledonides. Gondwana Res. 25, 2235–2256.

Glassley, W.E., Sørensen, K., 1980. Constant Ps-T amphibolite to granulite facies transition in Agto (West Greenland) metadolerites: implications and applications. J. Petrol. 21, 69–105.

Glassley, W.E., Korstgård, J.A., Sørensen, K., 2010. K-rich brine and chemical modification of the crust during continent–continent collision, Nagssugtoqidian Orogen, West Greenland. Precambr. Res. 180, 47–62.

Glassley, W.E., Korstgard, J.A., Sorensen, K., Platou, S.W., 2014. A new UHP metamorphic complex in the ~1.8 Ga Nagssugtoqidian Orogen of West Greenland, and the possible first terrestrial evidence for ringwoodite. Am. Mineral. 99, 1315–1334.

Gómez-Pugnaire, M.T., Rubatto, D., Ferńandez-Soler, J.M., Jabaloy, A., López Sánchez-Vizcáino, V., 2012. Late Variscan magmatism in the Nevado-Filábride Complex: U–Pb geochronologic evidence for the pre-Mesozoic nature of the deepest Betic complex (SE Spain). Lithos 146–147, 93–111.

González-Jiménez, J.M., Griffin, W.L., Proenza, J.A., Gervilla, F., O'Reilly, S.Y., Akbulut, M., Pearson, N.J., Arai, S., 2014. Chromitites in ophiolites: how, where, when, why?, Part II. The crystallization of chromitites. Lithos 189, 140–158.

Gordeev, E.I., Karpov, G.A., Anikin, L.P., Krivovichev, S.V., Filatov, S.K., Antonov, A.V., Ovsyannikov, A.A., 2014. Diamonds in lavas of the Tolbachik fissure eruption in Kamchatka. Dokl. Earth Sci. 454, 47–49.

Griffin, W.L., Yang, J.S., Robinson, P., Howell, D., Shi, R.D., O'Reilly, S.Y., Pearson, N.J., 2013. Going up or going down? Diamonds and super-reducing UHP assemblages in ophiolitic mantle. In: Goldschmidt 2013 Conference Abstracts, 1215.

Groppo, C., Beltrando, M., Compagnoni, R., 2009. P-T path of the UHP Lago di Cignana and adjoining HP meta-ophiolitic units: insights into the evolution of subducting Tethyan slab. J. Metamorph. Geol. 27, 207–231.

Guo, S., Ye, K., Wu, Y.F., Chen, Y., Yang, Y.H., Zhang, L.M., Liu, J.B., Mao, Q., Ma, Y.G., 2013. A potential method to confirm the previous existence of lawsonite in eclogite: the mass imbalance of Sr and LREEs in multistage epidote (Ganghe, Dabie UHP terrane). J. Metamorph. Geol. 31, 415–435.

Hacker, B.R., Ratscbacner, L., Liou, J.G., 2004. Subduction, collision, and exhumation in the Qinling-Dabie Orogen: a review. In: Malpas, John (Ed.), Aspects of the Tectonic Evolution of China. Geological Society of London, Special Paper 226, pp. 157–175.

Hacker, B.R., Anderson, T.B., Johnston, S., Kylander-Clark, A.R.C., Peterman, E.M., Walsh, E.O., Young, D., 2010. High-temperature deformation during continental-margin subduction and exhumation: the ultrahigh-pressure Western Gneiss Region of Norway. Tectonophysics 480, 149–171.

Hacker, B.R., Gerya, T.V., Gilotti, J.A., 2013. Formation and exhumation of ultrahigh-pressure terranes. Elements 9, 289–293.

Harley, S.L., 1998. On the Occurrence and Characterization of Ultrahigh-temperature Crustal Metamorphism. Geological Society, London, Special Publications 138, pp. 81–107.

Harlow, G.E., Davies, R., 2004. Status report on K-rich phases at mantle conditions. Selected Papers from the Eighth International Kimberlite Conference 2. Lithos 77, 647–653.

Harlow, G.E., Tsujimori, T., Sorensen, S.S., 2015. Jadeitites and plate tectonics. Annu. Rev. Earth Planet. Sci. 43, in press.

Harte, B., 2010. Diamond formation in the deep mantle: the record of mineral inclusions and their distribution in relation to mantle dehydration zones. Mineral. Mag. 74, 189–215.

Harte, B., 2011. Diamond window into the lower mantle. Science 334, 51–52.

Harte, B., Harris, J.W., Hutchison, M.T., Watt, G.R., Wilding, M.C., 1999. Lower mantle mineral associations in diamonds from Sao Luiz, Brazil. In: Fei, Y., Bertka, C.M., Mysen, B.O. (Eds.), Mantle Petrology: Field Observations and High Pressure Experimentation: A Tribute to Francis R. (Joe) Boyd. Geochemical Society Special Publication 6, pp. 125–153.

Helmstaedt, H.H., 2013. Tectonic relationships between E-type cratonic and ultrahigh-pressure (UHP) diamond: implications for craton formation and stabilization. In: Pearson, D.G. et al. (Eds.), Proceedings of 10th International Kimberlite Conference 1, Special Issue of the Journal of the Geological Society of India. http://dx.doi.org/10.1007/978-81-322-1170-9_4.

Helmstaedt, H., Doig, R., 1975. Eclogitic nodules from kimberlite pipes of the Colorado Plateau: samples of subducted Franciscan-type oceanic lithosphere. Phys. Chem. Earth 9, 95–111.

Hermann, J., Rubatto, D., 2014. Subduction of continental crust to mantle depth: geochemistry of ultrahigh-pressure rocks, . second ed.. In: Holland, H.D., Turekian, K.K. (Eds.), Treatise on Geochemistry second ed., vol. 4 Elsevier Science and Technology, Amsterdam, pp. 309–340.

Hermann, J., Zheng, Y.F., Rubatto, D., 2013. Deep fluids in subducted continental crust. Elements 9, 281–287.

Heylmun, E.B., 1999. California diamonds. California Min. J. 68, 45–47.

Hirajima, T., Zhang, R.Y., Li, J., Cong, B., 1992. Nyböite from the Donghai area, Jiangsu Province, eastern China. Mineral. Mag. 56, 37–46.

Hopkins, M., Harrison, T.M., Manning, C.E., 2008. Low heat flow inferred from > 4Gyr zircons suggest Hadean plate boundary interactions. Nature 456, 493–496.

Hopkins, M., Harrison, T.M., Manning, C.E., 2010. Constraints on Hadean geodynamics from mineral inclusions in >4 Ga zircons. Earth Planet. Sci. Lett. 298, 367–376.

Hopkins, M., Harrison, T.M., Manning, C.E., 2012. Metamorphic replacement of mineral inclusions in detrital zircon from Jack Hills, Australia: implications for the Hadean Earth: comment. Geology 40, e281.

Howarth, G.H., Sobolev, N.V., Pernet-Fisher, J.F., Barry, P.H., Penumalu, D., Puplampppu, S., Ketcham, R.A., Maisano, J.A., Pokhilenko, L.A., Taylor, D., Taylor, L.A., 2014. The secondary origin of diamonds: multi-modal radiation tomography of diamondiferous mantle eclogites. Int. Geol. Rev. 56, 1172–1180.

Howarth, G.H., Sobolev, N.V., Pernet-Fisher, J.F., Ketcham, R.A., Maisano, J.A., Pokhilenko, L.A., Taylor, D., Taylor, L.A., in press. 3D X-ray tomography of diamondiferous mantle eclogite xenoliths, Siberia: a review. J. Asian Earth Sci.

Hu, X.-F., 1999. Origin of Diamonds in Chromitites of the Luobusa Ophiolite, South Tibet, China. MSc Thesis, Dalhousie University, Halifax, Nova Scotia, pp. 160.

Hu, N.G., Zhao, D.G., Xu, B.Q., Wang, T., 1995. Discovery of coesite-bearing eclogites from the Northern Qinling and its significances. Chin. Sci. Bull. 40, 174–176.

Huang, X., Xu, Y., Karato, S., 2005. Water content of the mantle transition zone from the electrical conductivity of wadsleyite and ringwoodite. Nature 434, 746–749.

Huang, M.X., Yang, J.J., Powell, R., Mo, X., 2014. High-pressure metamorphism of serpentinitzed chromitite at Luobusha (Southern Tibet). Am. J. Sci. 314, 400–433.

Hwang, S.L., Shen, P., Chu, H.T., Yui, T.F., 2000. Nanometer-size α-PbO₂-type TiO₂ in garnet: a thermobarometer for ultrahigh-pressure metamorphism. Science 288, 321–324.

Hwang, S.L., Shen, P., Chu, H.T., Yui, T.F., Liou, J.G., Sobolev, N., Zhang, R.Y., Shatsky, S., Zayachkovsky, A.A., 2004. Kokchetavite, a new K-feldspar polymorph from the Kokchetav ultrahigh-pressure terrane. Contrib. Miner. Petrol. 148, 380–389.

Hwang, S.L., Shen, P., Chu, H.T., Yui, T.F., 2006. A new occurrence and new data on akdalaite, a retrograde mineral from UHP whiteschist, Kokchetav massif, northern Kazakhstan. Int. Geol. Rev. 48, 754–764.

Hwang, S.-L., Shen, P., Chu, H.T., Yui, T.F., Liou, J.G., Sobolev, N.V., 2009. Kumdykolite, an orthorhombic polymorph of albite, from the Kokchetav ultrahigh-pressure massif, Kazakhstan. Eur. J. Mineral. 21, 1325–1334.

Hwang, S.-L., Yui, T.F., Chu, H.T., Shen, P., Liou, J.G., Sobolev, N.V., 2013. Oriented kokchetavite compound rods in clinopyroxene of Kokchetav ultrahigh-pressure rocks. J. Asian Earth Sci. 63, 56–69.

IGCAGS (Institute of Geology, Chinese Academy of Geological Science), 1981. The discovery of alpine-type diamond bearing ultrabasic intrusions in Xizang (Tibet). Geol. Rev. 27, 455–457 (in Chinese).

Imamura, K., Ogasawara, Y., Yurimoto, H., Kusaka, M., 2012. Carbon isotope heterogeneity in metamorphic diamond from the Kokchetav UHP dolomite marble, northern Kazakhstan. Int. Geol. Rev. 55, 453–467.

Ingle, S., Weis, D., Frey, F.A., 2002. Indian continental crust recovered from Elan Bank, Kerguelen Plateau (ODP Leg 183, Site 1137). J Petrol. 43, 1241–1257.

Jacob, D., Foley, S.F., 1999. Evidence for Archean ocean crust with low high field strength element signature from diamondiferous eclogite xenoliths. Lithos 48, 317–336.

Jacob, D., Jagoutz, E., Lowry, D., Mattey, D., Kudrjavtseva, G., 1994. Diamondiferous eclogites from Siberia: remnants of Archean oceanic crust. Geochim. Cosmochim. Acta 58, 5191–5207.

Jahn, B.M., Cornichet, J., Cong, B.L., Yui, T.F., 1996. Ultra-high εNd eclogites from an ultra-high pressure metamorphic terrane of China. Chem. Geol. 127, 61–79.

Janák, M., Krogh Ravana, E.J., Kullerund, K., Yoshida, K., Milovsky, R., Hirajima, T., 2013a. Discovery of diamond in the Tromso Nappe, Scandinavian Caledonides (N. Norway). J. Metamorph. Geol. 31, 691–703.

Janák, M., van Roermund, H., Majka, J., Gee, D., 2013b. UHP metamorphism recorded by kyanite-bearing eclogites from the Seve Nappe Complex of northern J€amtland, Swedish Caledonides. Gondwana Res. 23, 865–879.

Jaques, A.L., Hall, A.E., Sheraton, J.W., Smith, C.B., Sun, S.S., Drew, R.M., Foudoulis, C., Ellingsen, K., 1989. Composition of crystalline inclusions and C isotopic composition of Argyle and Ellendale diamonds. In: Ross, J. (Ed.), Kimberlites and Related Rocks. Geological Society of Australia Special Publication 14, pp. 966–989.

Ji, S., Xu, Z., 2009. Drilling deep in ultrahigh-pressure terrane. Tectonophysics 475, 201–203.

Kahoui, M., Kaminsky, F.V., Griffin, W.L., Belousova, E., Mahdjoub, Y., Chabane, M., 2012. Detrital pyrope garnets from the El Kseibat area, Algeria: a glimpse into the lithospheric mantle beneath the northeastern edge of the West African Craton. J. Afr. Earth Sci. 63, 1–11.

Kaminsky, F.V., 2012. Mineralogy of the lower mantle: a review of 'super-deep' mineral inclusions in diamond. Earth Sci. Rev. 110, 127–147.

Kaminsky, F.V., Khachatryan, G.K., Andreazza, P., Araujo, D., Griffin, W.L., 2009. Super-deep diamonds from kimberlites in the Juina area, Mato Grosso State, Brazil. Lithos 112, 833–842.

Katayama, I., Maruyama, S., 2009. Inclusion study in zircon from ultrahigh-pressure metamorphic rocks in the Kokchetav massif: an excellent tracer of metamorphic history. J. Geol. Soc. London 166, 783–796.

Katayama, I., Nakashima, S., 2003. Hydroxyl in clinopyroxene from the deep subducted crust: evidence for H₂O transport into the mantle. Am. Mineral. 88, 229–234.

Katayama, I., Ota, M., Ogasawara, Y., 2002. Phengite exsolution in diopside in diamond-bearing marbles from Kumdy-Kohl. In: Parkinson, C.D., Katayama, I., Liou, J.G., Maruyama, S. (Eds.), The Diamond-bearing Kokchetav Massif, Kazakhstan: Petrochemistry and Tectonic Evolution of a Unique Ultrahigh-pressure Metamorphic Terrane. Universal Academy Press Inc., Tokyo, Japan, pp. 181–190.

Kawai, K., Tsuchiya, T., 2012. Phase stability and elastic properties of the NAL and CF phases in the NaMg₂Al₅SiO₁₂ system from first principles. Am. Mineral. 97, 305–314.

Kelemen, P.B., Dick, H.B., Quick, J.E., 1992. Formation of harzburgite by pervasive melt/rock reaction in the upper mantle. Nature 358, 635–641.

Kelsey, D.E., 2008. On ultrahigh-temperature crustal metamorphism. Gondwana Res. 13, 1–29.

Kohn, M.J., 2010. Carbon isotope compositions of terrestrial C3 plants as indicators of (paleo)ecology and (paleo)climate. Proc. Natl. Acad. Sci. 107, 19691–19695.

Konzett, J., Frost, D.J., 2009. The high P–T stability of hydroxyl-apatite in natural and simplified MORB-an experimental study to 15 GPa with implications for transport and storage of phosphorus and halogens in subduction zones. J. Petrol. 50, 2043–2062.

Konzett, J., Rhede, D., Frost, D.J., 2012. The high PT stability of apatite and Cl partitioning between apatite and hydrous potassic phases in peridotite: an experimental study to 19 GPa with implications for the transport of P, Cl and K in the upper mantle. Contrib. Miner. Petrol. 163, 277–296.

Kopf, R.W., Hurlbut, C.S., Koivula, J.I., 1990. Recent discoveries of large diamonds in Trinity County, California. Gems Gemol. 25, 212–219.

Kopylova, M.G., Afanasiev, V.P., Bruce, L.F., Thurston, P.C., Ryder, J., 2011. Metaconglomerate preserves evidence for kimberlite, diamondiferous root and medium grade terrane of a pre-2.7 Ga Southern Superior protocraton. Earth Planet. Sci. Lett. 312, 213–225.

Kotková, J., O'Brien, P.J., Ziemann, M.A., 2011. Diamond and coesite discovered in Saxony-type granulite: solution to the Variscan garnet peridotite enigma. Geology 39, 667–670.

Kotková, J., Skoda, R., Mchovic, V., 2014. Kumdykolite from the ultrahigh-pressure granulite of the Bohemian Massif. Am. Mineral. 99, 1798–1801.

Kylander-Clark, A.R.C., Hacker, B.R., Mattinson, C.G., 2012. Size and exhumation rate of ultrahigh-pressure terranes linked to orogenic stage. Earth Planet. Sci. Lett. 321–322, 115–120.

Li, G., Shi, N., Xiong, M., Ma, Z., Bai, W., Fang, Q., 2007a. Rietveld structure refinement of new mineral luobusaite (βFeSi₂). J. Mineral. Petrol. 27, 1–5 (in Chinese with English abstract).

Li, G., Shi, N., Xiong, M., Ma, Z., Bai, W., Fang, Q., 2007b. X-ray diffraction investigation of native Si–Fe alloy minerals from Luobusha, Tibet. Front. Earth Sci. 1, 21–25.

Li, G., Fang, Q., Shi, N., Bai, W., Yang, J.S., Xiao, M., Ma, Z., Rong, H., 2009. Zangboite, TiFeSi₂, a new mineral species from Luobusha, Tibet, China, and its crystal structure. Can. Mineral. 47, 1265–1274.

Li, Z.H., Xu, Z.Q., Gerya, T.V., 2011. Flat versus steep subduction: contrasting modes for the formation and exhumation of high- to ultrahigh-pressure rocks in continental collision zones. Earth Planet. Sci. Lett. 301, 65–77.

Li, G., Bai, W., Shi, N., Fang, Q., Xiong, M., Yang, J.S., Ma, Z., 2012. Linzhiite, FeSi₂, a redefined and revalidated new mineral species from Luobusha, Tibet, China. Eur. J. Mineral. 24, 1047–1057.

Liou, J.G., Tsujimori, T., 2013. The fate of subducted continental crusts: evidence from recycle UHP–UHT minerals. Element 9, 248–250.

Liou, J.G., Zhang, R.Y., 1996. Occurrence of intergranular coesite in ultrahigh-P rocks from the Sulu region, eastern China: implications for lack of fluid during exhumation. Am. Mineral. 81, 1217–1221.

Liou, J.G., Zhang, R.Y., Ernst, W.G., Rumble III, D., Maruyama, S., 1998. High pressure minerals from deeply subducted metamorphic rocks. Rev. Mineral. 37, 33–96.

Liou, J.G., Hacker, B.R., Zhang, R.Y., 2000. Into the Forbidden zone. Science 287, 1215–1216.

Liou, J.G., Tsujimori, T., Zhang, R.Y., Katayama, I., Maruyama, S., 2004. Global UHP metamorphism and continent subduction/collision. The Himalayan Model. Int. Geol. Rev. 46, 1–27.

Liou, J.G., Ernst, W.G., Jahn, B.M., Song, S., 2009a. Tectonics and HP–UHP metamorphism of northern Tibet. J. Asian Earth Sci. 35, 191–198.

Liou, J.G., Ernst, W.G., Zhang, R.Y., Tsujimori, T., Jahn, B.M., 2009b. Ultrahigh-pressure minerals and metamorphic terranes – The view from China. J. Asian Earth Sci. 35, 199–231.

Liou, J.G., Zhang, R.Y., Liou, F.L., Zhang, Z.M., Ernst, W.G., 2012. Mineralogy, petrology, U-Pb geochronology, and geologic evolution of the Dabie-Sulu classic ultrahigh-pressure metamorphic terrane, East-Central China. Am. Mineral. 97, 1533–1543.

Liu, F.L., Liou, J.G., 2011. Zircon as the best mineral for P–T–time history of UHP metamorphism: a review on mineral inclusions and U-Pb SHRIMP ages of zircon from the Sulu-Dabie UHP rocks. J. Asian Earth Sci. 40, 1–39.

Liu, L., Zhang, J., Green II, H.W., Jin, Z., Bozhilov, K.N., 2007. Evidence of former stishovite in metamorphosed sediments, implying subduction to >350 km. Earth Planet. Sci. Lett. 263, 180–191.

Liu, L., Wang, C., Chen, D., Zhang, A., Liou, J.G., 2009. Petrology and geochronology of HP-UHP rocks from the south Altyn Tagh, northwestern China. J. Asian Earth Sci. 35, 232–244.

Liu, Y.S., Gao, S., Hu, Z.C., Gao, C.G., Zong, L.Q., Wang, D.B., 2010. Continental and oceanic crust recycling-induced melt-peridotite interactions in the Trans-North China orogen: U–Pb dating, Hf isotopes and trace elements in zircons from mantle xenoliths. J. Petrol. 51, 537–571.

Liu, F.L., Robinson, P.T., Liu, P.H., 2012. Multiple partial melting events in the Sulu UHP terrane: zircon U-Pb dating of granitic leucosomes within amphibolite and gneiss. J. Metamorph. Geol. 30, 887–906.

Lussier, A., Ball, N.A., Hawthorne, F.C., Henry, D.J., Shimizu, R., Ogasawara, Y., Ota, T., 2014. Maruyamaite. Mineral. Mag. 78, 549–558.

Ma, C., Tschauner, O., Beckett, J.R., 2014. Liebermannite, IMA 2013–128. CNMNC Newsletter No. 20, June 2014, page 551. Mineral. Mag. 78, 549–558.

Malaviarchichi, S.P.K., Makishima, A., Tanimoto, M., Kuritani, T., Nakamura, E., 2008. Highly unradiogenic lead isotope ratios from the Horoman peridotite in Japan. Nat. Geosci. 1, 859–863.

Malaviarchichi, S.P.K., Makishima, A., Nakamura, E., 2010. Melt-peridotite reactions and fluid metasomatism in the upper mantle, revealed from the geochemistry of peridotite and gabbro from the Horoman peridotite massif, Japan. J. Petrol. 51, 1417–1445.

Malkovets, V.G., Griffin, W.L., O'Reilly, S.Y., Wood, B.J., 2007. Diamond, subcalcic garnet, and mantle metasomatism: kimberlite sampling patterns define the link. Geology 35, 339–342.

Martin, L., Wood, B.J., Turner, S., Rushmer, T., 2011. Experimental measurements of trace element partitioning between lawsonite, zoisite and fluid and their implication for the composition of arc magmas. J. Metamorph. Geol. 52, 1049–1075.

Martin, L., Hermann, J., Gauthiez-Putallaz, L., Whitney, D.L., Vitale-Brovarone, A., Fornash, K.F., Evans, N.J., 2014. Lawsonite geochemistry and stability – implication for trace element and water cycles in subduction zones. J. Metamorph. Geol. 32, 455–478.

Maruyama, S.M., Liou, J.G., 1998. Initiation of UHP metamorphism and its significance on the Proterozoic/ Phanerozoic boundary. Island Arc, 35–76.

Maruyama, S., Liou, J.G., Terabayashi, M., 1996. Blueschists and eclogites of the world, and their exhumation. Int. Geol. Rev. 38, 485–594.

Maruyama, S., Yuen, D.A., Windley, B.F., 2007. Dynamics of plumes and superplumes through time. In: Yuen, D.A., Maruyama, S., Karato, S., Windley, B.F. (Eds.), Superplumes: Beyond Plate Tectonics. Springer, pp. 41–502.

Massonne, H.-J., 2001. First find of coesite in the ultrahigh-pressure metamorphic region of the Central Erzgebirge, Germany. Eur. J. Mineral. 13, 565–570.

Massonne, H.-J., 2013. Constructing the P–T path of ultrahigh-pressure rocks. Elements 9, 5–14.

Massonne, H.-J., Tu, W., 2007. δ^{13}C-signature of early graphite and subsequently formed microdiamond from the Saxonian Erzgebirge, Germany. Terra Nova 19, 476–480.

Massonne, H.-J., Kennedy, A., Nasdala, L., Theye, T., 2007a. Dating of zircon and monazite from diamondiferous quartzofeldspathic rocks of the Saxonian Erzgebirge. Mineral. Mag. 71, 407–425.

Massonne, H.-J., Willner, A.P., Gerya, T., 2007b. Densities of psammopelitic rocks at elevated temperatures and high to ultrahigh pressure conditions: what are the geodynamic consequences? Earth Planet. Sci. Lett. 256, 12–27.

Massonne, H.-J., Opitz, J., Theye, T., Nasir, S., 2013. Evolution of a very deeply subducted metasediment from As Sifah, northeastern coast of Oman. Lithos 156–159, 171–185.

McClelland, W.C., Lapen, T.J., 2013. Linking time to the pressure–temperature path for ultrahigh-pressure rocks. Elements 9, 273–279.

Medaris Jr., L.G., Wang, H.F., Jelinek, E., Jakes, P., 2003. Garnet peridotite in the Moldanubian zone in the Czech Republic—a heat source for Variscan metamorphism? J. Czech Geol. Soc. 48, 92–93.

Medaris Jr., L.G., Wang, H., Jelínek, E., Mihaljevič, M., Jakeš, P., 2005. Characteristics and origins of diverse Variscan peridotites in the Gfohl Nappe, Bohemian Massif, Czech Republic. Lithos 82, 1–23.

Meibom, A., Krot, A.N., Robert, F., Mostefaoui, S., Russell, S.S., Petaev, M.I., Gounelle, M., 2007. Composition of the sun inferred from a high-temperature solar nebular condensate. Astrophys. J. 656, 33–36.

Menneken, M., Nemchin, A.A., Geisler, Th., Pidgeon, R.T., Wilde, S., 2007. Hadean diamonds in zircon from Jacks Hills, Western Australia. Nature 448, 917–920.

Metcalf, R.V., Shervais, J.W., 2008. Suprasubduction-zone ophiolites: is there really an ophiolite conundrum? Geol. Soc. Am. Spec. Pap. 438, 191–222.

Meyer, H.O.A., 1985. Genesis of diamond: a mantle saga. Am. Mineral. 70, 344–355.

Meyers, P.A., 2014. Why are the δ^{13}C values in Phanerozoic black shales more negative than in modern marine organic matter? Geochem. Geophys. Geosyst. 25. http://dx.doi.org/10.1002/2014GC005305.

Miller, C.E., Kopylova, M.G., Ryder, J., 2012. Vanished diamondiferous cratonic root beneath the Southern Superior province. Evidence from diamond inclusions in the Wawa metaconglomerate. Contrib. Miner. Petrol. 164, 697–714.

Miura, M., Arai, S., Armed, A.H., Mizukami, T., Okuno, M., Yamamoto, S., 2012. Podiform chromitite classification revisited: a comparison of discordant and concordant chromitite pods from Wadi Hilti, northern Oman ophiolite. J. Asian Earth Sci. 59, 52–61.

Naemura, K., Hirajima, T., Svojtka, K., 2009. The pressure-temperature path and the origin of phlogopite in spinel-garnet peridotites from the Blansky Les Massif of the Moldanubian Zone, Czech Republic. J. Petrol. 50, 1795–1827.

Naemura, K., Ikuta, D., Kagi, H., Odake, S., Ueda, T., Ohi, S., Kobayashi, Y., Svojtka, M., Hirajima, T., 2011. Diamond and other possible ultra-deep evidence discovered in the orogenic spinel-garnet peridotite from the Moldanubian Zone of the Bohemian Massif, Czech Republic. In: Dobrzhinetskaya, L.F., Faryad, S.W., Wallis, S., Cuthbert, S. (Eds.), UHPM: 25 year after Discovery of Coesite and Diamond. Elsevier, pp. 77–112.

Naemura, K., Shimizu, I., Hirajima, T., Svojtka, M., 2013. In-situ finding of micro-diamond in chromite from the spinel-garnetperidotite, Moldanubian Zone of the Bohemian Massif. In: Tenth International Eclogite Conference, p. 93.

Nahodilová, R., Faryad, S.W., Dolejš, D., Tropper, P., Konzett, J., 2011. High-pressure partial melting and melt loss in felsic granulites in the Kutná Hora complex, Bohemian Massif (Czech Republic). Lithos 125, 641–658.

Nakamura, D., Svojtka, M., Naemura, K., 2004. Very high-pressure (>4 GPa) eclogite associated with the Moldanubian zone garnet peridotite (Nove Dvory, Czech Republic). J. Metamorph. Geol. 22, 593–603.

Nasdala, L., Massonne, H.-J., 2000. Microdiamonds from the Saxonian Erzgebirge, Germany: in situ micro-Raman characterisation. Eur. J. Mineral. 12, 495–498.

Nemchin, A.A., Whitehouse, M.J., Menneken, M., Geisler, Th., Pidgeon, R.T., Wilde, S., 2008. A light carbon reservoir recorded in zircon-hosted diamond from the Jack Hills. Nature 454, 92–95.

Ogasawara, Y., 2005. Diamonds: microdiamonds in ultrahigh-pressure metamorphic rocks. Elements 1, 91–95.

Ogasawara, Y., Ohta, M., Fukasawa, K., Katayama, I., Maruyama, S., 2000. Diamond-bearing and diamond-free metacarbonate rocks from Kymdi-Kol in the Kokchetav massif, northern Kazakhstan. Island Arc 9, 400–416.

Ogasawara, Y., Fukasawa, K., Maruyama, S., 2002. Coesite exsolution from supersilicic titanite in UHP marble from the Kokchetav Massif, northern Kazakhstan. Am. Mineral. 87, 454–461.

Ohtani, E., Litasov, K., Hosoya, T., Kubo, T., Kondo, T., 2004. Water transport into the deep mantle and formation of a hydrous transition zone. Phys. Earth Planet. Int. 143–144, 255–269.

Okamoto, K., Maruyama, S., 1999. The high-pressure synthesis of lawsonite in the MORB + H_2O system. Am. Mineral. 84, 362–373.

Palot, M., Cartigny, P., Harris, J.W., Kaminsky, F.V., Stachel, T., 2012. Evidence for deep mantle convection and primordial heterogeneity from nitrogen and carbon stable isotopes in diamond. Earth Planet. Sci. Lett. 357–358, 179–193.

Parkinson, C.D., Motoki, A., Onishi, C.T., Maruyama, S., 2001. Ultrahigh-pressure pyrope-kyanite granulites and associated eclogites in Neoproterozoic Nappes of Southeast Brazil. UHPM Workshop 2001. Waseda University, pp. 87–90.

Pearson, D.G., Brenker, F.E., Nestola, F., McNeill, J., Nasdala, L., Hutchison, M.T., Matveev, S., Mather, K., Schmitz, S., Vekemans, B., Vincze, L., 2014. Hydrous mantle transition zone indicated by rinwoodite included within diamond. Nature 507, 221–224.

Pernet-Fisher, J.F., Howarth, G.H., Liu, Y., Barry, P.H., Carmody, L., Valley, J.W., Bodnar, R.J., Spetsius, Z.V., Taylor, L.A., 2014. Komsomolskaya diamondiferous eclogites: evidence for oceanic crustal protoliths. Contrib. Miner. Petrol. 167, 981. http://dx.doi.org/10.1007/s00410-014-0981-y.

Perraki, M., Faryad, S.W., 2014. First findings of microdiamond, coesite and other UHP phases in felsic granulites in the Moldanubian Zone: implications for deep subduction and a revised geodynamic model for Variscan Orogeny in the Bohemian Massif. Lithos 202–203, 157–166.

Platt, J.P., Anczkiewicz, R., Soto, J., Kelley, S.P., Thirwall, M., 2006. Early Miocene continental subduction and rapid exhumation in the western Mediterranean. Geology 34, 981–984.

Platt, J.P., Behr, W.M., Johanesen, K., Williams, J.R., 2013. The Betic-Rif Arc and its orogenic hinterland: a review. Annu. Rev. Earth Planet. Sci. 41, 313–357.

Powell, R., Holland, T., 2010. Using equilibrium thermodynamics to understand metamorphism and metamorphic rocks. Elements 6, 309–314.

Proyer, A., Baziotis, I., Mposkos, E., Rhede, D., 2014. Ti- and Zr-minerals in calcite-dolomite marbles from the ultrahigh-pressure Kimi Complex, Rhodope Mountains, Greece. Implication for the P–T evolution based on reaction textures, petrogenetic grids, and geothermobarometry. Am. Mineral. 99, 1429–1448.

Ragozin, A.L., Liou, J.G., Shatsky, V.S., Sobolev, N.V., 2009. The timing of retrograde partial melting in the Kumdy-Kol region (Kokchetav massif, northern Kazakhstan). Lithos 109, 274–284.

Ren, Y.F., Fei, Y.W., Yang, J.S., Bai, W.J., Xu, Z.Q., 2009. SiO_2 solubility in rutile at high temperature and pressure. J. Earth Sci. 20, 274–283.

Riches, A.J.V., Liu, Y., Day, J.M.D., Spetsius, Z.V., Taylor, L.A., 2010. Subducted oceanic crust as diamond hosts revealed by garnets of mantle xenoliths from Nyurbinskaya, Siberia. Lithos 120, 368–378.

Robinson, P.T., Bai, W.J., Malpas, J., Yang, J.S., Zhou, M.F., Fang, Q.S., Hu, X.F., Cameron, S., Staudigel, H., 2004. Ultra-high Pressure Minerals in the Luobusa Ophiolite, Tibet and Their Tectonic Implications. Geological Society London, Special Publications 226, pp. 247–271.

Robinson, P., Trumbull, R.B., Schmitt, A., Yang, J.S., Li, J., Zhou, M.F., Erzinger, J., Dare, S., Xiong, F., 2014. The origin and significance of crustal minerals in ophiolitic chromitites and peridotites. Gondwana Res.. http://dx.doi.org/10.1016/j.gr.2014.06.003.

Root, D.B., Hacker, B.R., Gans, P.B., Ducea, M.N., Eide, E.A., Mosenfelder, J.L., 2005. Discrete ultrahigh-pressure domains in the Western Gneiss Region, Norway: implications for formation and exhumation. J. Metamorph. Geol. 23, 45–61.

Ruiz Cruz, M.D., Sanz de Galdeano, C., 2012. Diamond and coesite in ultrahigh-pressure-ultrahigh-temperature granulites from Ceuta, Northern Rif, northwest Africa. Mineral. Mag. 76, 683–705.

Ruiz Cruz, M.D., Sanz de Galdeano, C., 2013. Coesite and diamond inclusions, exsolution microstructures and chemical patterns in ultrahigh pressure garnet from Ceuta (Northern Rif, Spain). Lithos 177, 184–206.

Ruiz Cruz, M.D., Sanz de Galdeano, C., 2014. Garnet variety and zircon ages in UHP metasedimentary rocks from the Jubrique zone (Alpujárride Complex, Betic Cordillera, Spain): evidence for a pre-Alpine emplacement of the Ronda peridotite. Int. Geol. Rev. 56, 845–868.

Ruiz, L., McCandless, T.E., Helmstaedt, H.H., 1998. Re–Os model ages for eclogite xenoliths from the Colorado Plateau, USA. In: Gurney, J.J., Pasce, M.D., Richardson S.H. (Eds.), Proceedings of the 7th International Kimberlite Conference, vol. 2, pp. 736–740.

Saito, T., Wakabayashi, K., Yamashita, S., Sasabe, M., 2005. Production of Fe-Ti-Si alloys from the ilmenite ore and their magnetic properties. J. Alloys Compd. 388, 258–261.

Sakamaki, K., Ogasawara, Y., 2013. Hydroxyl in clinopyroxene and titanite in UHP diamond-free garnet-clinopyroxene rock from the Kokchetav Massif, northern Kazakhstan. Int. Geol. Rev. 56, 133–149.

Schertl, H.-P., O'Brien, P.O., 2013. Continental crust as mantle depths: key minerals and microstructures. Elements 9, 261–266.

Schertl, H.-P., Sobolev, N.V., 2013. The Kokchetav Massif, Kazakhstan: "Type locality" of diamond-bearing UHP metamorphic rocks. J. Asian Earth Sci. 63, 5–38.

Schertl, H.-P., Neuser, R.D., Sobolev, N.V., Shatsky, V.S., 2004. UHP-metamorphic rocks from Dora Maira/Western Alps and Kokchetav/Kazakhstan: new insights using cathodoluminescence petrography. Eur. J. Mineral. 16, 49–57.

Schmandt, B., Jacobsen, S.T., Becker, T.W., Lin, Z., Ducker, K.G., 2014. Dehydration melting at the top of the lower mantle. Science 344, 1265–1268.

Schulze, D.J., Helmstaedt, H., 1988. Coesite–sanidine eclogites from kimberlite – products of mantle fractionation or subduction. J. Geol. 96, 435–443.

Schulze, D.J., Valley, J.W., Spicuzza, M.J., 2000. Coesite eclogites from the Roberts Victor Kimberlite, South Africa. Lithos 54, 23–32.

Schulze, D.J., Harte, B., Valley, J.W., Brenan, J.M., Channer, D.M.D., 2003. Extreme crustal oxygen isotope signature preserved in coesite in diamond. Nature 423, 68–70.

Schulze, D.J., Harte, B., Page, F.Z., Valley, J.W., Channer, D.D., Jaques, A.L., 2013. Anti-correlation between low δ^{13}C of eclogitic diamonds and high δ^{18}O of their coesite and garnet inclusions requires a subduction origin. Geology 41, 455–458.

Schulze, D.J., Flemming, R.L., Shepherd, P.H.M., Helmstaedt, H., 2014. Mantle-derived guyanaite in a Cr-omphacitite xenolith from Moses Rock diatreme, Utah. Am. Mineral. 99, 1277–1283.

Sharp, Z.D., Essene, E.J., Smyth, J.R., 1992. Ultra-high temperatures from oxygen isotope thermometry of a coesite–sanidine grospydite. Contrib. Miner. Petrol. 112, 358–370.

Shcheka, S.A., Ignat'ev, A.V., Nechaev, V.P., Zvereva, V.P., 2006. First diamonds from placers in Primorie. Petrology 14, 99–317.

Shi, R., Alard, O., Zhi, X., O'Reilly, S.Y., Pearson, N.J., Griffin, W.L., Zhang, M., Chen, X., 2007. Multiple events in the Neo-Tethyan oceanic upper mantle: evidence from Ru–Os–Ir alloys in the Luobusa and Dongqiao ophiolitic podiform chromitites Tibet. Earth Planet. Sci. Lett. 261, 33–48.

Shi, N., Bai, W.J., Li, G., Xiong, M., Fang, Q., Yang, J.S., Ma, Z., Rong, H., 2009. Yarlongite: a new metallic carbide mineral. Acta Geol. Sin. 83, 52–56.

Shi, N.C., Bai, W.J., Li, G.W., Xiong, M., Yang, J.S., Ma, Z.S., Rong, H., 2012. Naquite, FeSi, a new mineral species from Luobusha, Tibet Western China. Acta Geol. Sin. 86, 533–538.

Shimizu, R., Ogasawara, Y., 2005. Discovery of K-tourmaline in diamond-bearing quartz-rich rock from the Kokchetav Massif, Kazakhstan. Mitteil. sterreichischen Mineral. Gesellschaft 150, 141.

Shimizu, R., Ogasawara, Y., 2013. Diversity of potassium-bearing tourmalines in diamondiferous Kokchetav UHP metamorphic rocks: a geochemical recorder from peak to retrograde metamorphic stages. J. Asian Earth Sci. 63, 39–55.

Shirey, S.B., Richardson, S.H., 2011. Start of the Wilson cycle at 3 Ga shown by diamonds from subcontinental mantle. Science 333, 434–436.

Shirey, S.B., Cartigny, P., Frost, D.J., Keshav, S., Nestola, F., Nimis, P., Pearson, D.G., Sobolev, N.V., Walter, M.J., 2013. Diamonds and the geology of mantle carbon. Rev. Mineral. Geochem. 75, 355–421.

Sizova, E., Gerya, T., Brown, M., 2012. Exhumation mechanisms of melt-bearing ultrahigh pressure crustal rocks during collision of spontaneously moving plates. J. Metamorph. Geol. 30, 957–972.

Smart, K.A., Heaman, L.M., Chacko, T., Simonetti, A., Kopylova, M., Mah, D., Daniels, D., 2009. The origin of high-MgO eclogites from the Jericho kimberlite, Nunavut. Earth Planet. Sci. Lett. 284, 527–537.

Smart, K.A., Chacko, T., Stachel, T., Muehlenbachs, K., Stern, R.A., Heaman, L.M., 2011. Diamond growth and carbon sources beneath the Northern Slave Craton, Canada: a δ^{13}C–N study of eclogite-hosted diamonds from the Jericho kimberlite. Geochim. Cosmochim. Acta 75, 6027–6047.

Smart, K.A., Chacko, T., Simonetti, A., Sharp, Z.D., Heaman, L.M., 2014. A record of Paleoproterozoic subduction preserved in the Northern Slave Cratonic Mantle: Sr-Pb-O isotope and trace-element investigations of eclogite xenoliths from the Jericho and Muskox Kimberlites. J. Petrol. 55, 549–583.

Smit, K.V., Stachel, T., Creaser, R.A., Ickert, R.B., DuFrane, S.A., Stern, R.A., Seller, M., 2014. Origin of eclogite and pyroxenite xenoliths from the Victor kimberlite, Canada, and implications for Superior craton formation. Geochim. Cosmochim. Acta 125, 308–337.

Smith, D.C., 1984. Coesite in clinopyroxene in the Caledonides and its implications for geodynamics. Nature 310, 641–644.

Smith, D., 2010. Antigorite peridotite, metaserpentinite, and other inclusions within diatremes on the Colorado Plateau, SW USA: implications for the mantle wedge during low-angle subduction. J. Petrol. 51, 1355–1379.

Smith, D.C., Godard, G., 2013. A Raman spectroscopic study of diamond and disordered sp^3-carbon in the coesite-bearing Straumen eclogite pod, Norway. J. Metamorph. Geol. 31, 19–33.

Smith, C.B., Bulanova, G.P., Kohn, S.C., Milledge, H.J., Hall, A.E., Griffin, B.J., Pearson, D.G., 2009. Nature and genesis of Kalimantan diamonds. Lithos 112, 822–832.

Smyth, J.R., 1977. Quartz pseudomorphs after coesite. Am. Mineral. 62, 1252–1257.

Smyth, J.R., Hatton, C.J., 1977. A coesite–sanidine grospydite from the Roberts-Victor Kimberlite. Earth Planet. Sci. Lett. 34, 284–290.

Snyder, G.A., Taylor, L.A., Jerde, E.A., Clayton, R.N., 1995. Archean mantle heterogeneity and the origin of diamondiferous eclogites, Siberia: evidence from stable isotopes and hydroxyl in garnet. Am. Mineral. 80, 799–809.

Snyder, G.A., Taylor, L.A., Crozaz, G., Halliday, A.N., Beard, B.L., Sobolev, V.N., Sobolev, N.V., 1997. The origins of Yakutian eclogite xenoliths. J. Petrol. 38, 85–113.

Sobolev. N.V., 1974. Deep-seated inclusions in kimberlites and the problem of the composition of the Upper mantle. Novosibirsk, Nauka Publ. House (in Russian). English Translation: 1977, Boyd, F.R. (Ed.), Washington. D.C. American Geological Union.

Sobolev, N.V., Shatsky, V.S., 1990. Diamond inclusions in garnets from metamorphic rocks: a new environment for diamond formation. Nature 343, 742–746.

Sobolev, V.S., Sobolev, N.V., 1980. New evidence of subduction to great depths of the eclogitized crustal rock. Dokl. Akad. Nauk SSSR 250, 683–685.

Sobolev, N.V., Kuznetsova, I.K., Zyuzin, N.I., 1968. The petrology of grospydite xenoliths from the Zagadochnaya kimberlite pipe in Yakutia. J. Petrol. 9, 253–280.

Sobolev, N.V., Efimova, E.S., Koptil, V.I., Lavrent'yev, Yu.G., Sobolev, V.S., 1976. Inclusions of coesite, garnet and omphacite in Yakutian diamond: the first discovery of coesite paragenesis. Dokl. Akad. Nauk SSSR 230, 1442–1446 (in Russian).

Sobolev, N.V., Galimov, E.M., Ivanovskaya, I.N., Efimova, E.S., 1979. Isotopic composition of carbon from diamonds containing crystalline inclusions. Dokl. Akad. Nauk SSSR 249, 1217–1220.

Sobolev, N.V., Efimova, E.S., Lavrent'yev, Y.G., Sobolev, V.S., 1984. Dominant calcsilicate association of crystalline inclusions in placer diamonds from southeastern Australia. Dokl. Akad. Nauk SSSR 279, 172–178.

Sobolev, N.V., Efimova, E.S., Channer, D.M.de R., Anderson, P.F.M., Barron, K.M., 1998. Unusual upper mantle beneath Guaniamo, Guyana Shield, Venezuela: evidence from diamond inclusions. Geology 26, 971–974.

Sobolev, N.V., Logvinova, A.M., Zedgenizov, D.A., Yefimova, E.S., Seryotkin, Y.V., Floss, K., Taylor, L.A., 2004. Mineral inclusions in microdiamonds and macrodiamonds from Yakutian kimberlites: a comparative study. Lithos 77, 225–242.

Sobolev, A.V., Hofmann, A.W., Kuzmin, D.V., Yaxley, G.M., Arndt, N.T., Chung, S.L., Danyushevsky, L.V., Elliott, T., Frey, F.A., Garcia, M.O., Gurenko, A.A., Kamenetsky, V.S., Kerr, A.C., Krivolutskaya, N.A., Matvienkov, V.V., Nikogosian, I.K., Rocholl, A., Sigurdsson, I.A., Sushchevskaya, N.M., Teklay, M., 2007. The amount of recycled crust in sources of mantle-derived melts. Science 316, 412–417.

Spaggiari, C.V., Pidgeon, R.T., Wilde, S.A., 2007. The Jack Hills greenstone belt, Western Australia. Part 2: lithological relationships and implications for the deposition of ⩾4.0 Ga detrital zircons. Precambr. Res. 155, 261–286.

Spandler, C., Pirard, C., 2013. Element recycling from subducting slabs to arc crust: a review. Lithos 170–171, 208–223.

Spencer, L.K., Dikinis, S.D., Keller, P.C., Kane, R.E., 2008. The diamond deposits of Kalimantan, Borneo. Gems Gemol. 24, 67–80.

Spetsius, Z.V., Taylor, L.A., Valley, J.W., Deangelis, M.T., Spicuzza, M., Ivanov, A.D., Banzerak, V.I., 2008. Diamondiferous xenoliths from crustal subduction: garnet oxygen isotopes from the Nyurbinskaya pipe, Yakutia. Eur. J. Mineral. 20, 375–385.

Spetsius, Z.V., Wiggers de Vries, D.F., Davies, G.R., 2009. Combined C isotope and geochemical evidence for a recycled origin for diamondiferous eclogite xenoliths from kimberlites of Yakutia. Lithos 112, 1032–1042.

Stachel, T., Harris, J.W., Brey, G.P., Joswig, W., 2000. Kankan diamonds (Guinea) II: lower mantle inclusion parageneses. Contrib. Miner. Petrol. 140, 16–27.

Stachel, T., Brey, G.P., Harris, J.W., 2005. Inclusions in sublithospheric diamonds: glimpses of deep earth. Elements 1, 73–78.

Stagno, V., Ojwang, D.O., McCammon, C.A., Frost, D.J., 2013. The oxidation state of the mantle and the extraction of carbon from Earth's interior. Nature 493, 84–90.

Stern, R.J., Tsujimori, T., Harlow, G.E., Groat, L.A., 2013. Plate tectonic gemstones. Geology 41, 723–726.

Tappert, R., Stachel, T., Harris, J.W., Muelenbachs, K., Ludwig, T., Brey, G.P., 2005. Subducting oceanic crust: the source of deep diamonds. Geology 33, 565–568.

Tappert, R., Foden, J., Stachel, T., Muelenbachs, K., Tappert, M., Wills, K., 2009. Deep mantle diamonds from South Australia: a record of Pacific subduction at the Gondwanan margin. Geology 37, 43–46.

Tatarintsev, V.I., Sandomirskaya, S.M., Tsumbal, S.N., 1987. First discovery of titanium nitride (osbornite) in terrestrial rocks. Dokl. Akad. Nauk SSSR 296, 1458–1461.

Taylor, L.A., Anand, M., 2004. Diamonds: time capsules from the Siberian Mantle. Chem. Erde 64, 1–74.

Terry, M.P., Robinson, P., Krogh Ravana, E.J., 2000. Kyanite eclogite thermobarometry and evidence for thrusting of UHP over HP metamorphic rocks, Nordoyane, Western Gneiss Region, Norway. Am. Mineral. 85, 1637–1650.

Tomilenko, A.A., Kovyazin, S.V., Pokhilenko, L.N., Sobolev, N.V., 2009. Primary hydrocarbon inclusions in garnet of diamondiferous eclogite from the Udachanaya kimberlite pipe, Yakutia. Dokl. Earth Sci. 42, 695–698.

Trommsdorff, V., Evans, B.W., 1972. Progressive metamorphism of antigorite schist in the Bergell tonalite aureole (Italy). Am. J. Sci. 272, 423–437.

Tropper, P., 2014. Small grains and big implications: accessory Ti- and Zr-minerals as petrogenetic indicators in HP and UHP marbles. Am. Mineral. 99, 1197–1198.

Tsujimori, T., Ernst, W.G., 2014. Lawsonite blueschists and lawsonite eclogites as proxies for paleosubduction zone processes: a review. J. Metamorph. Geol. 32, 437–454.

Tsujimori, T., Harlow, G.E., 2012. Petrogenetic relationships between jadeitite and associated high-pressure and low-temperature metamorphic rocks in worldwide jadeitite localities: a review. Eur. J. Mineral. 24, 371–390.

Tsujimori, T., Sisson, B., Liou, J.G., Harlow, G.E., Sorensen, S.S., 2006. Very low-temperature record in subduction process: a review of global lawsonite-eclogites. Lithos 92, 609–624.

Usui, T., Nakamura, E., Kobayashi, K., Maruyama, S., Helmstaedt, H., 2003. Fate of the subducted Farallon plate inferred from eclogite xenoliths in the Colorado Plateau. Geology 31, 589–592.

Usui, T., Nakamura, E., Helmstaedt, H., 2006. Petrology and geochemistry of eclogite xenoliths from the Colorado Plateau: implications for the evolution of subducted oceanic crust. J. Petrol. 47, 929–964.

Van Roermund, H.L.M., Carswell, D.A., Drury, M.R., Heijboe, T.C., 2002. Microdiamond in a megacrystic garnet websterite pod from Bardane on the Island of Fjortoft, western Norway: evidence for diamond formation in mantle rocks during deep continental subduction. Geology 30, 959–962.

Vitale Brovarone, A.V., Beyssac, O., 2014. Lawsonite metasomatism: a new route for water to the deep Earth. Earth Planet. Sci. Lett. 393, 275–284.

Vitale Brovarone, A., Alard, O., Beyssac, O., Martin, L.A.J., Picatto, M., 2014. Lawsonite metasomatism and trace element recycling in subduction zones. J. Metamorph. Geol. 32, 489–514.

Vrabec, M., Janák, M., Froitzheim, N., De Hoog, J.C.M., 2012. Phase relations during peak metamorphism and decompression of the UHP kyanite eclogites, Pohorje Mountains (Eastern Alps, Slovenia). Lithos 144–145, 40–55.

Vrijmoed, J.C., Smith, D.C., van Roermund, H.L.M., 2008. Raman confirmation of micro-diamond in the Svartberget Fe-Ti type garnet peridotite, Western Gneiss Region, western Norway. Terra Nova 20, 295–301.

Wain, A., 1997. New evidence for coesite in eclogites and gneiss: defining an ultrahigh-pressure province in the Western Gneiss Region of Norway. Geology 25, 927–930.

Wain, A., Waters, D., Jephcoat, A., Olijnyk, H., 2000. The high-pressure to ultrahigh-pressure transition in the Western Gneiss Region, Norway. Eur. J. Mineral. 12, 667–687.

Walter, M.J., Kohn, S.C., Araujo, D., Bulanova, G.P., Smith, C.B., Gillou, E., Wang, J., Steele, A., Shirey, S.B., 2011. Deep mantle cycling of oceanic crust: evidence from diamonds and their mineral inclusions. Science 334, 54–57.

Wang, L., Rouse, R.C., Essene, E.J., Peacor, D.R., Zhang, Y., 2000. Carmichaelite, a new hydroxyl-bearing titanate from Garnet Ridge, Arizona. Am. Mineral. 85, 792–800.

Wang, H., Wu, Y.-B., Gao, S., Zheng, J.P., Liu, Q., Liu, X.C., Qin, Z.W., Yang, S.H., Gong, H.J., 2014. Deep subduction of continental crust in accretionary orogen: evidence from U-Pb dating on diamond-bearing zircons from the Qinling orogen, central China. Lithos 190–191, 420–429.

Warren, J.M., Shirey, S.B., 2012. Lead and osmium isotopic constraints on the oceanic mantle from single abyssal peridotite sulfides. Earth Planet. Sci. Lett. 359–360, 279–293.

Warren, C.J., Beaumont, C., Jamieson, R.A., 2008a. Modelling tectonic styles and ultra-high pressure (UHP) rock exhumation during the transition from oceanic subduction to continental collision. Earth Planet. Sci. Lett. 267, 129–145.

Warren, C.J., Beaumont, C., Jamieson, R.A., 2008b. Formation and exhumation of UHP rocks during continental collision: role of detachment in the subduction channel. Geochem. Geophys. Geosyst. 9, Q04019. http://dx.doi.org/10.1029/2007GC001839.

Watson, K.D., Morton, D.M., 1969. Eclogite inclusions in kimberlite pipes at Garnet Ridge, Northeastern Arizona. Am. Mineral. 54, 267–285.

Wei, C.J., Qian, H., Tian, Z.L., 2013. Metamorphic evolution of medium-temperature ultra-high pressure (MT-UHP) eclogites from the South Dabie orogen, Central China: an insight from phase equilibria modeling. J. Metamorph. Geol. 31, 469–504.

Whitney, D.L., Evans, B., 2010. Abbreviations for names of rock-forming minerals. Am. Mineral. 95, 185–187.

Wina, T.T., Daviesb, R.M., Griffin, W.L., Wathanakulc, P., Frencha, D.H., 2001. Distribution and characteristics of diamonds from Myanmar. J. Asian Earth Sci. 19, 563–577.

Wirth, R., Rocholl, A., 2003. Nanocrystalline diamond from the Earth's mantle underneath Hawaii. Earth Planet. Sci. Lett. 211, 357–369.

Wirth, R., Vollmer, C., Brenker, F., Matsyuk, S., Kaminsky, F., 2007. Nanocrystalline hydrous aluminum silicate in superdeep diamonds from Juina (Mato Grosso State, Brazil). Earth Planet. Sci. Lett. 259, 384–399.

Wirth, R., Kaminsky, F., Matsyuk, S., Schreiber, A., 2009. Unusual micro- and nano-inclusions in diamonds from the Juina Area, Brazil. Earth Planet. Sci. Lett. 286, 292–303.

Withers, A.C., Essene, E.J., Zhang, Y., 2003. Rutile/TiO$_2^{II}$ phase equilibria. Contrib. Miner. Petrol. 145, 199–204.

Wu, X.-L., Meng, D.-W., Hanm, Y.-J., 2005. Λ-PbO$_2$-type nanophase of TiO$_2$ from coesite-bearing eclogite in the Dabie Mountains, China. Am. Mineral. 90, 1458–1461.

Xu, Z.Q., 2007. Continental deep subduction and exhumation: evidence from the main hole of the Chinese continental Scientific Drilling and the Sulu UHP/HP metamorphic terrane. Acta Petrol. Sin. 23, 3041–3053 (in Chinese with English Abstract).

Xu, X.Z., Yang, J.S., Chen, S.Y., Fang, Q.S., Bai, W.J., Ba, D.Z., 2009. Unusual mantle mineral group from chromitite orebody Cr-11 in Luobusa ophiolite of the Yarlung-Zangbo suture zone, Tibet. J. Earth Sci. 20, 284–302.

Xu, X.Z., Yang, J.S., Ba, D.Z., Guo, G.L., Robinson, P.T., Li, J.Y., 2011. Petrogenesis of the kangjinla peridotite in the luobusa ophiolite, southern tibet. J. Asian Earth Sci. 42, 553–568.

Yagi, A., Suzuki, T., Akaogi, M., 1994. High pressure transitions in the system KAlSi$_3$O$_8$-NaAlSi$_3$O$_8$. Phys. Chem. Miner. 21, 12–17.

Yamamoto, H., Yamamoto, S., Kaneko, Y., Terabayashi, M., Komiya, T., Katayama, K., Iizuka, T., 2007a. Imbricate structure of the Luobusa Ophiolite and surrounding rock units, southern Tibet. J. Asian Earth Sci. 29, 296–304.

Yamamoto, S., Maruyama, S., Windly, B.F., Omori, S., Shibuya, T., Kawai, T., Sawaki, Y., 2007. An ultrahigh-pressure origin of podiform chromitites in the Ballantrae Complex ophiolite, SW Scotland: silicate exsolution lamellae in chromites. In: 29th International Eclogite Field Symposium in Lochalsh Scotland Programme and Abstracts, 126.

Yamamoto, S., Senshu, H., Rino, S., Omori, S., Maruyama, S., 2009a. Granite subduction: arc subduction, tectonic erosion and sediment subduction. Gondwana Res. 15, 443–453.

Yamamoto, S., Komiya, T., Hirose, K., Maruyama, S., 2009b. Coesite and clinopyroxene exsolution lamellae in chromites: in-situ ultrahigh-pressure evidence from podiform chromitites in the Luobusa ophiolite, southern Tibet. Lithos 109, 314–322.

Yamamoto, S., Komiya, T., Yamamoto, H., Kaneko, Y., Terabayashi, M., Katayama, I., Iizuka, T., Maruyama, S., Yang, J.S., Kon, Y., Hirata, T., 2013. Recycled crustal zircons from podiform chromitites in the Luobusa ophiolite, southern Tibet. Island Arc 22, 89–103.

Yan, B.G., Liang, R.X., Fang, Q.S., Yang, F.Y., Yuan, C.Y., 1986. The basic characteristics of diamond and diamond-bearing ultramafic rocks of Qiaoxi and Hongqu, Tibet. J. Inst. Geol. Chin. Acad. Geol. Sci. 14, 52–56 (in Chinese).

Yang, F.Y., Kang, Z.Q., Liu, S.C., 1981. A new octahedral pseudomorph of lizardite and its origin. Acta Mineral. Sin. 1, 52–54 (in Chinese).

Yang, J.S., Xu, Z.Q., Dobrzhinetskaya, L.F., Green, H.W., Shi, R.D., Wu, C.L., Wooden, J.L., Zhang, J.X., Wan, Y.S., Li, H.B., 2003a. Discovery of metamorphic diamonds in central China: an indication of a ~4000-km-long zone of deep subduction resulting from multiple continental collisions. Terra Nova 15, 370–379.

Yang, J.-S., Bai, W.J., Fang, Q.S., Yan, B.G., Shi, N.C., Ma, Z.S., Dai, M.Q., Xiong, M., 2003b. Silicon rutile-an ultra-high pressure (UHP) mineral from an ophiolite. Prog. Nat. Sci. 23, 528–531.

Yang, J.S., Liu, F.L., Wu, C.L., Xu, Z.Q., Shi, R.D., Chen, S.Y., Deloule, E., Wooden, J.L., 2005. Two ultrahigh-pressure metamorphic events recognized in the Central Orogenic Belt of China: evidence from the U-Pb dating of coesite-bearing zircons. Int. Geol. Rev. 47, 327–343.

Yang, J.S., Dobrzhinetskaya, L., Bai, W.J., Fang, Q.S., Robinson, P.T., Zhang, J.F., Green II, H.W., 2007. Diamond- and coesite-bearing chromitites from the Luobusa ophiolite, Tibet. Geology 35, 875–878.

Yang, J.S., Bai, W.J., Fang, Q.S., Rong, H., 2008. Ultrahigh-pressure minerals and new minerals from the Luobusa ophiolitic chromitites in Tibet: a review. Acta Geosci. Sin. 29, 263–274.

Yang, J.S., Robinson, P.T., Zhang, Z.M., 2011. Introduction to the special issue "Subduction and Exhumation History Recorded in HP-UHP Metamorphic Rocks". J. Asian Earth Sci. 42, 511–513.

Yang, J.S., Wirth, R., Xu, X., Robinson, P.T., Rong, H., 2012. Mineral inclusions in diamonds from ophiolitic peridotite and chromites. Geol. Soc. Am. Abstr. Progr. 44 (7), 200.

Yang, J.S., Xu, X.Z., Zhang, Z.M., Rong, H., Li, Y., Xiong, F.H., Liang, F.H., Liu, Z., Liu, F., Li, J.Y., Li, Z.L., Chen, S.Y., Guo, G.L., Robinson, P., 2013. Ophiolite-type diamond and deep genesis of chromitite. Acta Geosci. Sin. 34, 643–653 (in Chinese with English abstract).

Yang, J.S., Robinson, P., Dilek, I., 2014. Diamonds in ophiolite. Element 10, 127–130.

Yang, J.S., Meng, F.C., Xu, X.Z., Robinson, P.T., Dilek, Y., Makeyev, A.B., Wirth, R., Wiedenbeck, M., Griffin, W.L., Cliff, J., 2014. Diamonds, native elements and metal alloys from chromitites of the Ray-Iz ophiolite of the Polar Urals. Gondwana Res.. http://dx.doi.org/10.1016/j.gr.2014.07.004.

Yu, Z.X., 1984. Two new minerals, gupeiite and xifengite, in cosmic dusts from Yanshan. Acta Petrol. Mineral. Anal. 3, 231–238 (in Chinese with English abstract).

Yui, T.F., Ogasawara, L., Zhang, L.F., Tsai, C.H., 2013. Editorial: HP and UHP metamorphic belts in Asia. J. Asian Earth Sci. 63, 1–4.

Zhang, R.Y., Liou, J.G., 1997. Partial transformation of gabbro to coesite-bearing eclogite from Yangkou, the Sulu terrane, eastern China. J. Metamorph. Geol. 15, 183–202.

Zhang, S.-B., Zheng, Y.-F., 2013. Formation and evolution of precambrian continental lithosphere in South China. Gondwana Res. 23, 1241–1260.

Zhang, H.Y., Ba, D.Z., Guo, T.Y., Mo, X.X., Xue, J.Z., Ruan, G.F., Wang, Z.X., 1996. Study of Luobusha Typical Chromite Ore Deposit Qusong County, Tibet (Xizang): Lhasa. Xizang People Press, pp. 1–181 (in Chinese).

Zhang, R.Y., Liou, J.G., Shau, J.F., 2002. Hydroxyl-rich topaz in high-pressure and ultrahigh-pressure kyanite quartzites, with retrograde woodhouseite, from the Sulu terrane, eastern China. Am. Mineral. 87, 445–453.

Zhang, R.Y., Liou, J.G., Ernst, W.G., 2009a. The Dabie-Sulu continental collision zone: a comprehensive review. Gondwana Res. 16, 1–2.

Zhang, R.Y., Liou, J.G., Iizuka, Y., Yang, J.S., 2009b. First record of K-cymrite in North Qaidam UHP eclogite, Western China. Am. Mineral. 94, 222–228.

Zhang, R.Y., Liou, J.G., Omori, S., Sobolev, N.V., Shatsky, V.S., Ogasawara, Y., 2012. Tale of the Kulet eclogite from the Kokchetav massive, Kazakhstan: initial tectonic setting and transition from amphibolite to eclogite. J. Metamorph. Geol. 30, 537–559.

Zheng, Y.-F., 2012a. Metamorphic chemical geodynamics of continental subduction zones. Chem. Geol. 328, 5–48.

Zheng, Y.-F., 2012b. A perspective view on ultrahigh-pressure metamorphism and continental collision in the Dabie-Sulu orogenic belt. Chin. Sci. Bull. 53, 3081–3104.

Zheng, Y.-F., Chen, R.K., Zhao, E.F., 2009. Chemical geodynamics of continental subduction-zone metamorphism: insights from studies of the Chinese Continental Scientific Drilling (CCSD) core samples. Tectonophysics 475, 327–358.

Zheng, Y.-F., Xia, X.-Q., Chen, R.-X., Gao, X.-Y., 2011. Partial melting, fluid super-criticality and element mobility in ultrahigh-pressure metamorphic rocks during continental collision. Earth Sci. Rev. 107, 342–374.

Zheng, Y.-F., Zhang, L.F., McClelland, W.C., Cuthbert, S., 2012. Processes in continental collision zones: preface. Lithos 136–139, 1–9.

Zhou, M.F., 1995. Petrogenesis of the podiform chromitites in the Luobusa ophiolites, Southern Tibet. Ph.D. thesis, Dalhousie University, Canada.

Zhou, M.F., Robinson, P.T., Malpas, J., Li, Z., 1996. Podiform chromitites in the Luobusa ophiolite (southern Tibet): implications for melt-rock interaction and chromite segregation in the upper mantle. J. Petrol. 37, 3–21.

Zhou, M.F., Sun, M., Keays, R.R., Kerrich, R.W., 1998. Controls on platinum-group elemental distributions of podiform chromitites: a case study of high-Cr and high-Al chromitites from Chinese orogenic belts. Geochim. Cosmochim. Acta 62, 677–688.

Zhou, M.F., Robinson, P.T., Malpas, J., Edwards, S.J., Qi, L., 2005. REE and PGE geochemical constraints on the formation of dunites in the Luobusa ophiolite, southern Tibet. J. Petrol. 46, 615–639.